Mechanism of Germ Cell Specification in Early Zebrafish Embryogenesis

Doctoral Thesis

Dissertation for the award of the degree

“Doctor rerum naturalium (Dr. rer. nat)”

in the GGNB program: Genes and Development

at the Georg August University Göttingen

Faculty of Biology

Submitted by

Roshan Priyarangana Perera

Born in Sri Lanka

Göttingen, June 2020

Members of the Thesis Committee

Supervisor

Dr. (PD). Roland Dosch (Reviewer)

Institute for Human Genetics, Georg August University Göttingen

Second member of the thesis committee

Professor. Markus T.Bohnsack (Reviewer)

Institute for Molecular Biology, Georg August University Göttingen

Third member of the thesis committee

Dr. Achim Dickmanns

Department for Structural Biology, Georg August University Göttingen

Examination board members

Professor. Gregor Bucher

Department of Developmental Biology, Georg August University Göttingen

Dr. Nico Posnien

Department of Developmental Biology, Georg August University Göttingen

Dr. Ufuk Günesdogan

Department of Developmental Biology, Georg August University Göttingen

Date of Oral examination:

Affidavit

Herewith I declare that I prepared the PhD thesis "**Mechanism of Germ Cell Specification in Early Zebrafish Embryogenesis**" on my own and with no other sources and aids than quoted.

04.06.2020

_____

Roshan Perera

Acknowledgement

I wish to express my sincere gratitude to my supervisor, Dr. Roland Dosch, the one who convincingly guided and encouraged me to be professional and do the right things even when the road got more tough than I expected.

Besides my supervisor, I would like to thank my thesis committee: Prof. Markus Bohnsack and Dr. Achim dickmann, for their encouragement, insightful comments, and constructive questions.

I thank my fellow labmates in the Dosch Lab: Dr. Pritesh Krishnakumar, Dr. Alexander Goloborodko, Nadia Rostam, Hazem Khalifa and Vranda Garg for nice discussions, arguments, for the sleepless nights we were working together in the lab, and for all the fun we have had in the last four years.

Words cannot express how grateful I am for you Alaa Shaikhqasem. Thank you for your help and useful advice! I am incredibly fortunate to have a friend like you. I could not have done my Ph.D. without you. Also, I would like to thank Piotr Neumann, Tim Garbers, and Florian Hamann for your support for my studies.

I specially thank my friend Leoni Witte: You are a wonderful friend. You inspired me during a difficult time when I needed words of encouragement, and I appreciate your, kindness, support, and generosity shared with me during the last four years. Also, my deep appreciation goes to my friends Dolma Choezom, Pradhipa Karuna, and Esther Essel who helped me in numerous ways during various stages of my Ph.D.

I am indebted to all my rotation students, Lukas Amann, Aishwarya Tagat, Indrani Mukarji, and Florian Fink for their valuable contribution to my research project.

My thanks also go out to Gudrun Krach, Mona Honemann, and Katja Ditter who were always so helpful and provided me with their kind assistance. In addition, I thank to Dr. Julia Gross allowing me to do cell culture experiments.

This work would not have been possible without financial support from Deutscher Akademischer Austausch Dienst/German Academic Exchange Service. Therefore, I express my heartfelt thanks to the for funding thought out my Ph.D. Special thanks go to Göttingen Graduate Center for Neurosciences, Biophysics, and Molecular Biosciences (GGNB)for their enormous support during my Ph.D.

I wish to acknowledge the support and great love of my Mother, Father, and other family members. They kept me going on and this work would not have been realized without their support.

List of Abbreviations

°C	Degrees Celsius
A	Adenine
aa	Amino acids
amol	Attomolar
bp	Base pairs
BSA	Bovine serum albumin
C	Cytosine
C. elegans	*Caenorhabditis elegans*
cDNA	Complementary DNA
CMV	Cytomegalovirus
Co-IP	Co-immunoprecipitation
C-terminus	Carboxy-terminus
DAZ	Deleted in azoospermia
dH_2O	Distilled water
Dm	*Drosophila melanogaster*
DNA	Deoxyribonucleic acid
dNTP	Deoxynucleotide triphosphate
dpf	Days post fertilization
E. coli	*Escherichia coli*
EDTA	Ethylenediaminetetraacetic acid
eGFP	Enhanced green fluorescent protein
EGTA	Ethylene glycol tetraacetic acid
et al.	Et alii
fw	Forward
g	Gram
G	Guanine

GFP	Green fluorescent protein
h	Hour
HMM	Hidden Markov models
hpf	Hours post fertilization
IP	Immunoprecipitation
Kb	Kilo base pairs
kDa	Kilodalton
LB	Lysogeny broth
M	Molar
mg	Milligram
min	Minute
miRNA	Micro RNA
ml	Millilitre
mM	Millimolar
mRNA	Messenger RNA
n	Number
ng	Nanogram
nl	Nanolitre
N-terminus	Amino-terminus
ORF	Open reading frame
PAGE	Polyacrylamide gel electrophoresis
PBS	Phosphate-buffered saline
PBT	Phosphate-buffered saline Triton X-100
PCR	Polymerase chain reaction
pg	Picogram
PGC	Primordial germ cell
pH	Potentium hydrogenium
piRNA	Piwi-interacting RNA

RNA	Ribonucleic acid
RNase	Ribonuclease
RNP	Ribonucleo-protein granule
rpm	Rounds per minute
RRM	RNA recognition motif
RT-qPCR	Reverse transcription quantitative real-time PCR
rv	Reverse
s	Second
SDS	Sodium dodecyl sulfate
SH3	SRC Homology 3
T	Thymine
TAE	Tris-Acetate-EDTA
Taq	Thermus aquaticus
TBE	Tris-Borate-EDTA
Tris	Tris(hydroxymethyl)aminomethane
U	Units
UAS	Upstream activation sequence
UTR	Untranslated region
UV	Ultraviolet
V	Volt
Zf	Zebrafish
µg	Microgram
µl	Microlitre
µm	Micrometer
µM	Micromolar

Abstract

Reproduction is an essential feature of life that ensures the perpetuation and survival in many multicellular organisms while passing the genetic information to the next generation. The zebrafish germline is specified during early embryogenesis by maternal RNP granules collectively called germ plasm. It has been discovered that the zebrafish *bucky ball* gene, which is a key gene responsible for germ plasm formation and encodes a novel vertebrate-specific protein with unknown biochemical function. Overexpression experiments revealed that Buc induces ectopic primordial germ cells (PGCs) *in vivo*. So far, only the Oskar protein in *Drosophila* shows equivalent activities. Remarkably, we recently revealed that Oskar induces ectopic PGCs in zebrafish, albeit Oskar does not share sequence homology with Buc. Moreover, zebrafish Vasa is also sufficient to induce PGCs *in vivo* suggesting that Buc and Vasa act in the same molecular process involving in germ cell specification. This conserved activity between Oskar and Buc suggests that both proteins share a similar biochemical interactome, whose molecular identity is unknown.

In this study, I characterize the interaction of Buc and the RNA helicase Vasa investigating their binding motifs. I identified a peptide encoding amino acids 372-394 in Buc as Vasa Binding Motif (VBM) and a peptide encoding amino acids 600-625 in Vasa as Buc Binding Motif (BBM) using bimolecular fluorescence complementation (BiFC). Further, I show that the Buc-VBM is highly conserved in vertebrates. Moreover, Buc and Vasa directly interact *in vitro* and independent of RNA. The Buc-VBM encodes an intrinsically disordered peptide, but CD spectroscopy reveals that a crowding agent induces formation of an α-helix. Fascinatingly, I discovered that Buc activates Vasa ATPase activity annotating the first biochemical function of Buc as a helicase activator. Collectively, these results propose a model in which the activity of Vasa helicase is a central regulator of PGC formation, which is tightly controlled by the germ plasm organizer Buc.

Table of Contents

1. Introduction

Reproduction is an essential feature of life that ensures the perpetuation and survival in many multicellular organisms while passing the genetic information from one generation to the next (Santos & Lehmann, 2004; Marlow, 2010; Jostes & Schorle, 2018; Cieri et al., 2018).

1.1. Sexual reproduction

Sexual reproduction needs two parents to produce female and male germ cells *i.e.* eggs and sperm. During fertilization, egg and sperm fuse and form a zygote. The zygote undergoes embryonic development to form an offspring of the same species, but is genetically a combination of the parents (Dudgeon et al., 2017).

All germ cells arise from **primordial germ cells (PGCs)** (Dudgeon et al., 2017). In many animals, a population of PGCs segregates from the somatic cells during early embryonic development (Dudgeon et al., 2017). However, the mechanism of PGC specification is diverse among animal species (Santos & Lehmann, 2004; Marlow, 2015). Nevertheless, two distinct mechanisms specify PGCs.

1.2. Modes of germ cell specification

The first mechanism is the induction mode of germ cell specification (Figure. 1). There, a subset of pluripotent embryonic cells is specified to PGCs by cell-cell communication through zygotic signaling molecules (Santos & Lehmann, 2004; Carr, R. M., Oranu, A., & Khungar, 2016; Marlow, 2015; Gustafson & Wessel, 2010; Saitou & Yamaji, 2010). This mode of germ cell specification can be seen in mammals such as mice and humans and some insects like *Gryllus bimaculatus* (cricket) (Extavour & Akam, 2003; Nakamura & Extavour, 2016; Krishnakumar & Dosch, 2018; Marlow, 2015)

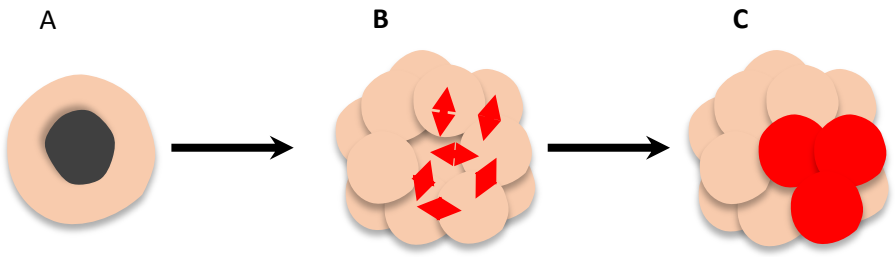

Figure 1 : Induction mode of germ cell specification.

A) Zygote (brown) and the nucleus (black). (B) Early embryogenesis with several blastomeres (light brown) and a subset of blastomeres sends inductive signals to each other to specify germ cells (red arrows). (C) Later stage of early embryo with specified PGCs (red)

The second mechanism is called inherited mode of germ cell specification (Figure. 2). In this mode, the newly fertilized, totipotent embryo inherits a cytoplasmic determinant referred as germ plasm (Gp). Gp is already deposited in the oocyte during oogenesis. During early embryogenesis, certain cells of the embryo inherit Gp, which develop into PGCs (Santos & Lehmann, 2004; Carr, R. M., Oranu, A., & Khungar, 2016; Marlow, 2015; Gustafson & Wessel, 2010; Saitou & Yamaji, 2010). Invertebrate species like *Drosophila*, *C. elegans* and vertebrate species like *Xenopus*, zebrafish, and birds display inherited mode of germ cell specification (Extavour & Akam, 2003; Krishnakumar & Dosch, 2018; Marlow, 2015).

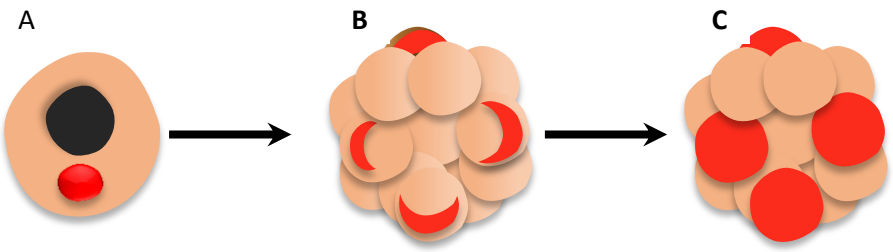

Figure 2: Inherited mode of germ cell specification.

(A) Oocyte (brown) with nucleus (black) and maternally inherited germ plasm (red). (B) Early embryogenesis with several blastomeres (brown). During the early embryogenesis, germ plasm (red) asymmetrically distribute among few blastomeres. (C) Later stage of early embryo with specified PGCs (red).

Regardless of the mode of specification, PGCs give rise to a continual supply of germ cells showing stemness properties like totipotency and immortality, that are distinct from those of somatic cells (Nakamura et al., 2019; Juliano et al., 2010). In addition PGCs express many

conserved germ line genes such as *Vasa, Nanos and Piwi* among different species suggesting that the development of PGCs uses similar molecular mechanisms during evolution (Extavour & Akam, 2003; Juliano et al., 2010; Liang et al., 1994). However, the molecular function of these conserved genes in PGC specification is poorly understood. In the past, *Drosophila*, *C. elegans*, and the mouse have been used as model organisms to understand the molecular mechanisms of germ cell specification. In this thesis, I used zebrafish as a model organism to investigate vertebrate germ cell specification as zebrafish combines the advantages of forward genetics as in *Drosophila* or *C. elegans* but is a vertebrate like the mouse.

1.3. Germline development in zebrafish

In zebrafish, PGCs are specified by the inheritance of maternal germ plasm (Figure. 3A). During oogenesis germ plasm is assembled in a huge ribonucleo-protein granule (RNP) also known as Balbiani body. The Balbiani body is assembled vegetal to the oocyte nucleus at the beginning of oogenesis (stage IB). Later during oogenesis in stage III oocytes, the Balbiani body is dispersed at the vegetal pole (Dosch, 2015; Kloc et al., 2014; Bontems et al., 2009; Heim et al., 2014; O.H. Kaufman and F.L. Marlow, 2017). The germ plasm comprises of maternally supplied RNAs, proteins, cell organelles like endoplasmic reticulum (ER), Golgi and mitochondria (Raz, 2003; Kloc et al., 2004; O.H. Kaufman and F.L. Marlow, 2017; Kloc et al., 2014; Marlow, 2015). After fertilization, vegetally localized germ plasm moves to the animal blastodisc during cytoplasmic streaming (Dosch, 2015).

Subsequent germ plasm positioning during early embryonic development has been demonstrated tracing molecular germ plasm markers such as *vasa*, *nanos3*, and *dazl* mRNA or Buc protein (Raz, 2000; Yoon et al., 1997; Braat et al., 1999; Hashimoto et al., 2004; Köprunner et al., 2001; Riemer et al., 2015). These molecular markers revealed that germ plasm localizes forming four spots at the distal end of the cleavage furrows after the first two cell cleavages (Figure. 3D).

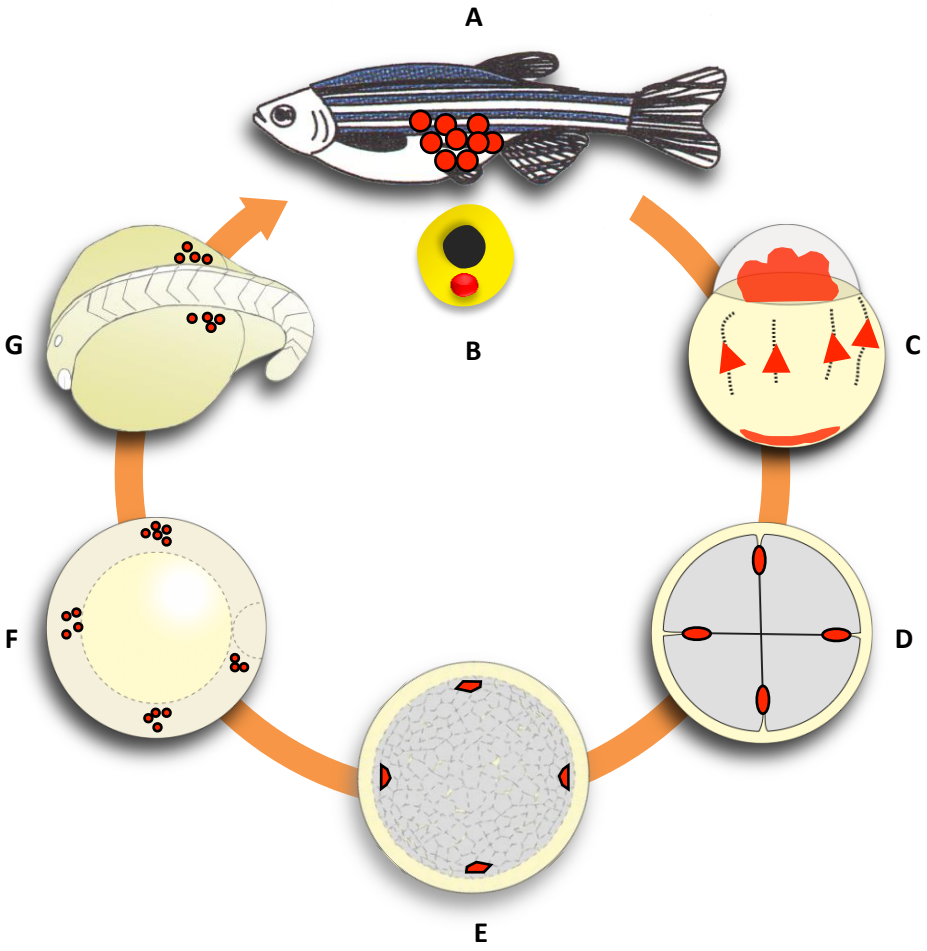

Figure 3: Germ line development of zebrafish.

(A) A female zebrafish with symbolized oocytes (red circles). (B) Stage I oocyte (yellow) with germ plasm/Balbiani body (red) vegetal to the nucleus (black). (C) Lateral view of fertilized egg, animal to the top. Red arrows indicate the migration of vegetal germ plasm to the animal blastodisc during cytoplasmic streaming. (D) Four-cell (grey) stage embryo, animal view. During the first two cleavages, germ plasm localizes to the distal region of the four cleavage furrows (red spots). However, no further germ plasm spots are formed during later stages. (E) 1k-cell embryo (3 hpf), animal view. This is approximately after the 10^{th} cell division with around 1000 cells. Only four out of 1000 cells inherited germ plasm during asymmetric cleavage. These blastomeres are specified as PGCs (red). (F) Embryo in the gastrula stage with four PGCs clusters. These PGCs then start to migrate during further embryonic development. The dotted line on the right side denotes the shield, the zebrafish Spemann's organizer. (G) Dorsolateral view of embryo at 15-somite stage, head to the left and back to the top. Migrating PGCs form two clusters at either side of the midline, where the prospective gonads form. During sexual maturation, PGCs eventually differentiate and mature into sperm in males, or oocytes in females (A) to start another generation

During subsequent cell divisions, germ plasm is asymmetrically inherited to one of the two daughter cells forming four cells with germ plasm at the 1'000-cell stage (3 hpf) (Figure. 3E). The other cells differentiate into somatic cells (Raz, 2003; Hashimoto et al., 2004; Riemer et al., 2015). After this embryonic stage of PGCs specification, germ plasm is symmetrically inherited between daughter cells during cell division forming four PGCs clusters (Figure. 3F). These PGCs then migrate to the prospective gonads (Figure. 3G) where they differentiate into mature male and female germ cells (Raz, 2000; Hashimoto et al., 2004; Dosch, 2015). Taken together, the inheritance of germ plasm into a subset of blastomeres during early embryogenesis is critical for the formation of PGCs, but also for the correct development of somatic tissues like neurons or the cardiovascular system.

1.4. Germ plasm is critical for the formation of PGCs

Intriguingly, many studies have shown that germ plasm plays a pivotal role for the formation of PGCs. For example, Ultraviolet (UV) irradiation of the vegetal pole of early anuran amphibian embryos *Rana* and *Xenopus*, led to complete absence of PGCs in the descendent tadpoles (Ikenishi et al., 1974; Smith, 1966; Tanabe & Kotani, 1974). Further, surgically removal of vegetal germ plasm from *Xenopus* fertilized eggs caused to form sterile tadpoles (Buehr & Blackler, 1970) demonstrating that germ plasm is essential for PGC development.

By contrast, microinjection of aspirated and purified germ plasm into UV-irradiated fertilized *Rana* eggs (Wakahara, 1977) and transplantation of *Xenopus* blastomeres containing microinjected germ plasm form PGCs in tadpoles (Ikenishi et al., 1986) demonstrating that germ plasm is sufficient to induce PGC development. Also, transplantation of EGFP labeled *Xenopus* germ plasm into animal blastomeres induced viable ectopic PGCs (Tada et al., 2012).

Similarly, after transplantation of *Drosophila* posteriorly localized pole plasm into the anterior end, recipient embryos form ectopic PGCs which are morphological and functionally similar to that of endogenous PGCs (Illmensee & Mahowald, 1974). In addition, removal of

cytoplasm containing germ plasm components at the ends of the cleavage furrows of four-cell stage zebrafish embryos resulted in a severe reduction in the number of germ cells (Hashimoto et al., 2004). Collectively, these results suggest that maternally deposited germ plasm factors are indispensable for the formation of PGCs in different animal species. These data also initiated several studies to identify the molecular nature of germ plasm components, which are necessary for the formation of PGCs.

1.5. Roles of known germ plasm components during germ cell specification

Germ plasm components required for germ plasm assembly and PGCs formation are well studied in *Drosophila*. For instance, *Oskar,* which is originally discovered from a genetic screen for maternal-effect posterior group genes in *Drosophila* is recognized as a gene necessary to assemble the germ plasm and germ cells at the posterior pole of the oocyte (Figure. 4B) (Lehmann & Nüsslein-Volhard, 1986; Ephrussi, Anne; Lehmann, 1992). Further, it has been discovered that the overexpression of *oskar* mRNA to the anterior pole of the oocyte was sufficient to form ectopic germ plasm and functional germ cells at the anterior pole of the oocyte (Figure. 4C) (Smith et al., 1992; Ephrussi et al., 1991).

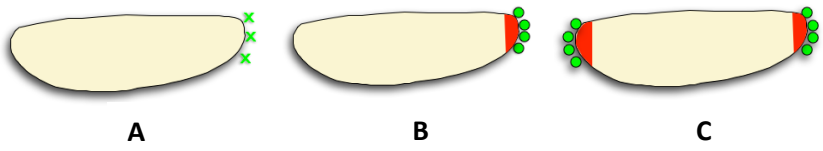

Figure 4: Drosophila Oskar is sufficient and necessary for germ cell formation.

All embryos are at stage 5 and shown in lateral view, anterior to the left. (A) *Oskar* mutant embryos do not assemble germ plasm and therefore do not form PGCs (green x). (B) In wild-type, Oskar assembles germ plasm at the posterior pole (red) and induces PGCs. (C) Ectopic expression of Oskar at the anterior pole forms extra germ plasm and thus induces ectopic PGCs.

In addition, the other germ plasm components such as Vasa, Staufen, Tudor and Valois have also been identified as essential genes for the assembly of germ plasm and germ cell formation in *Drosophila* (Schüpbach & Wieschaus, 1986). *Drosophila* Vasa mutants fail to assemble germ plasm and hence, no PGCs form (Styhler et al., 1998; Lasko & Ashburner,

1988; Tomancak et al., 1998; Schupbach & Wieschaus, 1986). Further, Vasa has been recognized as a translational regulator for *gurken* mRNA in oocytes and *Mei-P26* mRNA in the ovary (Johnstone & Lasko, 2004; Tomancak et al., 1998; Liu et al., 2009).

Moreover, *Drosophila* Vasa interacts with Piwi-interacting RNAs, piRNAs, to maintain the genome integrity of germ cells by silencing transposons (Pek et al., 2012; Xiol et al., 2014). *Drosophila* females mutant for *tudor* also abolish germ cell formation due to the failure of germ plasm assembly (Boswell & Mahowald, 1985). The *Drosophila* RNA binding protein Staufen, which was identified in a genetic screen for the posterior group genes, is essential for the localization of *osk* mRNA to the posterior pole of the oocyte (Schüpbach & Wieschaus, 1986; Ephrussi et al., 1991; Kim-Ha et al., 1991; St Johnston et al., 1991). These data conclude that the germ plasm components are essential for the assembly of germ plasm and also ochestrate germ cell formation.

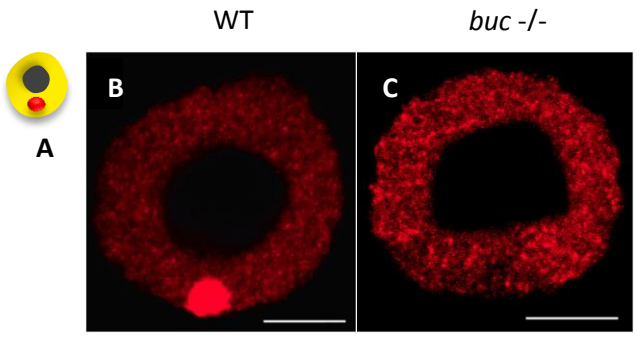

Figure 5: Buc is required to organize germ plasm in zebrafish.

(A) A cartoon of a lateral view of a stage I oocyte (yellow) showing germ plasm (Balbiani body; red) vegetal to the nucleus (dark grey). (B) Lateral view of stage I wild-type oocyte. Fluorescent *in-situ* hybridization against germ plasm marker, *nanos3* mRNA highlights aggregated germ plasm (red) vegetal to the nucleus (black circle). (C) *Buc* mutants are unable to organize germ plasm but instead *nanos3* mRNA is dispersed ubiquitously in the ooplasm (red patches). Scale bar is 500 µm. This image modified from (Bontems *et al.*, 2009).

1.6. Bucky ball is a novel vertebrate specific germ plasm organizer protein

The germ plasm organizer *bucky (buc) ball* gene was discovered in a forward genetic maternal-effect screen in zebrafish (Dosch et al., 2004; Wagner et al., 2004). Oocytes produced by *buc* mutant females do not have a properly aggregated Balbiani body; instead, the RNP granules are ubiquitously dispersed in the ooplasm (Figure 5). This interprets *buc* as the first gene which is necessary for Balbiani body formation in vertebrates (Dosch et al., 2004; Bontems et al., 2009). Moreover, *buc* mutant oocytes and eggs exhibited a defect in animal-vegetal polarity (Dosch et al., 2004; Florence L. Marlow and Mary C. Mullins, 2008) (Figure 6). Therefore, embryos with polarity defects do not develop beyond the one-cell stage (Dosch et al., 2004).

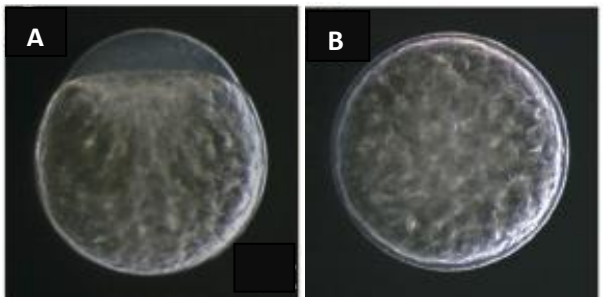

Figure 6: Phenotype of *buc* wild-type and *buc* mutant embryos.

buc mutants show a defect in embryonic animal-vegetal polarity. (A) In the wild-type embryo, the blastodisc is formed at the animal pole due to cytoplasmic streaming. (B) The b*uc* mutant embryo does not form blastodisc at the animal pole, instead cytoplasm radially accumulates around the central yolk. Embryos at 30 (minutes post fertilization) mpf are shown with animal to the top. This image modified from Dosch et al. (2004).

Mapping the isolated *buc* mutation to the genome and positional cloning of the Buc cDNA revealed a novel gene in zebrafish (Bontems et al., 2009). Examining the conservation of the *buc* gene by BLAST searches and synteny identified homologous sequences for Buc in all vertebrate classes such as fish, amphibian, birds and mammals (Bontems et al., 2009). Further, alignment of 15 Buc related proteins from different vertebrates discovered two highly conserved N-terminal sequence motifs within the conserved BUVE motif (Krishnakumar et al., 2018) (Figure. 7).

In addition to BUVE motif, the same sequence alignment identified another conserved motif, which shows higher sequence conservation corresponding to amino acid 372-394 (Figure 7). However, the function of this highly conserved motif in Buc is still unknown. Therefore, Buc represents a novel vertebrate specific protein with powerful biological activities whose biochemical function still needs to be uncovered (Bontems et al., 2009).

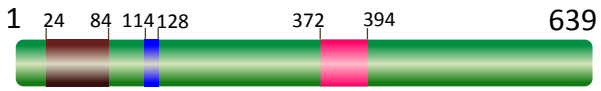

Figure 7: Schematic representation of evolutionary conserved motifs in Buc.

Buc protein (green bar) contains three conserved motifs. The N-terminal BUVE motif (amino acid 23 - 136) comprises two sub motifs encoding amino acid 24-84 (brown box) and 114-128 (blue box) and the highly conserved motif encoding amino acid 372-394 (pink) adopted from (Krishnakumar et al., 2018)

1.7. Buc mirrors the dynamic localization of germ plasm

Using a novel anti-Buc antibody, we labeled the germ plasm of zebrafish (Riemer et al., 2015). In wild-type oocytes, anti-Buc antibody specifically recognized the Balbiani body (Figure 8A) but not the mutant *bucP*^{106} (Figure 8B).

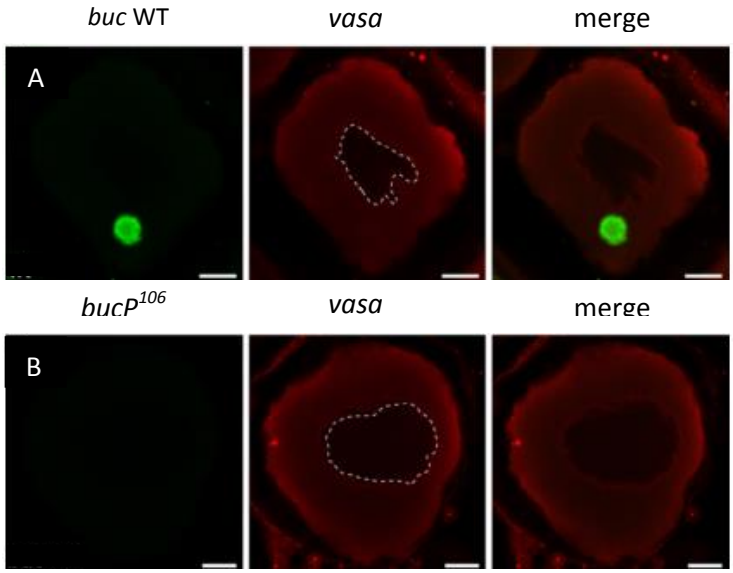

Figure 8: Anti-Buc antibody specifically recognize Buc.

Upper and lower panel shows the lateral view of **s**tage IB oocytes, animal to the top. (A) Anti Buc antibody recognizes the Buc protein in the Balbiani body (green) but not mutant BucP^{106} (B). (C) Besides, perinuclear Vasa is not changed. Nuclear is demarcated in dashed line. Scale bar 10 µm. (adopted from (Riemer et al., 2015).

Further, dynamic of germ plasm localization have been investigated labeling germ plasm using anti-Buc antibody (Figure 9) (Riemer et al., 2015).

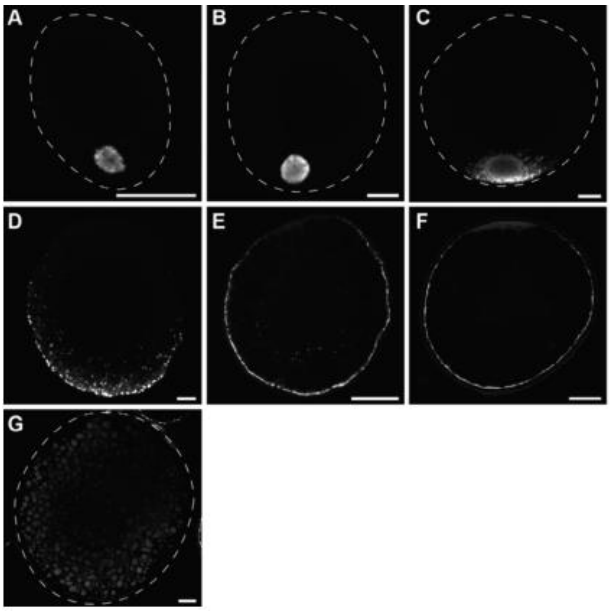

Figure 9: Dynamic of Buc localization during oogenesis

Images represent the lateral view of stage IA (A), early IB (B), late IB (C, D), early II (E), late II (F) and III (G), animal to the top. Buc protein is labeled with anti-Buc antibody (white). During oogenesis, Buc localizes with the germ plasm to the vegetal pole. Stippled line is denoted outline of oocytes. Scale bar 10 µm. This image modified from (Riemer et al., 2015)

.

In addition, overexpression of *buc-GFP* mRNA into early oocyte revealed that Buc localizes to the Balbiani body and later in oogenesis, Buc actively localize more to the vegetal pole of the oocyte. Similarly, overexpression of *buc-GFP* mRNA into once-cell stage embryos divulged that Buc-GFP aggregate in the four cleavage furrows at the eight-cell stage (Bontems et al., 2009). Fascinatingly, Buc-GFP transgenic fish are reminiscent of the overexpression results. (Figure 10) (Riemer et al., 2015). Therefore, Buc mirrors the dynamic of germ plasm localization during oogenesis and early embryogenesis, which is consistent with its function as a germ plasm organizer.

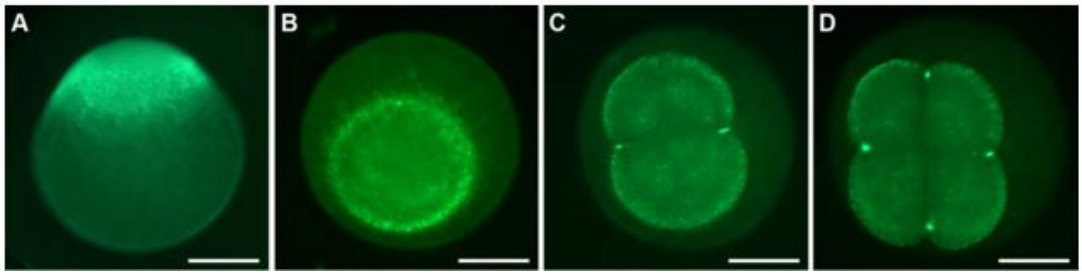

Figure 10: Buc-GFP transgenic embryos mimics the dynamics of germ plasm localization.

One-cell stage embryos show fluorescent blastodics (A: lateral view, B: animal view). At the two-cell stage (B: animal view) and four-cell stage (D: animal view) germ plasm localize to the distal cleavage furrow. Scale bar 200 µm. (adopted from (Riemer et al., 2015)**.**

1.8. Buc induces ectopic germ cells after injection of mRNA into a somatic cell

As mentioned above, *buc-GFP* overexpression leads to its aggregation at four spots at the eight-cell stage. Beyond the eight-cells stage, the spots remain as four foci until high stage suggesting that Buc specifies germ cells in vertebrates (Bontems et al., 2009). Indeed, the germ cell induction assay (16-cell assay) revealed that Buc expression in a somatic cell induces ectopic formation of germ cells during early embryogenesis (Bontems et al., 2009) (Figure 11). Such an *in vivo* activity was hitherto not described for any vertebrate gene.

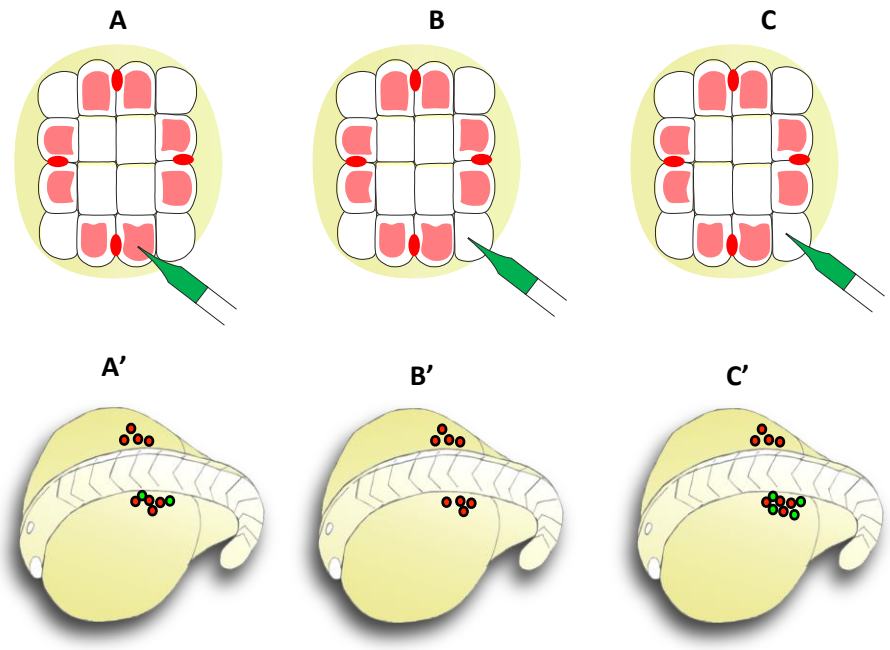

Figure 11: Schematic illustration of germ cell induction assay.

Upper panel (A-B) shows embryos at the 16-cell stage (animal view) with localized germ plasm (red oval) together with potential to form future PGCs (middle blastomeres in light red). After injection (green needle tip), embryos were examined for germ cells after 15-18 somite stage. Lower panel (A'-C') illustrates the activity of the germ cell reporter (green) in an 18-somite stage embryo (dorsolateral view, anterior to the left). (A) Injection of PGC reporter (*GFP-nanos3-3'UTR* mRNA; citation) into a middle cell as a positive control and (A') embryos show a fraction of endogenous germ cells positive for PGC reporter (green circles) next to unlabeled germ cells (red circle; invisible in the experiment). (B) Injection of reporter RNA into a somatic, corner blastomere as a negative control leads to embryos (B') without fluorescent PGCs but endogenous germ cells (red circles). (C) Injection of reporter RNA together with *buc* mRNA into a somatic, corner blastomere leads to embryos (C') whose somatic cells are reprogrammed into extra PGCs (green circles) in addition to the endogenous germ cells (red).

1.9. Oskar Induces germ cells in zebrafish

After localization to the posterior pole of the oocyte, *Drosophila* oskar mRNA is translated into two isoforms, Long (lOskar) and Short Oskar (sOskar) (Vanzo & Ephrussi, 2002). However, only sOskar is responsible for the assembly of germ plasm and formation of germ cells whereas lOskar anchors *oskar* mRNA and sOskar protein at the posterior pole (Vanzo & Ephrussi, 2002).

As stated, Buc is a vertebrate specific novel protein without having any sequence homology for other proteins with known functions (Riemer et al., 2015). Thus, understanding the

molecular function of Buc in germ cell specification is a great challenge. Thus, finding a protein in which the genetic function is evolutionary conserved provide an alternative approach to investigate function of a novel protein (Jensen et al., 2003). Therefore, our lab used an innovative approach in which Oskar was used as a functional homolog without related amino acid sequence to investigate the function of Buc in germ cell specification (Bontems et al. 2009).

Fascinatingly, overexpression of *Drosophila sOskar* mRNA (amino acid 139-606) induces ectopic germ cells in the zebrafish germ cell induction assay (Figure 12C), whereas mutant sOskar (*osk*^{84}*,* amino acid 139-254) was unable to induce ectopic germ cells (Krishnakumar et al., 2018). This result is reminiscent of the overexpression of wild-type (amino acid 1-639) and mutant *buc* (*buc*^{p43} amino acid 1-362) mRNA. In this assay, wild-type *buc* mRNA induced ectopic germ cells but not mutant *buc* (Bontems et al., 2009; Krishnakumar et al., 2018). Both *osk*^{84} *and buc*^{p43} mRNA have the identical nucleotide sequence to wild type with only one nucleotide change generating a premature STOP codon (Kim-Ha et al., 1991; Bontems et al., 2009). This reveals that Buc and sOskar but not their RNA is sufficient for germ cell induction.

Surprisingly, Oskar and Buc do not share sequence homology although they perform the same biological activity (Krishnakumar et al., 2018). Therefore, these results reveal for the first time the functional equivalence of two germ plasm organizers in germ cell specification without sequence homology (Krishnakumar et al., 2018). More importantly, these results suggest that sOskar and Buc use a similar biochemical mechanism to induce germ cells in zebrafish.

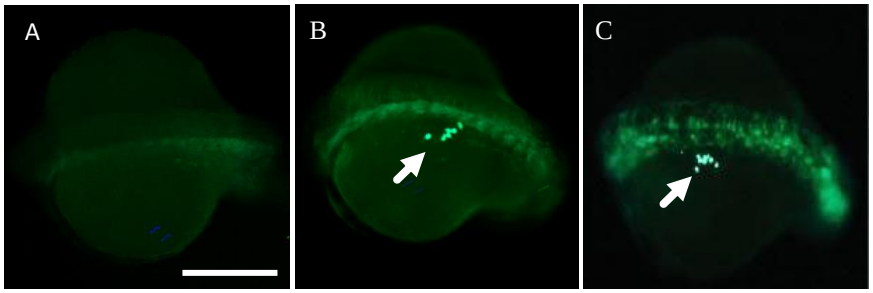

Figure 12: Buc and Oskar in germ cell induction assay.

Dorsolateral view of living embryos at 15-18 somite stage, anterior to the left. (A) Injection of PGC reporter (*GFP-nano3-3' UTR*) into a corner blastomere does not induce extra germ cells. Co-injection of reporter together *buc* (B) or *soskar* mRNA (C) induces extra fluorescent germ cells (green, white arrow).

1.10. Buc and Oskar share conserved biochemical interaction during germ cell specification

As described previously, proteins with similar amino acid sequences share a similar biological function. Surprisingly, we showed functional equivalence between *Drosophila* sOskar and zebrafish Buc even though they do not share sequence homology. Nonetheless, this result postulates that both sOskar and Buc likely share similar biochemical interactions during the formation of germ cells. Oskar binds to Smaug, Valois and Vasa proteins (Dahanukar et al., 1999; Anne, 2010; Breitwieser et al., 1996). Especially the direct Vasa - Oskar binding has been a major focus, because this interaction is essential for germ plasm assembly and germ cell specification (Breitwieser et al., 1996; Jeske et al., 2015).

1.11. The RNA helicase Vasa is a key player in germ cell specification

Vasa was originally discovered from a genetic screen for maternal-effect genes in *Drosophila* required for the formation of germ cells (pole cells) and abdominal segments (Schupbach & Wieschaus, 1986). Thereafter, Vasa has been identified as a conserved germ cell specific protein in variety of animal taxa such as sponges, cnidarians, flatworms, annelids, nematodes, echinoderms, tunicates, mollusks, insects, crustaceans, fish, amphibians, reptiles, birds, and mammals (Hickford et al., 2011). As a result of this conservation, Vasa is used nowadays as a universal marker for germ cell lineage (Gustafson & Wessel, 2010; Hickford et al., 2011; Raz, 2003). Functionally, Vasa, aka DDX4 (DEAD [Asp-Glu-Ala-Asp] box polypeptide 4), is an ATP-dependent RNA helicase belonging to the DEAD box protein family (Linder, 2006; Hickford et al., 2011).

1.12. Structural characteristics of Dead box helicases

DEAD box family RNA helicases form the largest helicase family and are found in all three kingdoms of life *i.e.* Bacteria, Archea and, Eukaryotes (Jankowsky, 2011). Essentially, these helicases participate in nearly all aspects of RNA metabolism such as transcription, translation initiation, ribosome biogenesis, splicing, RNA editing, RNA export from the nucleus, and RNA degradation. In these processes, RNA helicases remodel higher-order RNA

secondary or tertiary structures and RNA-protein complexes in an ATP dependent manner (Jankowsky, 2011; Linder, 2006; Linder & Lasko, 2006; Popovic et al., 2019; Linder & Jankowsky, 2011).

DEAD box RNA helicases share a structurally highly conserved helicase core, which comprises of almost two identical RecA like domains. Each RecA like domain resembles that of bacterial recombination protein RecA and is connected by a flexible linker, which supports conformational changes of the helicase core during their catalytic activity (Linder, 2006; Jankowsky, 2011; Linder & Jankowsky, 2011). In addition, this protein family shows variable C- and N-terminal extensions on either sides of the helicase core which facilitates binding for additional protein-protein interactions (Linder & Jankowsky, 2011; Sloan & Bohnsack, 2018). The helicase core possesses at least 12 characteristic sequence motifs, which provide binding sites for ATP and RNA (Figure. 13) (Sloan & Bohnsack, 2018; Linder & Jankowsky, 2011; Linder & Lasko, 2006). Motifs I, Ia, Ib, II, and III are located in the N-terminal RecA-like domain (NTD) while motifs IV, V, and VI are located in the C-terminal domain (CTD) (Caruthers & McKay, 2002; Hickford et al., 2011). The motif II, which harbors the conserved four amino acids, Asp-Glu-Ala-Asp, led to the designation “DEAD box” for this protein family (Linder & Jankowsky, 2011).

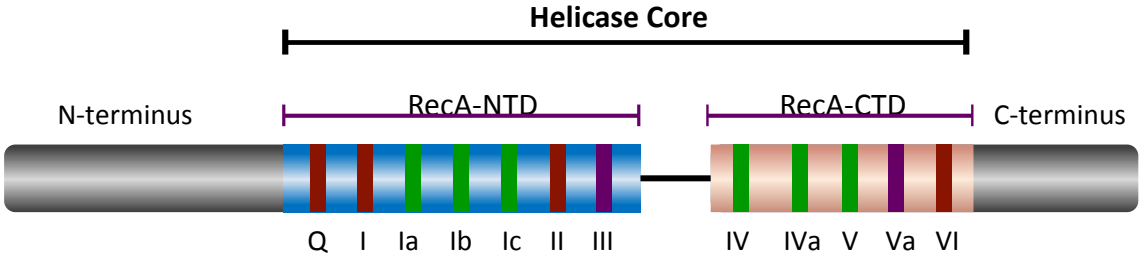

Figure 13: Schematic illustration of general features of DEAD box RNA helicase.

Dead box RNA helicases comprise a highly conserved helicase core. The Helicase core contains two RecA-like domains, RecA-NTD (Blue) and RecA-CTD (Salmon), which are connected with a flexible linker sequence (black line). Either side of the helicase core has N- and C-terminal flanking sequences (grey). Conserved sequence motifs located in each RecA-like domain are shown as horizontal colored boxes according to their primary functions, such as ATP binding and hydrolysis motifs (brown), RNA binding motifs (green) and motifs for communication between ATP binding and duplex unwinding (purple). This image modified from (Jankowsky, 2011).

1.13. Buc interacts with zebrafish Vasa during germ cell specification

It has been shown that the Oskar-Vasa interaction is required to promote efficient *oskar* mRNA translation and phosphorylation of Oskar protein (Breitwieser et al., 1996). Further, it has also been reported that the LOTUS domain of Oskar directly binds the RecA like C-terminal domain of *Drosophila* Vasa. The binding of the LOTUS domain stimulates the ATPase activity of Vasa (Jeske et al., 2017, 2015)

Analysis of the Buc interactome using mass spectrometry discovered that zebrafish Vasa is highly enriched in the Buc-GFP pull-down assay (Krishnakumar et al., 2018). This enrichment suggests that Buc and Vasa might also interact with each other. Co-immunoprecipitiation indeed indicates that Buc and Vasa interact *in vivo* during germ cell specification confirming the mass spectrometry data (Figure. 14) (Krishnakumar et al., 2018). Further, it has been demonstrated that Buc and Vasa localization overlaps in the germ plasm during early embryogenesis including the period of germ cell specification (Krishnakumar et al., 2018). In chicken, it has been shown that overexpression of the Vasa homologue, Cvh reprograms embryonic stem cells to PGCs (Lavial et al., 2009). This data raised the hypothesis that Vasa has a critical role during germ cell specification in zebrafish. Indeed, overexpression of *vasa* mRNA in the zebrafish germ cell induction assay revealed that Vasa also induces ectopic germ cells identifying Vasa as the second protein with a germ cell specification activity (Krishnakumar et al., 2018).

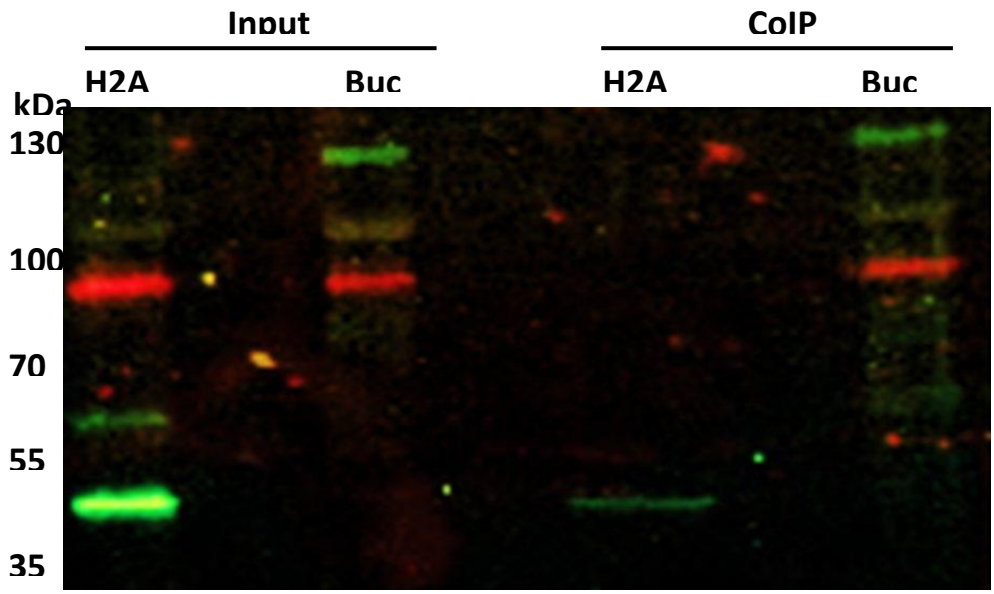

Figure 14: Buc interacts with Vasa during germ cell specification.

Western-blot after co-immunoprecipitation has been performed using Buc-GFP transgenic embryos. H2A-GFP transgenic line used as a control. Embryos at 3 hpf have been collected from both fish line. GFP pulldown assay has been performed after lysing cells. Input samples show the expression of H2A-GFP (42 kD, green band), Buc (130 kD, green band) and Vasa (80 kD, red band) presence in the sample. However, co-immunoprecipitation samples show only Buc-GFP pulldown Vasa but not H2A-GFP.

1.14. *Drosophila* Oskar interacts with zebrafish Vasa *in vitro*

With aforementioned findings, it is reasonable to hypothesize that ectopic germ cell formation by sOskar is mediated through zebrafish Vasa. To explore that, the coding sequence of sOskar fused to GFP (sOskar-GFP) and zebrafish Vasa were transcribed and translated in a cell free system followed by GFP pulldown assay. Results showed that sOskar interacts with zebrafish Vasa *in vitro* (Figure 15) supporting to the aforementioned hypothesis (Krishnakumar et al., 2018).

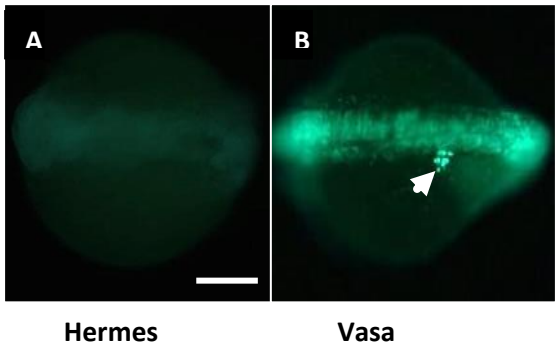

Figure 15: Vasa induce ectopic germ cell in zebrafish.

Dorsolateral view of embryo at 15-18-somite stage, animal to the left (A) Injection of Buc interacting protein, Hermes (Heim et al., 2014) into the corner blastomere in 16 cell stage embryos does not induce germ cells. (B) Injection of vasa mRNA into the corner cell induces ectopic germ cells (white arrow). Scale bar is 100 µm.

1.15. Similarity between Buc and Oskar

Buc is recognized as a novel vertebrate specific protein while Oskar was exclusively found in invertebrates like *Drosophila* (Bontems et al., 2009). Although Buc and Oskar do not share sequence homology, it seems that they have common biochemical functions. For instance, both proteins organize germ plasm and play a crucial role in germ cell formation. Mutant alleles of both proteins end up with a failure in germ plasm assembly and polarity defects in oocytes and embryos. In addition, Buc and Oskar can induce ectopic germ cells. Moreover, both Buc and Oskar interact with Vasa *in vivo* and in *vitro* (Jeske et al., 2015; Krishnakumar et al., 2018; Jeske et al., 2017). In addition, Buc and Oskar are composed of low complexity sequences hence predicted as intrinsically disordered proteins (Figure 16).

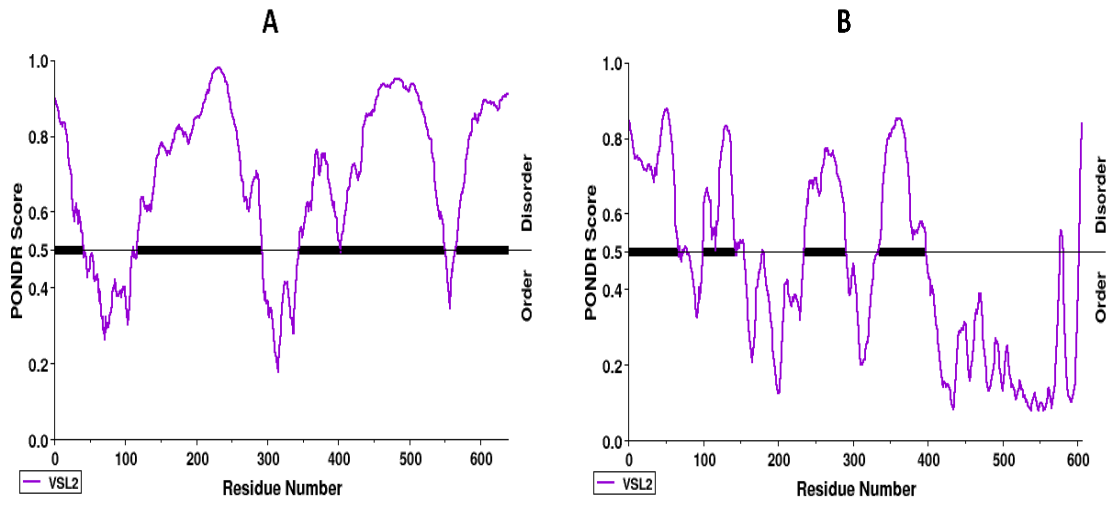

Figure 16: Buc and Oskar are intrinsically disordered proteins.

Intrinsically disordered properties of Buc (A) and Oskar (B) predicted using PONDR protein disorder predictor using VSL2 algorithm. Y-axis represents the generated disordered PONDR score. X-axis represents the number of amino acids for a given protein. Threshold value between ordered and disordered protein considered as 0.5 (thick horizontal black line). Distribution of the disordered and ordered properties are representing in purple colour. Protein regions above the threshold value are ordered while regions below the threshold value are disordered.

1.16. Objectives

Overexpression of Oskar in zebrafish induces ectopic germ cell formation. However, Buc and Oskar do not share sequence homology (Krishnakumar et al., 2018). This shows for the first time that two evolutionary distance proteins with no sequence homology perform equivalence biochemical function in germ cell specification (Krishnakumar et al., 2018). Therefore, we speculated Buc and Oskar have a conserved interactome in germ cell specification. To that end, it is revealed that Buc and Oskar interact with Vasa, a highly conserved germ plasm component across species, during germ cell specification. Interaction between Oskar and Vasa is exclusively characterized by different aspects. For example, it has been discovered that the LOTUS domain of Oskar physically binds to RecA like C-terminal domain of *Drosophila* Vasa (Jeske et al., 2017). Moreover, it has also been shown that Oskar LOTUS domain stimulates Vasa ATPase activity upon their interaction (Jeske et al., 2017). As Buc and Oskar are equivalent in function, I hypothesized that Buc and zebrafish Vasa are likely to perform similar biochemical function during germ cell specification. Thus far, there

is no known protein motif in Buc which interacts with Vasa or *vice versa*. Furthermore, no known biochemical activity is annotated to Buc apart from Buc as a scaffolding protein bringing together RNA binding proteins such as Hermes (Heim et al., 2014). Therefore, the aim of this work is to characterize the Buc and Vasa interaction during germ cell specification with following objectives.

I. Determine whether Buc and Vasa directly bind during germ cell specification

In vitro co-immunoprecipitation data and *in vivo* BiFC data clearly show that Buc interacts with Vasa during germ cell specification. So far, there are no studies characterizing Buc and Vasa interaction during zebrafish germ cell specification. Therefore, there is no any known protein motif has been identified in Buc which might interact with Vasa or vice versa. To that end, in this study, I will map Buc and Vasa binding motifs namely, Buc-Vasa binding motif (Buc-VBM) and Vasa-Buc binding motif (Vasa-BBM).

II. Investigate the structural changes upon Buc-Vasa interaction

From the recently published data, it is known that the LOTUS domain of Oskar interacts with RecA-like C-terminal domain of *Drosphophila* Vasa, and activates the Vasa ATPase activity upon interaction (Jeske et al., 2017). Consistent with this notion, I hypothesize that Buc induces zebrafish Vasa ATPase activity. Moreover, as described Buc and Oskar do not share sequence homology. Therefore, it is reasonable to postulate that both proteins perform equivalent functions adopting structural similarity. Importantly, it has been identified that eLOTUS domain of Oskar adopts a secondary structure α helix from its disordered state during interaction with *Drosophila* Vasa. Thus, I will investigate whether Buc performs the same structural changes during interaction with zebrafish Vasa.

III. Investigate regulation of Buc-Vasa interaction *in vivo*

It has been shown that the *Dosophila* Vasa localization to the posterior pole is dependent on Oskar protein (Breitwieser et al., 1996). Recently, it has been revealed that Oskar directly bind to Vasa and activates its ATPase activity (Jeske et al., 2017). In addition, it has been shown that Vasa mutant (*vasa⊿617*) unable interact with Oskar as wild-type counterpart and also *vasa⊿617 embryos* do not show germ cells (Johnstone & Lasko, 2004). These data suggest that the Oskar is upstream to Vasa during germ cell specification. As Buc and Oskar

are equivalence in function, probably Buc could be upstream to Vasa during germ cell specification. Thus, it is necessary to understand regulation of Buc and Vasa interaction during germ cell specification. Therefore, after identification of Buc-VBM and Vasa-BBM, first I will investigate requirement these motifs during germ cell specification in vivo generating mutations and deletion constructs for Buc and Vasa interaction motifs. Finally, these data will facilitate to understand the hierarchy of germ cell specification pathway in zebrafish.

2. Results

2.1. Mapping the Vasa binding motif (Buc-VBM) in Buc

Previously, we showed that Buc interacts with Vasa during the period of germ cell specification using co-immunoprecipitation. Therefore, I started to map the Buc and Vasa interaction domains using the same approach. To that end, I systematically truncated Buc and fused with GFP to the C-terminus of each fragment. Each GFP fusion fragment and full-length of Vasa proteins were transcribed and translated *in vitro* followed by GFP-pull-down assay. In my results, I observed that all Buc constructs I investigated interact with Vasa suggesting the lack of specificity in Buc and Vasa interaction with *in vitro* GFP-pull-down assay. This interaction pattern remains the same even after I performed many optimization for example, changing washing buffer, salt concentration of buffers, detergent type and its concentration, incubation time of GFP beads with samples Therefore, I switched to bimolecular fluorescence complementation assay (BiFC) as an alternative approach to investigate Buc and Vasa interaction *in vivo*. The BiFC assay is based on the reconstitution of an intact fluorescent protein complex if two complementary non-fluorescent fragments are brought in close proximity by two interacting proteins upon their expression in living cells (Kerppola, 2006, 2008) (Figure 17).

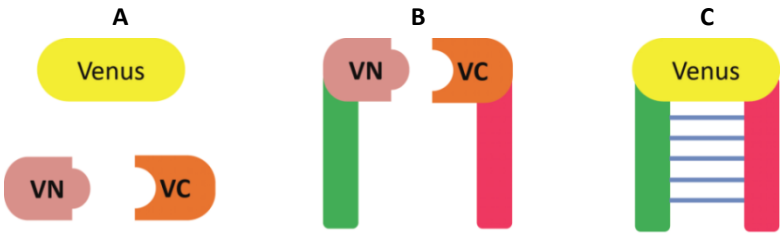

Figure 17: Schematic illustration of bimolecular fluorescence complementation assay (BiFC) assay.

(A) Venus protein (yellow) is split into two non-fluorescent parts, Venus N-terminus (VN; rose) and Venus C-terminus (VC; orange). (B) Target proteins are fused with VN- and VC-fragments (protein A; green and protein B; pink). (C) Association of protein A and B (horizontal blue lines) reconstitute a functional Venus protein forming a bimolecular fluorescent complex. This image modified from (Roshan Perera and Roland Dosch, submitted 2020).

Therefore, I fused Venus protein C-terminus (VC) to the both N-and C-terminus of Buc and Venus N-terminus (VN) to the N- and C-terminus of Vasa. After co-injection of Buc and Vasa

constructs into one-cell stage embryos, Buc-VC + Vasa-VN combination showed higher number of fluorescent positive embryos (79.4%) (Figure 18B) while VC-Buc + VN-Vasa combination showed a smaller number of fluorescent positive embryos (48.6%) (Figure 18E). Compared to above combinations, neither Buc-VC + VN-Vasa combination (Figure 18C) nor VC-Buc + Vasa-VN combination (Figure 18D) showed fluorescent embryos at 3 hpf. Collectively, these results suggest that the BiFC assay as a promising alternative to investigate the Buc and Vasa interaction *in vivo*. Besides, the results also provide some clues suggesting that the Buc and Vasa interaction motifs probably located in the C-terminal region of both proteins as the Buc-VC and Vasa-VN combination showed the highest number of fluorescent positive embryos. Therefore, I continued domain-mapping experiments fusing VC and VN fragments to the C-terminus of truncated Buc and Vasa constructs.

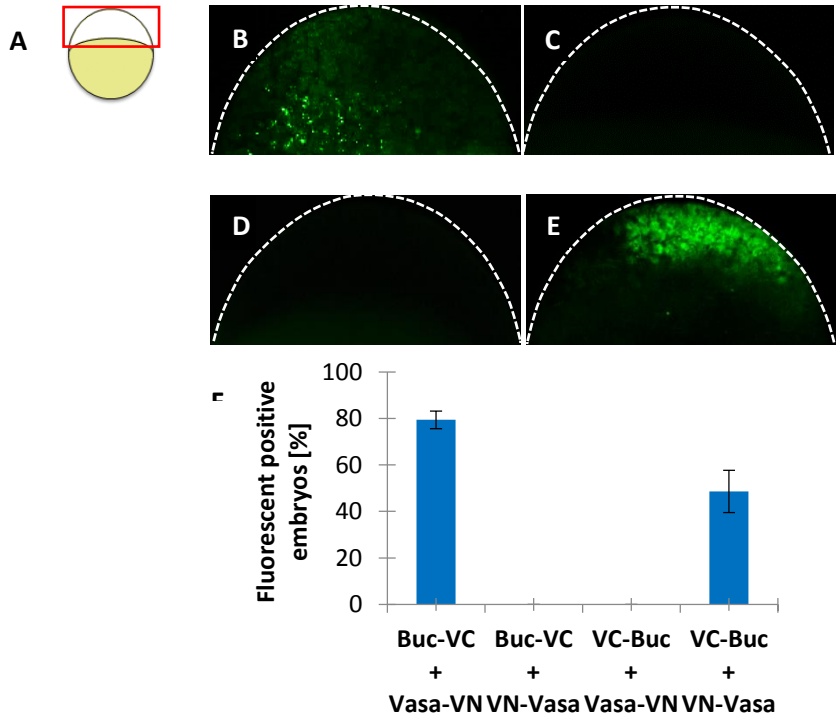

Figure 18: Buc and Vasa interact *in vivo* during germ cell specification.

(A) A cartoon illustrates the lateral view of embryos at 3 hpf, animal to the top. Confocal imaging area boxed in red. (B) Co-injection of Buc-VC and Vasa-VN showed fluorescent signal at the blastodisc (79.4 ± 3.8%, n = 80). Co-injection of Buc-VC with VN-Vasa (0 ± 0%, n = 73) in (C) and VC-Buc with Vasa-VN (0 ± 0%, n = 80) in (D) did not show a fluorescent signal. (E) Co-injection of VC-Buc with VN-Vasa showed fluorescence in the blastodisc (48.9 ± 9.6%, n = 66). (F) Quantification of fluorescent positive embryos based on the different combination of BiFC Buc and Vasa constructs. The data presented are averaged from three independent experiments. Y-axis represents percentage of fluorescent positive embryos from three independent experiments. X-axis represents injected constructs. Error bars represent standard deviation of the mean. Scale bar 100 µm.

Initially, I cloned BiFC expression vectors using traditional restriction enzyme-based cloning method. This method become troublesome, if I need to clone many truncated Buc and Vasa construct during interaction domain mapping. In recent years, recombination-based Gateway® cloning vectors have been developed to investigate robust and efficient gene functions (Kwan et al., 2007; Villefranc et al., 2007; Miles & Verkade, 2014). Therefore, to reduce the workload, I developed four Venus-BiFC Gateway adapted destination vectors (Roshan Perera and Roland Dosch submitted, 2020) (Figure. 19). These vectors are not only suitable for transcription of mRNA, but also allow to rapidly investigating interactions in tissue culture systems (Dr. Lukasz Smorag, Institute of Human Genetics, personal communication).

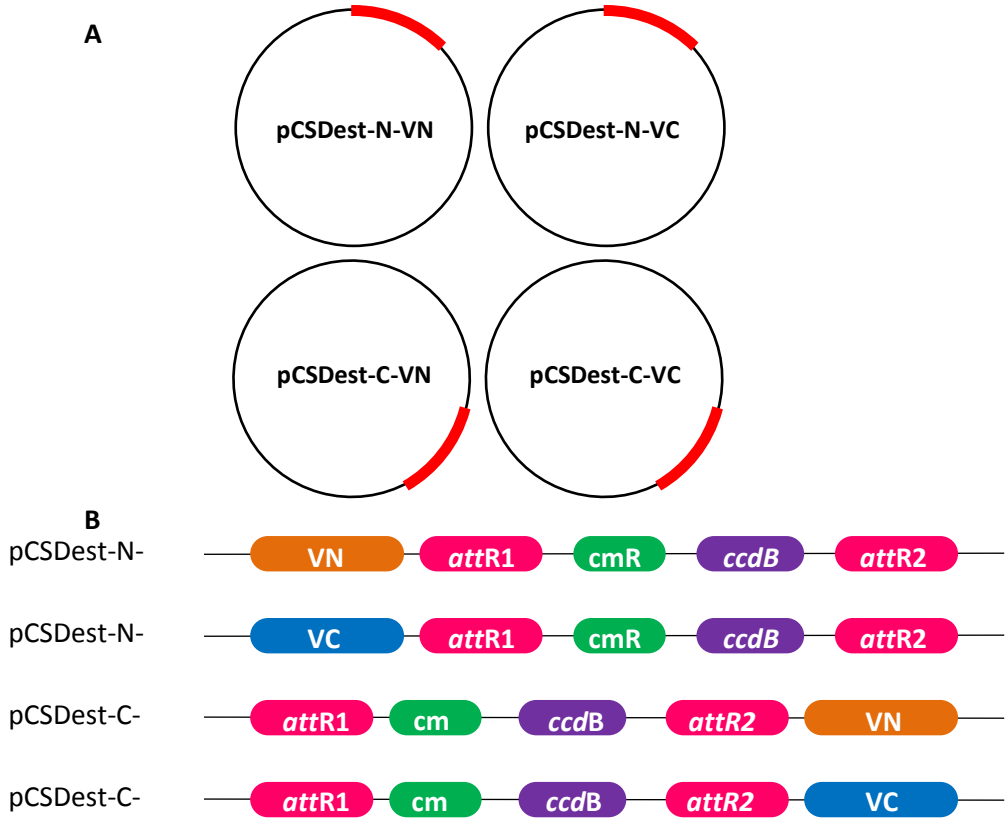

Figure 19: Expression Vector maps and key core elements of BiFC gateway destination vectors.

(A) Vector maps of four different BiFC gateway destination vectors, pCSDest N-VN, pCSDest N-VC, pCSDest C-VN, pCSDest C-VC. Black line represents the vector backbone and region colored in red represent the core features of the vector described in B. (B) The vectors comprise all features of the core cassette of gateway pCSDest destination vector for recombination reaction (Villefranc et al. 2007). The core gateway cassette contains two *att*R sites; *att*R1 and *att*R2 (pink) flanking the bacterial toxin gene *ccd*B (purple) for selection and the chloramphenicol resistance gene, cmR (green). Venus VN (orange) and VC (blue) are fused to the N-terminus of the core cassette to generate pCSDest N-VN or pCSDest N-VC while VN and VC are fused to the C-terminus of the core cassette to generate pCSDest C-VN or pCSDest C-VC BiFC destination vectors.

As described, Buc is predicted as an intrinsically disordered protein (Figure 16). Thus, after expressing recombinant protein in *Escherichia coli*, Buc is found in the insoluble pellet fraction but not in the soluble fraction. The recombinant Buc protein is highly aggregated and therefore, present in the pellet fraction as IDPs have a higher tendency to form hydrogen bonds, many electrostatic interactions via charged amino acids between proteins (Linding et al., 2004). Therefore, it is a great challenge to use full length of recombinant Buc protein to find out its structural features and biochemical functions. Alternatively, isolating a small motif, which interacts with Vasa, provides a promising approach to discover structural features and biochemical functions of Buc - Vasa interaction.

2.2. Buc amino acid 372-394 is the Vasa binding motif (Buc-VBM)

To identify the region of Buc that interacts with Vasa, I performed bimolecular fluorescence complementation (BiFC) assay as described in Figure 17 and 18. There, Buc protein was systematically truncated and Venus C-terminal (VC) half was fused to the C-terminus of Buc full-length (Buc-VC) and to the truncated protein fragment (Figure 20A). The Venus N-terminal (VN) half was fused to the C-terminus of full length of Vasa protein (Vasa-VN). At the beginning, Buc protein was divided into N-terminal (amino acids 1-362) and C-terminal (amino acids 363-639) halves. I co-injected mRNA encoding Buc full-length, truncated Buc constructs and Vasa-VN into one-cell stage zebrafish embryos and incubated at 28.5 ^{o}C. Then embryos were imaged at 3 hpf using fluorescence microscope. At 3 hpf, only the C-terminal region of Buc showed fluorescence signal in the blastodisc (Figure 20F) narrowing the Vasa binding motifs to amino acids 363-639 of Buc.

2.3. Buc-VBM is highly conserved in vertebrates

Previously, three conserved motifs of Buc have been predicted after multiple sequence alignment of vertebrate Buc orthologs (Krishnakumar et al., 2018). Of these three motifs, the central domain corresponding to amino acid 372-394, is predicted as a highly conserved domain among Buc orthologs. As the C-terminal region of Buc that I used for the BiFC assay

encompasses the highly conserved central domain, I next examined whether this motif is involved in the interaction with Vasa.

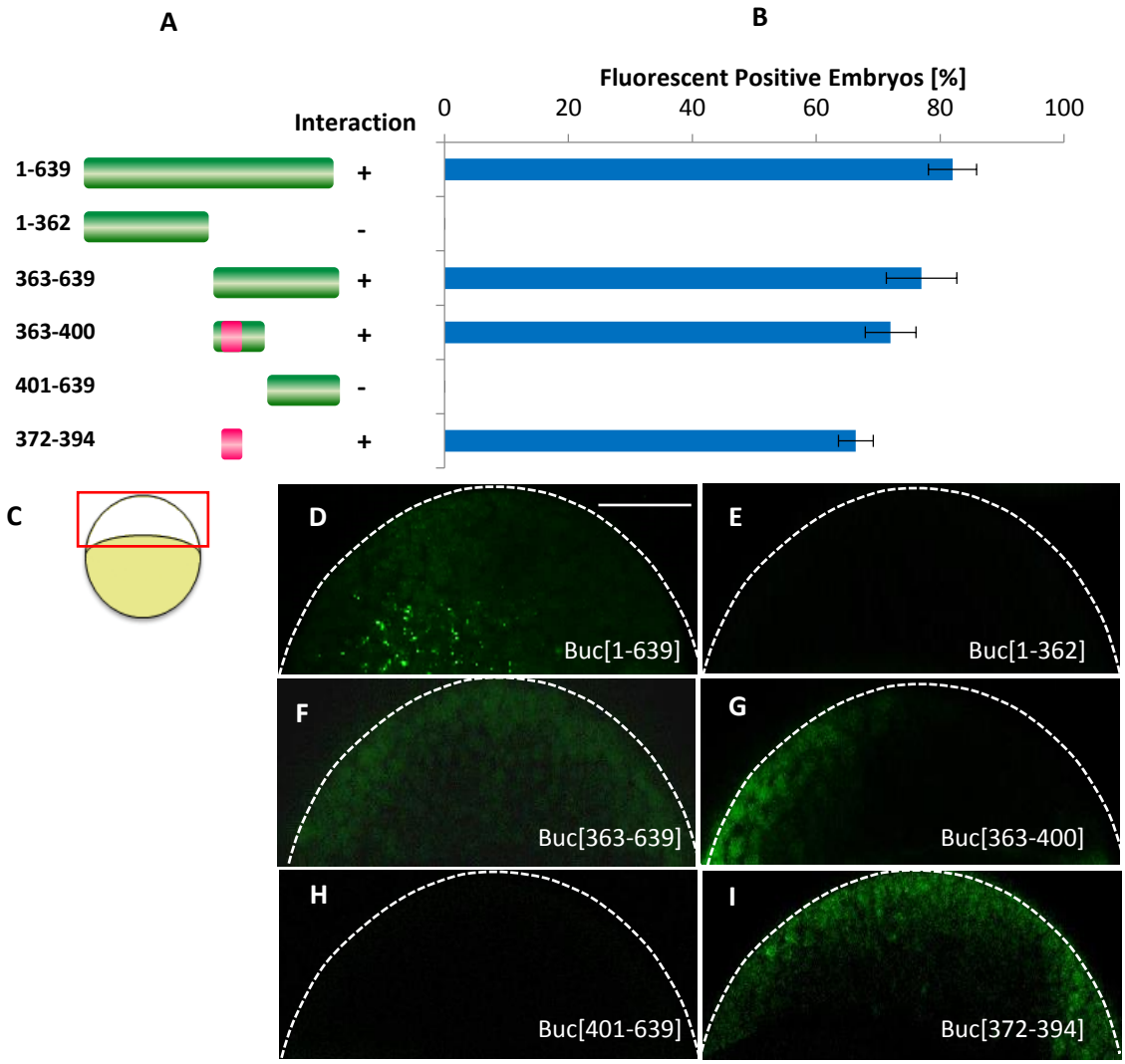

Figure 20: Identification of Buc-Vasa binding motif (Buc-VBM).

(A) Schematic illustration of systematic truncation of Buc (green). Numbers left to the colored bars indicate the corresponding amino acids. Interaction shown as '+', while no interaction shown as '-'. Buc-VBM highlighted in pink. (B) Quantification of fluorescent positive embryos based on the different combination of BiFC Buc and Vasa constructs. The data presented are averaged from three independent experiments. X-axis represents the percentage of fluorescent positive embryos and Y-axis represents injected constructs. Error bars represent standard deviation of the mean. (C) A cartoon illustrates the lateral view of embryos at 3 hpf, animal to the top. Confocal imaging area boxed in red. This region is outlined with a white dashed line in panel (D – I). All Buc constructs were co-injected with wild-type(full-length??) Vasa. (D) Injection of wild-type Buc shows fluorescent signal (82 ± 3.9%, n= 58). (E) However, Buc [1-362] and Vasa did not show fluorescent signal (0 ± 0%, n= 105). (F) After injection, Buc [363-639] shows fluorescent signal (77 ± 5.7%, n= 79). (G) Further, Buc [363-400] also shows fluorescence (72 ± 4.1%, n= 79). (H) Buc [401-639] did not show a fluorescent signal (0 ± 0%, n= 77). (I) Buc [372-394] shows fluorescent signal (66 ± 2.8%, n= 69). Scale bar 100 µm.

Next, I split the C-terminal region of Buc into two where the first fragment encompasses the highly conserved central domain encoding amino acid 363-400 while the second fragment bearing the remaining sequence encoding amino acid 401-639 (Figure 20A). Of these two fragments, only the fragment encoding amino acid 363-400 showed fluorescence signal in the blastodisc (Figure 20G). As this fragment bearing the highly conserved centennial (amino acid 372-394), I studied the interaction taking only the highly conserved central domain with Vasa-VN. Indeed, I observed fluorescent signal in the blastodiscs at 3 hpf suggesting that the highly conserved central domain is sufficient to interact with Vasa (Figure 20I).

2.4. Mapping of Buc binding motif in Vasa (Vasa-BBM)

To investigate the Buc binding domain in Vasa, I applied the same approach as described above for Buc. Essentially, the first 277 amino acids of Vasa are predicted to be intrinsically disordered; only amino acids 278-715, which included the helicase core (HC) with the conserved Rec-A like domains, are structured. Therefore, I cloned Vasa-IDR (amino acid 1-277) and Vasa HC (amino acid 278-715) fusing Venus VN half to the C-terminus of Vasa constructs (Figure 21A). After injection, at 3 hpf, I only found a positive BiFC signal using Vasa-HC with Buc but not with the Vasa-IDR (Figure 21F). These results indicate that Vasa-HC (amino acid 278-715) containing the RecA like domains interact with Buc.

It has been shown that the LOTUS domain of Oskar interacts with C-terminal RecA-like domain of *Drosophila* Vasa (Jeske et al., 2017). To examine whether Buc also interacts with the zebrafish Vasa RecA like domain, I divided the Vasa-HC (amino acid 278-715) into the N-terminal helicase core (N-HC; amino acid 278-495) and the C-terminal helicase core (C-HC; amino acid 496-715). The N-HC includes the N-terminal Rec-A like domain (RecA-NTD) while the C-HC includes the Rec-A like C-terminal domain (RecA-CTD; amino acids 496-623) together with an extended sequence (denoted as ‘e’) at the C-terminus of the RecA-CTD (eRecA-CTD; amino acids 624-715) (Figure 21A). After performing BiFC assay, I observed that the Vasa C-HC (amino acid 496-715) interacts with Buc (Figure 21H) but not the N-HC (amino

acid 278-495) (Figure 21G). This result suggests that zebrafish Vasa RecA-like C-terminal domain interacts with Buc as *Drosophila* Vasa RecA-like C-terminal domain binds to the Oskar LOTUS domain.

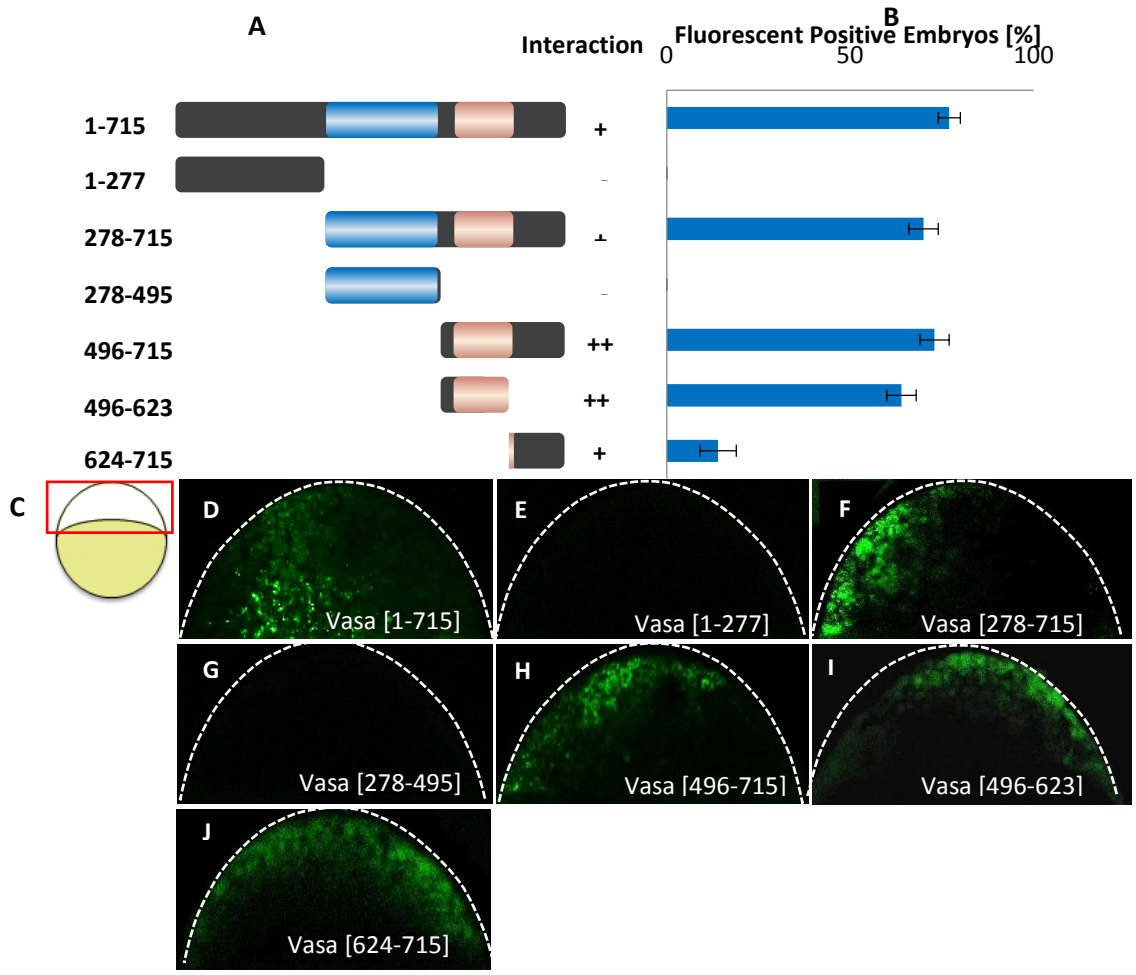

Figure 21: The Vasa-Buc binding motif (Vasa-BBM) is located in C-terminal region of Vasa.

(A) Schematic illustration of systematic truncations of Vasa (dark grey) with helicase core containing N-terminal (blue) and C-terminal (light rose) RecA-like domains. Numbers left to the colored bars indicate the corresponding amino acids. (B) Quantification of fluorescent positive embryos based on the different combination of BiFC Buc and Vasa constructs. The data presented are averaged from three independent experiments. X-axis represents percentage of fluorescent positive embryos and Y-axis represents injected constructs. Error bars represent standard deviation of the mean. Average fluorescent positive embryos ≥ 60% denoted as '++', average fluorescent positive embryos ≤ 40% as '+', and embryos with no fluoresce denoted as '-'. (C) A cartoon illustrates the lateral view of embryos at 3 hpf, animal to the top. Confocal imaging area boxed in red. This region is outlined with a white dashed line in the panels D – J. (D) Injection of wild-type Vasa shows a fluorescent signal (77 ± 3.0%, n= 96). (E) Vasa (1-277) did not show a fluorescent signal (0 ± 0%, n= 43). (F) However, Vasa (278-715) showed fluorescence (70 ± 4.0%, n= 85). (G) Further, Vasa (278-495) did not show a fluorescent signal (0 ± 0%, n= 57). (H) Besides, Vasa (496-715; 73 ± 4.0%, n= 77) showed fluorescent signal. (I) Vasa (496-623; 64 ± 4.0%, n= 76) showed fluorescent signal, whereas in (J) Vasa (624-715: 14 ± 5.0%, n= 55) showed a smaller number of fluorescent embryos. Scale bar 100 µm.

However, the structure solved for the LOTUS-Vasa complex revealed that the α2 helix of the *Drosophila* Vasa RecA-like C-terminal domain interfaces with α2 helix and α5 helix of the Oskar LOTUS domain during LOTUS -Vasa interaction (Jeske et al., 2017). As structural data for both Buc and Vasa are not available, I continued domain mapping using the BiFC assay to isolate a small peptide of Vasa, which is responsible for the interaction with Buc.

For this, I split the zebrafish Vasa C-terminal Helicase Core, C-HC (amino acid 496-715) into two fragments including the RecA-like C-terminal domain (amino acids 496-623) and the eRecA-CTD (amino acids 624-715) (Figure 21A). Both constructs generated fluorescent embryos upon injection with Buc in the BiFC assay. However, more fluorescent positive embryos were observed with RecA-like C-terminal domain (64%) than with eRecA-C-terminal domain (14%) (Figure 21B). The reason for this difference is not clear, but the Buc interaction domain in Vasa could spread over the RecA-C-terminal domain and eRecA- C-terminal domain.

I therefore changed my mapping strategy and continued by removing 50 amino acids from both the N-and the C-terminus of C-terminal helicase core (C-HC; amino acid 496-715) (Figure 22A). With this approach, I could narrow down the Vasa-BBM to amino acid 600-665 (Figure 22A). After deleting amino acids 665 to 615 from the C-terminus of Vasa-HC, the number of fluorescent embryos dramatically dropped from 71% to 24% (Figure A and B). This observation is similar to the results described above, where I observed a reduction of fluorescent embryos after splitting Vasa-Helicase Core into RecA-C-terminal domain and eRecA- C-terminal domain (Figure 21B). Taken together, these data suggest that the Buc-binding interface in Vasa is located between amino acids 600-665.

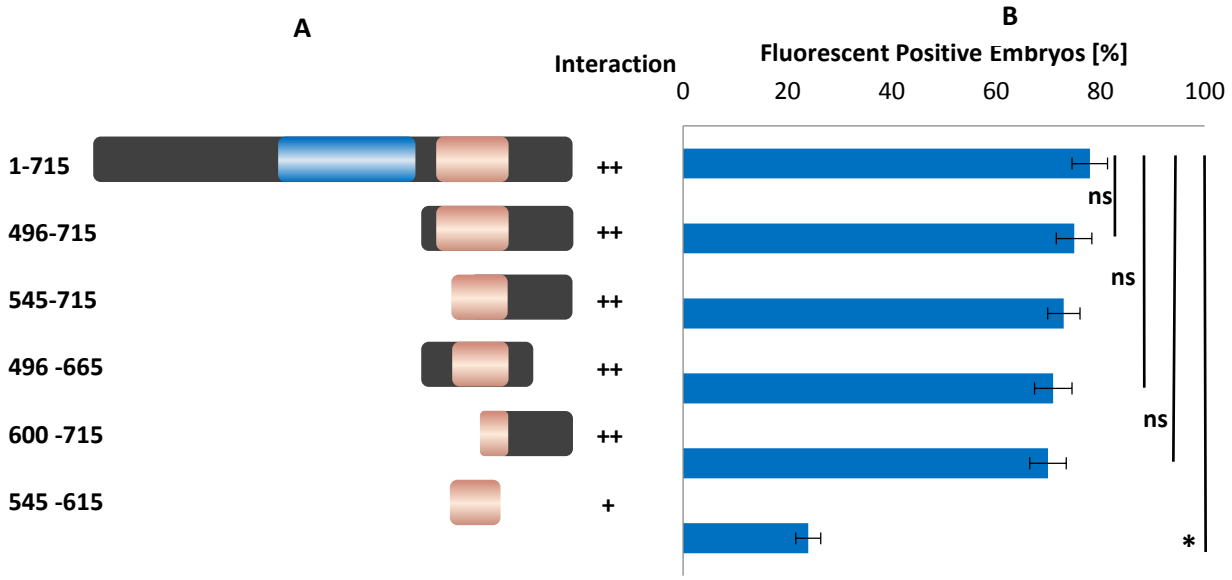

Figure 22: Vasa-BBM is potentially located in between amino acid 600-665.

(A) Schematic illustration of systematic truncations of Vasa (dark grey) with helicase core containing N-terminal (blue) and C-terminal (light rose) RecA-like domains. Numbers left to the colored bars indicate the corresponding amino acids. (B) Quantification of fluorescent embryos based on the different combination of BiFC Buc and Vasa constructs. The data presented are averaged from three independent experiments. X-axis represents percentage of average fluorescent positive embryos and Y-axis represents injected constructs. Error bars represent standard deviation of the mean. Fluorescent positive embryos ≥ 60% denoted as '++' and fluorescent positive embryos ≤ 40% shown as '+'. Test statistics: Student's t-test, * P< 0.05. All Vasa constructs were co-injected with wild-type, full-length Buc. Wild-type Vasa (positive control: 78±3.4%, n= 61), Vasa [496-715]; (75±3.4%, n= 85), Vasa [545-715]; (73±3.1%, n= 63), Vasa [496-665]; (71±3.6%, n= 58) and Vasa [600-665]; (70±3.5%, n= 58) constructs show ≥ 60% fluorescent embryos, while Vasa [545-615]; (24±2.4%, n= 53) shows ≤ 40% fluorescent embryos.

After I isolated the Buc interaction motif in amino acids 600-665 of Vasa, I again changed my mapping strategy to further narrow down the Buc binding site. I started to remove ten amino acids form the C-terminus of Vasa (600-665) to generate Vasa (amino acid 600-655), Vasa (amino acid 600-645), Vasa (amino acid 600-635), and Vasa (amino acid 600-625) (Figure 23A). After injection of these four constructs, I could narrow down the Buc interaction site in Vasa to a small peptide of amino acids 600-625 (Figure 23A and B).

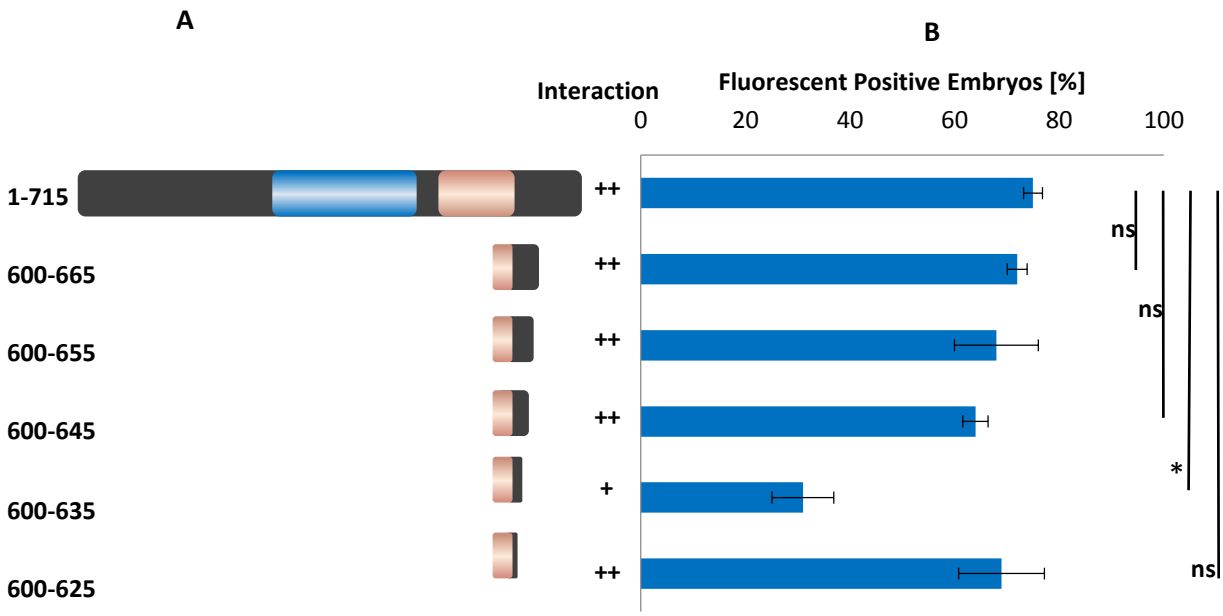

Figure 23: Vasa-BBM is located in amino acids 600-625.

(A) Schematic illustration of systematic truncation of Vasa (dark grey) with helicase core containing N-terminal (blue) and C-terminal (light rose) RecA-like domains. Numbers left to the colored bars indicate the corresponding amino acids. (B) Quantification of fluorescent positive embryos based on the different combination of BiFC Buc and Vasa constructs. The data presented are averaged from three independent experiments. The X-axis represents the percentage of fluorescent embryos and the Y-axis shows the injected constructs. Error bars represent standard deviation of the mean. Average fluorescent positive embryos ≥ 60% denoted as '++' and average fluorescent positive embryos ≤ 40% shown as '+'. Test statistics: Student's t-test, * P< 0.05. All the Vasa constructs were co-injected with wild-type Buc. There, wild-type Vasa (75±1.8%, n= 68), Vasa [600-665]; (72±1.9%, n= 80), Vasa [600-655]; (68±8.0%, n= 81) and Vasa [600-645]; (64±2.4%, n= 67) show ≥ 60% fluorescent embryos while Vasa [600-635]; (31±5.9%, n= 90) shows ≤ 40% fluorescent embryos. Interestingly, Vasa [600-625]; (69±8.2%, n= 64) shows ≥ 60% fluorescent embryos.

2.5. Buc-VBM and Vasa-BBM are required for their interaction

After identification of the binding motifs, I checked whether the identified Buc-VBM and Vasa-BBM are required for their interaction or whether there are still other binding motifs present in both proteins. For that, I generated a deletion construct of full-length of Buc, which lacks the amino acids 372-394 (BucΔVBM), and a construct of the full-length of Vasa, which lacks the amino acid 600-625 (VasaΔBBM) (Figure 24A). After injection, both deletions did not show any fluorescent signal with the wild-type binding partner in the BiFC assay (Figure 24D-F) suggesting that Buc-VBM and Vasa-BBM are essential for the Buc-Vasa interaction.

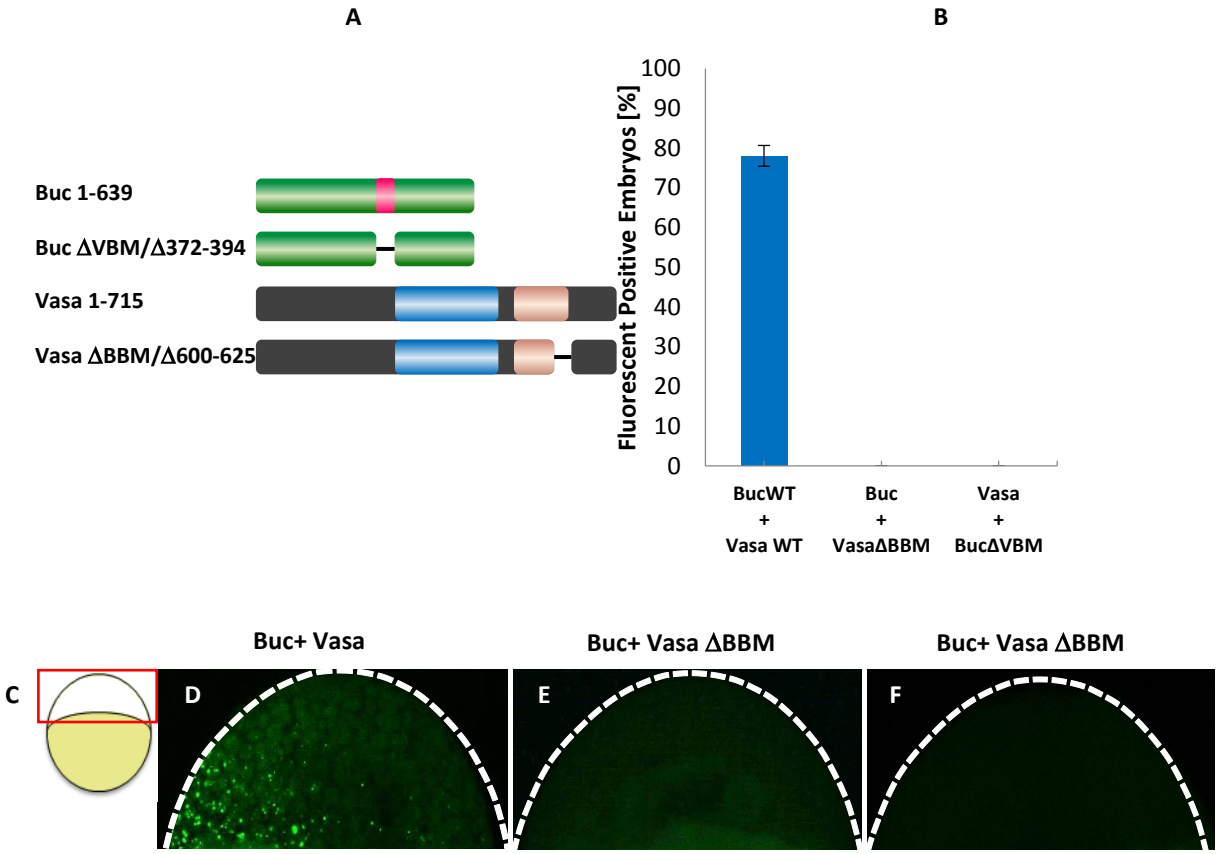

Figure 24: Buc-VBM and Vasa-BBM are required for Buc and Vasa interaction.

(A) Schematic representation of wild-type Buc, BucΔVBM, VasaΔBBM, and wild-type Vasa. Numbers left to the colored bar represent the corresponding amino acids. (B) Quantification of fluorescent positive embryos based on the different combination of BiFC Buc and Vasa constructs. The data presented are averaged from three independent experiments. The Y-axis represents the percentage of fluorescent embryos and the X-axis represents the injected constructs. Error bars represent standard deviation of the mean. (C) A cartoon illustrates the lateral view of embryos at 3 hpf, animal to the top. Confocal imaging area boxed in red. This region is outlined with a white dashed line in panel (D – F). Scale bar 100 µm. (D) Wild-type Buc and Vasa show fluorescent positive embryos (78±2.6, n = 72). However, wild-type Buc with VasaΔBBM (0±0%, n = 74). in (E) and wild-type Vasa with BucΔVBM in (F) did not show fluorescent positive embryos (0±0%, n = 71).

However, the deletion constructs might not be stable when expressed *in vivo*. As a specific antibody for the VC and VN fragments is not available, I fused the GFP protein to the C-terminus of all proteins to generate Buc-GFP, BucΔVBM-GFP, Vasa-GFP and VasaΔBBM-GFP. I then expressed equal amount of RNA (200 ng/ µl) in early zebrafish embryos and compared their fluorescence (Figure 25B-F). My results indicated that all the constructs are expressed *in vivo* and the level of fluorescence is comparable suggesting similar levels of translation and stability. Moreover, despite both BucΔVBM and VasaΔBBM expressed *in vivo*, they do

not bind to wild-type Vasa or Buc respectively. Therefore, my findings indicate that BucVBM and VasaBBM are required for their interaction during germ cell specification in early zebrafish embryogenesis. Nevertheless, it is a compelling question whether the deletion constructs are still folding into their native conformation without the binding motifs. I therefore aimed to obtain additional structural information about the Buc and Vasa interaction to perform "minimally invasive surgery" targeting point mutations on these proteins rather deleting entire stretch of binding motifs to further characterize their interaction during germ cell specification.

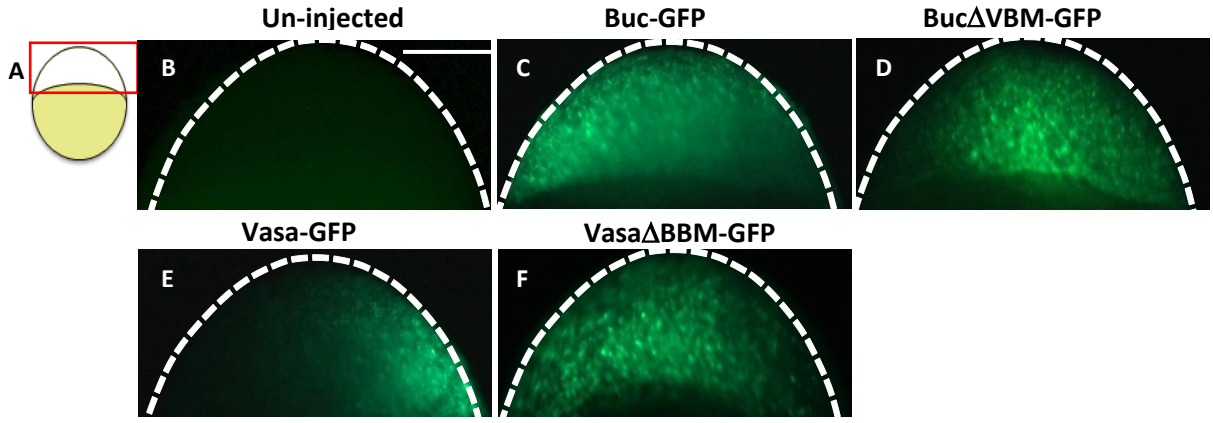

Figure 25: BucΔVBM-GFP and VasaΔBBM are expressed *in vivo.*

A) A cartoon illustrates the lateral view of embryos at 3 hpf, animal to the top. Confocal imaging area boxed in red. This region is outlined with a white dashed line in panel (B-F). (B-F) All the constructs; Buc-GFP, BucΔVBM-GFP, Vasa-GFP and VasaΔBBM showed fluorescent signal compared to the un-injected control. Scale bar 200 µm

2.6. Buc directly binds to Vasa

With the BiFC assay, I identified the Vasa-binding motif of Buc in amino acids 372-394 and the Buc binding motif of Vasa in amino acids 600-625 using BiFC. The fluorescent signal produced in the BiFC assay is dependent on the proximity of the non-fluorescent Venus fragments suggesting that Buc and Vasa bind directly to each other. However, under *in vivo* conditions like I used them in my experiments with a complex mixture of proteins, the possibility exists that the Venus fragment come close to each other and emit fluorescence, although there is no direct contact between two target proteins (Miller et al., 2016). I

therefore aimed to investigate whether Buc directly interacts with Vasa *in vitro* using GST pull-down assays with purified Buc and Vasa-fragments.

I fused glutathione-S-transferase (GST) to the N-terminus of the Buc-VBM (amino acid 363-400). I also generated an N-terminal GST-fusion of Vasa (amino acid 227-670). After expression in *E. coli*, I purified both proteins by GST affinity chromatography. Purified GST-Vasa treated with PreScission Protease enzyme to remove the GST-tag. After this treatment, I performed a GST pull-down assay incubating GST-Buc-VBM with Vasa. Coomassie Blue staining of the SDS-PAGE after GST-pulldown indicated that Buc-VBM directly interacts with Vasa (Figure 26). Increasing the concentration of Vasa in the binding assay did not pull-down more Vasa suggesting that the Buc and Vasa probably having a weak or transient interaction.

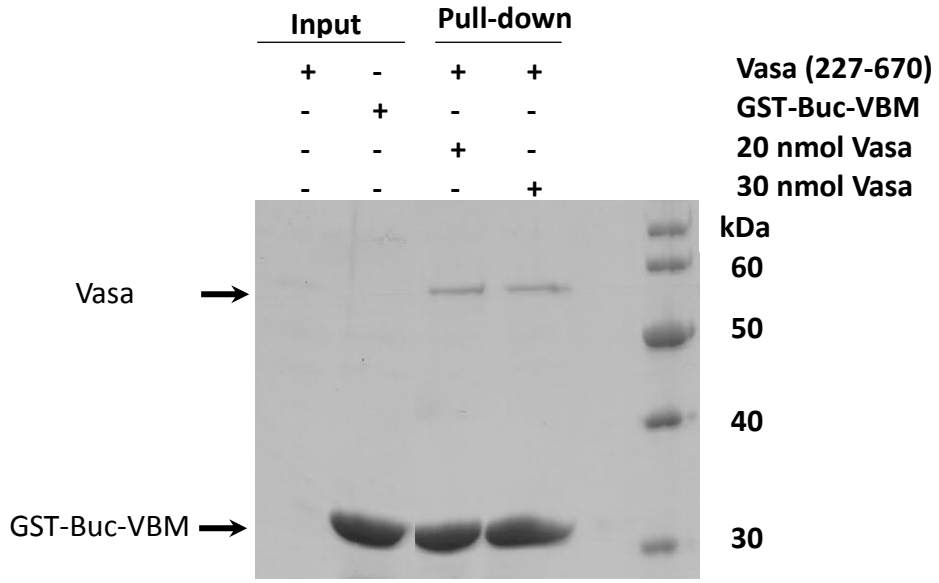

Figure 26: Buc directly interacts with Vasa.

SDS-PAGE (15%) stained with Coomassie Brilliant Blue. GST pull-down assay performed with recombinant GST-Buc-VBM (expected molecular weight approximately 32 kDa) and Vasa (residues 227–670; expected molecular weight approximately 56 kDa. Protein markers (in kDa) are indicated on the right. In the pull-down assay, GST-Buc-VBM pulls down Vasa suggesting that both fragments directly bind to each other. Further, there was no obvious difference observed in Buc-VBM and Vasa with increasing molar concentration of Vasa.

2.7. Homology modeling for zebrafish Vasa

As *Drosophila* Vasa and zebrafish Vasa are highly conserved in their sequence, I planned to examine the secondary structure of zebrafish Vasa using the conservation of *Drosophila* Vasa as a template. To that end, I aligned zebrafish Vasa encoding amino acids 227-670 which encompass the conserved helicase core with *Drosophila* Vasa encoding amino acids 200-623, whose crystal structure was already solved (Sengoku et al., 2006) (Figure 27). The alignment revealed that the secondary structures of zebrafish and *Drosophila* Vasa are highly conserved (Figure 27). More importantly, this result allowed me to perform homology modeling of zebrafish Vasa using the I-Tasser webserver (https://zhanglab.ccmb.med.umich.edu/I-TASSER/; Roy, Kucukural and Zhang, 2010).

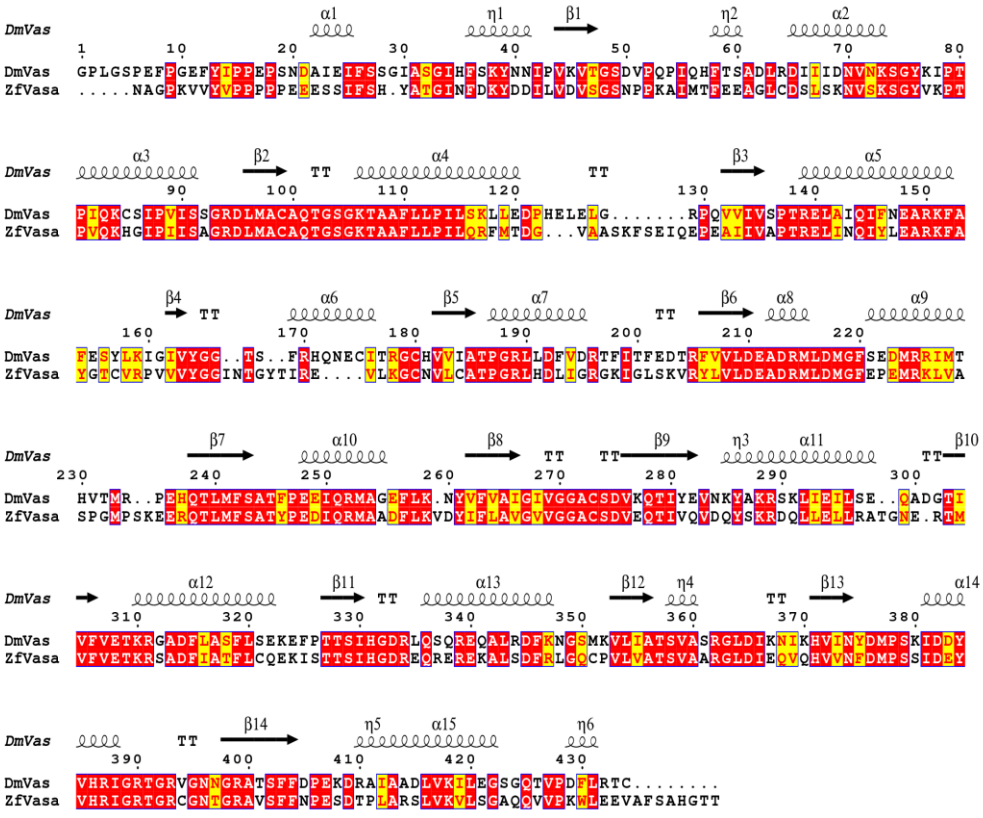

Figure 27: Pairwise amino acid sequence alignment of *Drosophila* and zebrafish Vasa.

Protein sequences were aligned using the T-Coffee multiple alignment server (Di Tommaso et al., 2011). For the alignment, I used partial sequences of *Drosophila* Vasa (DmVas; amino acids 200-623), whose structure is already solved, and zebrafish Vasa (ZfVasa; amino acids 227-670), which I used for purification. Identities are boxed in red, similarities of physico-chemical properties are boxed in yellow. Secondary structures indicated above the alignment were predicted using Espript 3.0 based on the *Drosophila* crystal structure PDB ID: 2DB3(Sengoku et al., 2006). Spirals indicate α-helices and arrows indicate β-sheets.

The I-Tasser program predicted four homology models. From these, I selected the final model with the highest C-score. The C-score calculates a confidence score as a significance of threading template alignments for the query sequence and the structure assembly. Usually, the C-score is in the range of from -5 to 2, where the higher C-score predicts the best model. After homology modeling, I selected a model with a C-score of -0.87 (Table 1) as the final model for zebrafish Vasa. I then aligned the selected structure against the published structure for *Drosophila* Vasa using PyMol software (The PyMOL Molecular Graphics System, Version 2.2.3 Schrödinger, LLC and Sengoku *et al.*, 2006). The structural alignment shows that the predicted secondary structure of zebrafish Vasa is nearly identical to *Drosophila* Vasa (Figure 28).

Table 1. C-score values for predicted zebrafish Vasa homology model

Model	C-score
1	-0.87
2	-1.02
3	-2.57
4	-3.37

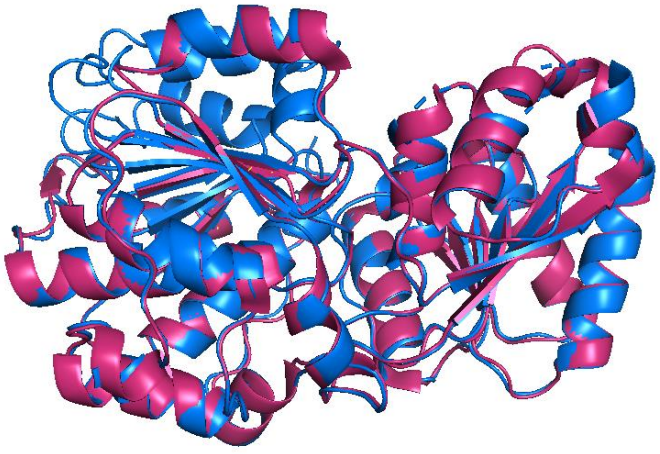

Figure 28: Alignment of a predicted zebrafish Vasa structure with the structure solved for *Drosophila* Vasa.

Both *Drosophila* Vasa (pink) and zebrafish Vasa (blue) structures were aligned using PyMol tool. The ribbon model shows that the two sequences have a nearly identical secondary structure.

2.8. *In silico* secondary structure prediction for Buc-VBM

As mentioned previously, the amino acid composition of Buc is predicted to form an intrinsically disordered protein (Figure 16). The algorithm predicts that the Buc-VBM (amino acid 363-400) is less disordered than the rest of the protein. Previously, we showed the functional equivalence between Buc and *Drosophila* Oskar protein despite there is no sequence similarity between the two proteins (Krishnakumar et al., 2018). This functional equivalence could be explained by two alternative mechanisms known as convergent or divergent evolution. (Krishnakumar et al., 2018)

In the convergent evolution model, two proteins evolved independently from unrelated ancestors and by selection, constraints developed a common interactome to specify germ cells in two different species. In the divergent evolution model, two proteins evolved from a common ancestor and by selection constraints maintained a common interactome to specify germ cells (Krishnakumar et al., 2018; Wake et al., 2011).

As Oskar and Buc are essential for fertility, which is key for evolution, convergence of Buc and Oskar is less likely. However, the unrelated sequence of both proteins is supported, if both proteins form similar structures, as observed in some proteins (Bayer et al., 1998). This model therefore hypothesizes Buc and Oskar form the same structure during their interaction with Vasa in the absence of sequence homology.

Interestingly, the crystal structure for the *Drosophila* Oskar LOTUS-Vasa complex revealed that the α2 helix of the *Drosophila* Vas-RecA-like C-terminal domain interfaces with the α2- and α5-helix of the LOTUS domain (Jeske et al., 2017). The α2-helix is part of the trihelical bundle of the winged helix -turn-helix (HTH) core of the LOTUS domain, while the α5-helix is found in the C-terminal region of the LOTUS domain (Figure 29).

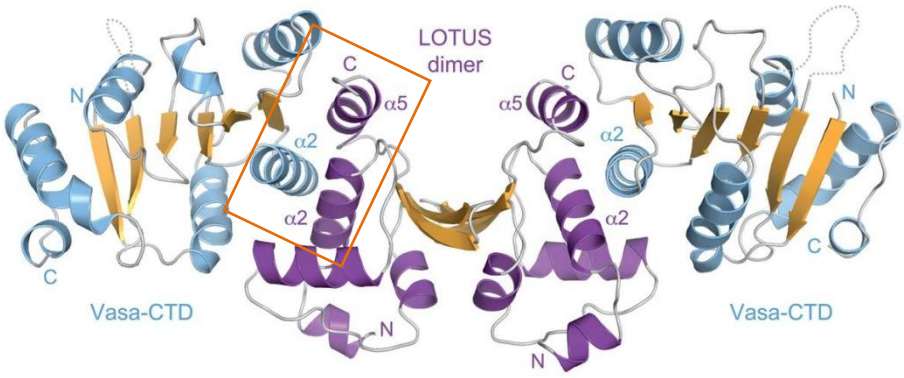

Figure 29: Illustration of *Drosophila* Vasa and Oskar LOTUS domain binding interface.

The LOTUS dimer of Oskar (middle) is shown in purple color and the RecA like C-terminal domain of *Drosophila* Vasa in light blue color. The interaction interface boxed in orange. During the interaction, the α2-helix of Vasa RecA like C-terminal domain interfaces with the α2-helix and α5-helix of the Oskar LOTUS domain. This image is modified from (Jeske et al., 2017).

Remarkably, the crystal structure did not show any secondary structure in the C-terminal region forming the α5-helix in the LOTUS-Vasa complex suggesting that this C-terminal extension of the LOTUS domain adopts an induced secondary structure upon interaction with Vasa (Jeske et al. 2017) (Figure 30).

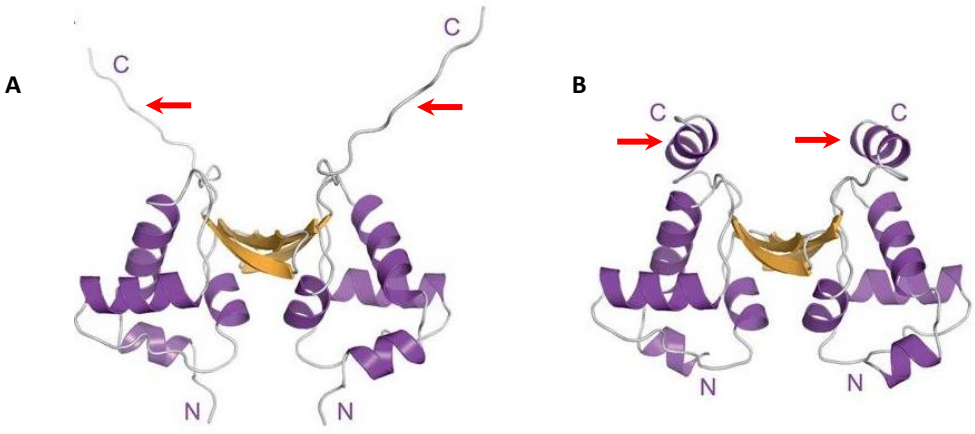

Figure 30: C-terminal extension of *Drosophila* Oskar LOTUS domain (eLOTUS) adopts an α-helix during interaction with *Drosophila* Vasa.

(A) Apo LOTUS dimer (Protein Data Bank [PDB] 5A48) (Jeske et al., 2015). Red arrows point disordered C-terminal eLOTUS domain of each monomer. (B) After interaction with *Drosophila* Vasa, each monomer of eLOTUS domain adopts an α-helix from its disordered state (red arrow). This image is modified from (Jeske et al., 2017)

To support the hypothesis that the Buc-Vasa complex would share structural identity with Oskar-Vasa during their interaction, I performed *in silico* secondary structure predictions for Buc-VBM (amino acid 363-400). For this prediction, I applied three different algorithms, namely CFSSP, PEP2D, and Jnet, which are predominantly used in structural biology to predict protein secondary structures (Ashok Kumar, 2013; Singh et al., 2019; Cole et al., 2008; Drozdetskiy et al., 2015).

The CFSSP algorithm predicts α-helices, ß-sheets and turns for a given protein sequence by calculating the relative occurrences of each amino acid compared to known protein secondary structures solved with X-ray crystallography (Ashok Kumar, 2013). The PEP2D algorithm is based on a random forest classification algorithm (Singh et al., 2019). For a submitted query peptide, the position-specific scoring matrix (PSSM) is calculated after aligning the given sequence with the known sequences obtained from PDB. This PSSM uses the occurrence of amino acids in secondary structures to calculate for each residue the probability values to predict α-helices, ß-sheets, and turns. Jnet is a sophisticated, artificial neural network (ANN) prediction algorithm (Cole et al., 2008; Drozdetskiy et al., 2015). In Jnet, the query sequence is searched against UniProt reference clusters to align with position-specific iterative basic local alignment search tool (PSI-BLAST) to generate a PSSM. An HHMer program produces a probabilistic HMM profile using alignment scores. Thereafter, the Jnet algorithm uses the generated PSSM and HMM profiles to predict the final secondary structures.

When I submitted the Buc-VBM (amino acid 363-400), the three algorithms predicted variable positions for ß-sheets and turns (Figure 31A-C) indicating that the formation of these secondary structures is less likely. However, all algorithms independently predicted two α-helices (Figure 31A-C), which share similar amino acids. The first α-helix (α1) consisted Glutamic acid (E), Arginine (R), Glutamine (Q) and Serine (S) (Figure 31A-C) while the second α-helix (α2) consisted Arginine (R), Aspartic acid (D), Glutamic acid (E) and Methionine (M) (Figure 31A-C). These results make the Vasa-binding motif in Buc an interesting object for further experiments to investigate its structure.

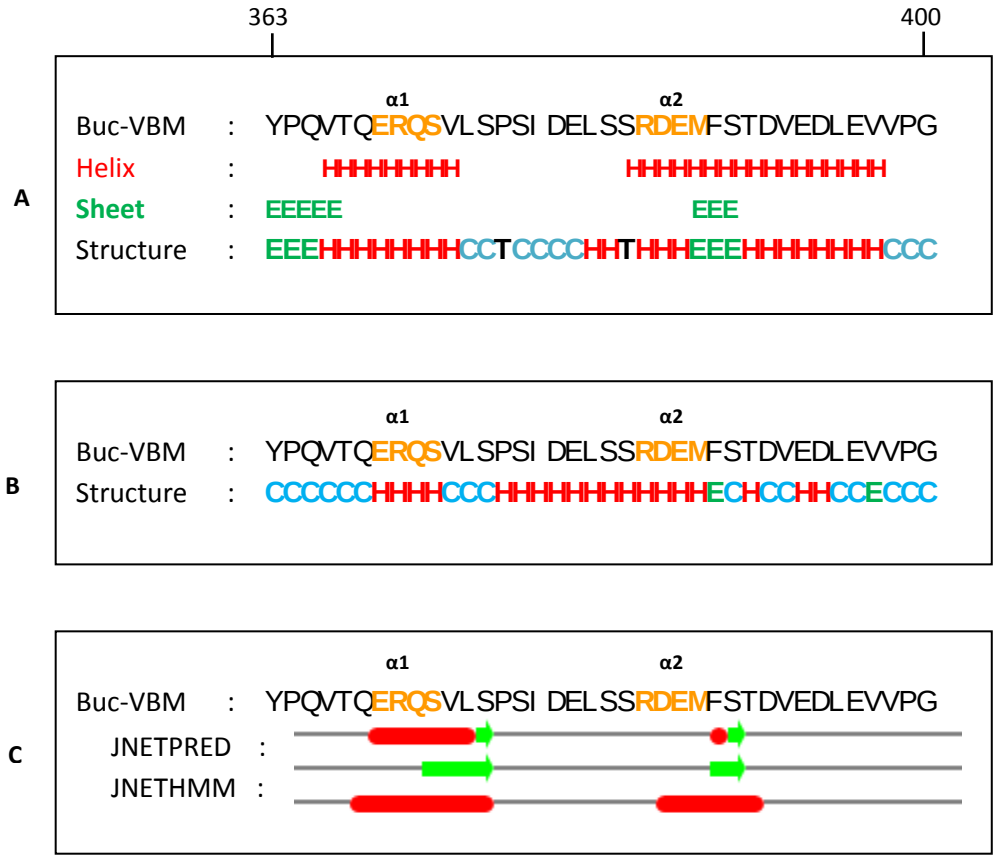

Figure 31: *In silico* secondary structure prediction for Buc-VBM.

In all three algorithms, predicted α-helices denoted as 'H' in red, ß-sheets as 'E' in green and turns as T in black. The consensus secondary structure is shown at the bottom. Note that random coils in the consensus structure are denoted as 'C' in light blue. The first (363) and last (400) amino acid sequence of the Buc-VBM is displayed on top of the sequence of panel A, which is common for the panel B and C. (A) Secondary structure prediction using the CFSSP algorithm. The algorithm predicted two α-helices, α1 and α2. The α1 contains amino acid ERQS (orange) and α2 contains amino acid RDEM (orange). It also predicted two ß-sheets, which contains amino acid YPQ from the N-terminus and MFS from the C-terminus. (B) Secondary structure prediction using PEP2D algorithm. The Buc-VBM amino acid sequence is displayed on top. The algorithm predicted two α-helices, α1 and α2, which shares the same amino acids predicted by CFSSP algorithm. (C) Secondary structure prediction using the Jnet algorithm. Buc-VBM sequence is displayed on top. The algorithm predicted two α-helices, α1 and α2, which shares the same amino acids predicted by CFSSP algorithm and Jnetpred program within the Jnet algorithm predicted two ß-sheets (green box; amino acid RQSV from the N-terminus and EMF from the C-terminus). JnetHMM shows the prediction of α-helices by the HMMER profile network in the Jnet algorithm.

2.9. Buc-VBM adopts α-helices from its disordered state

To confirm the *in silico* predicted secondary structures of Buc-VBM experimentally, I applied circular dichroism (CD) spectroscopy. CD-spectroscopy uses light absorption to measure the difference in absorbance of right- and left-handed circular-polarized light when it passes through optically active molecules (Norma J. Greenfield, 2012). Predominantly, amide groups of the polypeptide backbone are optically active and their CD spectrum changes with the local conformation of a secondary structure in the protein.

Structural elements such as α-helices, β-sheets, β-turn, and random coils have characteristic CD spectra over corresponding wavelength α-helices show negative CD spectra at 222 nm and 208 nm and positive spectra at 193 nm. Proteins with antiparallel β- sheets exhibit negative spectra at 218 nm and positive bands at 195 nm. Disordered proteins have considerably very low CD above 210 nm and negative spectra near 195 nm (Figure 32A). (Norma J. Greenfield, 2012).

To perform CD-spectroscopy, I used purified Buc-VBM (amino acid 363-400) after removing the GST moiety by treatment with PreScission Protease. Next, I rebuffered the protein by dialysis to provide appropriate conditions for CD-spectroscopy. At native, aqueous conditions and neutral pH, I calculated the molar ellipticity ([θ]deg×cm^2/dmol) for Buc-VBM. It showed a strong negative molar ellipticity at 200 nm, low negative molar ellipticity at 210–230 nm, and 190 nm (Figure 31B). Therefore, the CD profile of Buc-VBM is typical for disordered proteins, which lack any secondary structure (Fig. 32A).

To assess whether a disordered protein has the propensity to form stable secondary structures, the organic solvent trifluoroethanol (TFE) with its crowding properties has been used to induce secondary structures in short peptides (Laureto et al., 2001). TFE disrupts hydrogen bond formation between water molecules in the solvent shell and the amide proton of the peptide backbone. Consequently, intramolecular hydrogen bond formation is strengthened and the stability of secondary structures increases (Walgers et al., 1998;

Kaczka et al., 2014). In the presence of 30% as well as 50% TFE, I observed that Buc-VBM displays the typical CD spectra for α-helices (Figure 32B). These results suggest that Buc-VBM is prone to adopt an ordered conformation from its disordered nature, when it loses its hydration shell as it occurs during protein-protein interaction. Together, my *in silico* secondary structure predictions and CD-spectroscopy data provide strong support for the hypothesis that the Buc-Vasa interaction show structural similarities to the binding of the eLOTUS domain of Oskar with *Drosophila* Vasa RecA-like C-terminal domain.

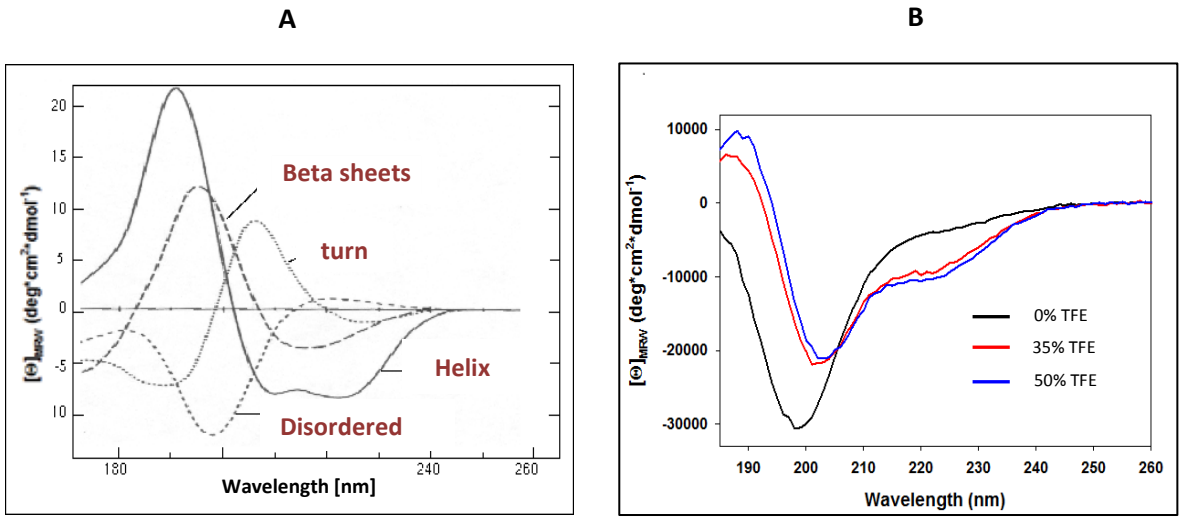

Figure 32: Secondary structure prediction for Buc-VBM (amino acid 363-400) using CD-spectroscopy.

The Y-axis represents the molar ellipticity ([θ]) which is CD corrected for concentration. The X-axis represents the corresponding wavelength. (A) A representation of reference CD-spectra (Norma J. Greenfield, 2012) CD-spectra for characteristic secondary structures are labelled. α-helices show negative CD spectra at 222 nm and 208 nm and positive spectra at 193 nm. Proteins with antiparallel β- sheets exhibit negative spectra at 218 nm and positive bands at 195 nm. Disordered proteins have very low CD spectra above 210 nm and negative spectra near 195 nm. (B) Represents the CD-spectra for Buc-VBM. In the native aqueous conditions and neutral pH, the CD spectra calculated for Buc-VBM was typical for a disordered protein (black line). After addition of different concentration of TFE (35%-red line and 50%-blue line), Buc-VBM shows CD-spectra characteristic for α-helices from its disordered state with the TFE crowding agent.

2.10. Buc-VBM is a novel activator of zebrafish Vasa helicase activity

My data show that Buc directly binds to Vasa, but also raise the question what are the biochemical consequences of this interaction. It has been previously shown that the helicase activity of DEAD box proteins is modulated by protein cofactors. Fascinatingly, it has been discovered that the Oskar LOTUS domain stimulates the ATPase activity of *Drosophila* Vasa upon their interaction albeit Oskar is not belonging to a canonical protein family of putative helicase regulating cofactors (Jeske et al., 2017). Therefore, I next aimed to check whether Buc-VBM could modulate the ATPase activity of zebrafish Vasa during their interaction. To quantify the Vasa activity, I used an *in vitro* NADH/LDH coupled ATPase assay (Kiianitsa et al., 2003).

In principle, this assay monitors the reduction of NADH absorbance at 340 nm, which is directly proportionate to the rate of ATP hydrolysis. For each cycle of ATP hydrolysis by RNA helicases, phosphoenolpyruvate (PEP) is converted to pyruvate by pyruvate kinase (PK), which is coupled to the regeneration of ATP. Subsequently, pyruvate is reduced to lactate by lactate dehydrogenase (LDH) while oxidizing NADH to NAD+, which I measured at 340 nm. (Figure 33).

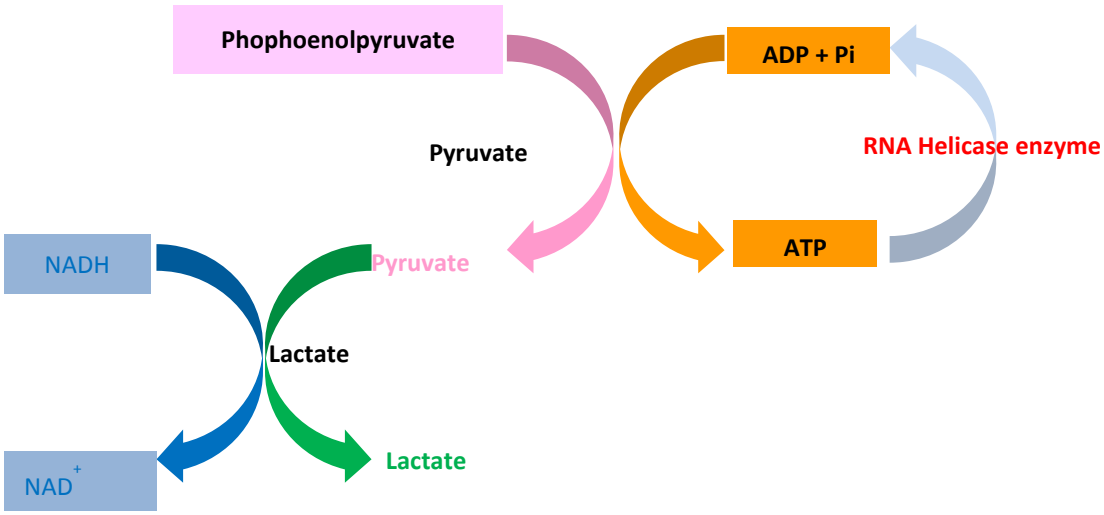

Figure 33: Schematic representation of NADH/LDH coupled ATPase assay.

This assay monitors the reduction of NADH absorbance at 340 nm, which is directly proportional to the rate of ATP hydrolysis. For that, substrates such as Phophoenolpyruvate (pink box), NADH (light blue box) ATP (orange box) are mixed with pyruvate kinase/lactate dehydrogenase enzyme mixture. For each cycle of ATP hydrolysis by RNA helicases, phosphoenolpyruvate is converted to pyruvate by pyruvate kinase, which is coupled to the regeneration of ATP. Consequently, pyruvate is reduced to lactate by lactate dehydrogenase (LDH) while oxidizing NADH to NAD+, which measured at 340 nm.

In control experiments, I observed a mild ATPase activity after incubating 5 µM Vasa together with 2.5 mM ATP compared to samples incubated with only 100 µM Buc (Figure 34). Remarkably, ATPase activity was strongly induced when I added 100 µM Buc-VBM to Vasa. These results suggest that Buc-VBM functions as a novel cofactor, which stimulates the ATPase activity of zebrafish Vasa (Figure 34). More importantly, this discovery reveals for the first time a biochemical function for the Buc protein during germ cell specification.

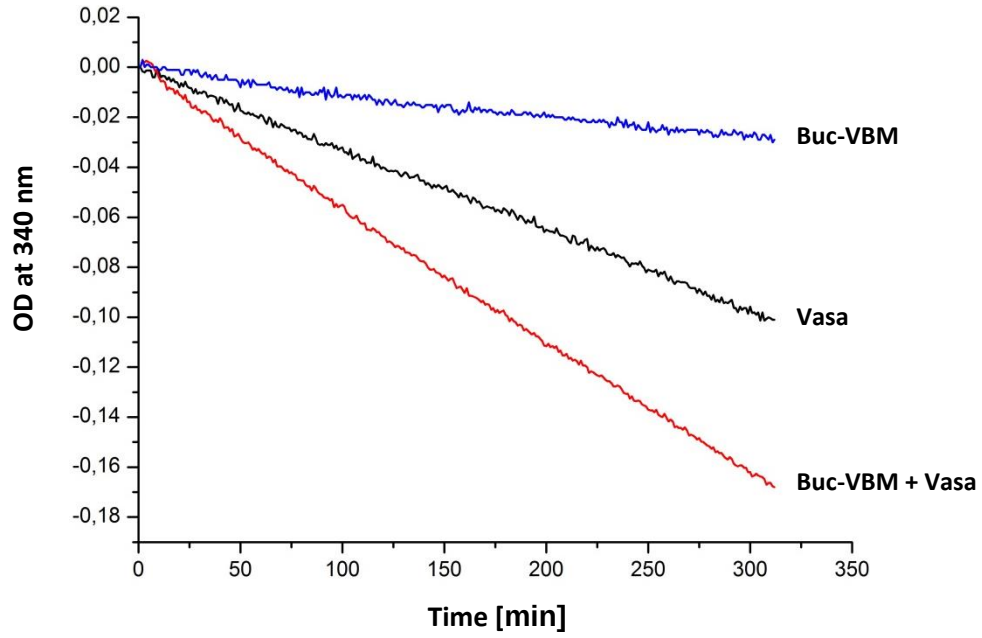

Figure 34: Buc-VBM activates Vasa helicase activity.

Y-axis denotes the reduction of NADH absorption, which is directly proportional to the rate of ATP hydrolysis. The absorbance was measured at 340 nm. X-axis denotes the incubation time in minutes. The data presented are averaged from three independent experiments. Incubation of 100 µM Buc-VBM with 2.5 mM ATP showed very mild ATPase activity (Negative control, blue line). A higher background ATPase activity was observed after incubation of 5 µM Vasa with 2.5 mM ATP (black line). Fascinatingly, ATPase activity was approximately doubled when 100 µM Buc-VBM was added to 5 µM Vasa, and 2.5 mM ATP. Data sheet is attached in the appendix I.

2.11. Buc-Vasa binding motifs and intrinsically disordered region is not sufficient for germ cell formation

Previously, we showed that wild-type Buc and Vasa induce ectopic germ cells when inject into a somatic cell in 16-cell stage of embryos. With this assay, I wanted to check whether the Buc-VBM or Vasa-BBM is sufficient to induce ectopic germ cells. To test for germ cell induction, I injected mRNA of wild-type Buc, Buc-VBM and Vasa-BBM into a somatic cell of 16-cell stage embryos. In my results, except wild-type Buc, Buc-VBM and Vasa-BBM did not show ectopic germ cells at 15-18 somite stage embryos (Figure 35A-C). It has been shown that Buc, Oskar, and Vasa are intrinsically disordered proteins. Therefore, these proteins aggregate through the IDRs. Thus, it is arguable that the induction of ectopic germ cells is dependent on IDR of the proteins in addition to Buc and Vasa binding motifs. To test this, in the same assay I injected mRNA of mutant Buc encoding amino acids 1-601 ($BucP^{106}$), which

lacks the terminal 38 amino acids yet retains most of the IDRs. As a control, I injected mRNA of an unrelated protein called human fused in sarcoma (hFUS), which is strongly intrinsically disordered, into a somatic cell of a 16-cell stage zebrafish embryo. In my results, neither hFUS (Figure 35D) nor BucP^{106} did induce ectopic germ cells (Figure 35E), even though Buc^{p106} contains the Buc-VBM (amino acid 363-400). Collectively, these results postulate that neither aggregation of these proteins via their IDRs nor interaction through their binding motifs are sufficient to form ectopic germ cells.

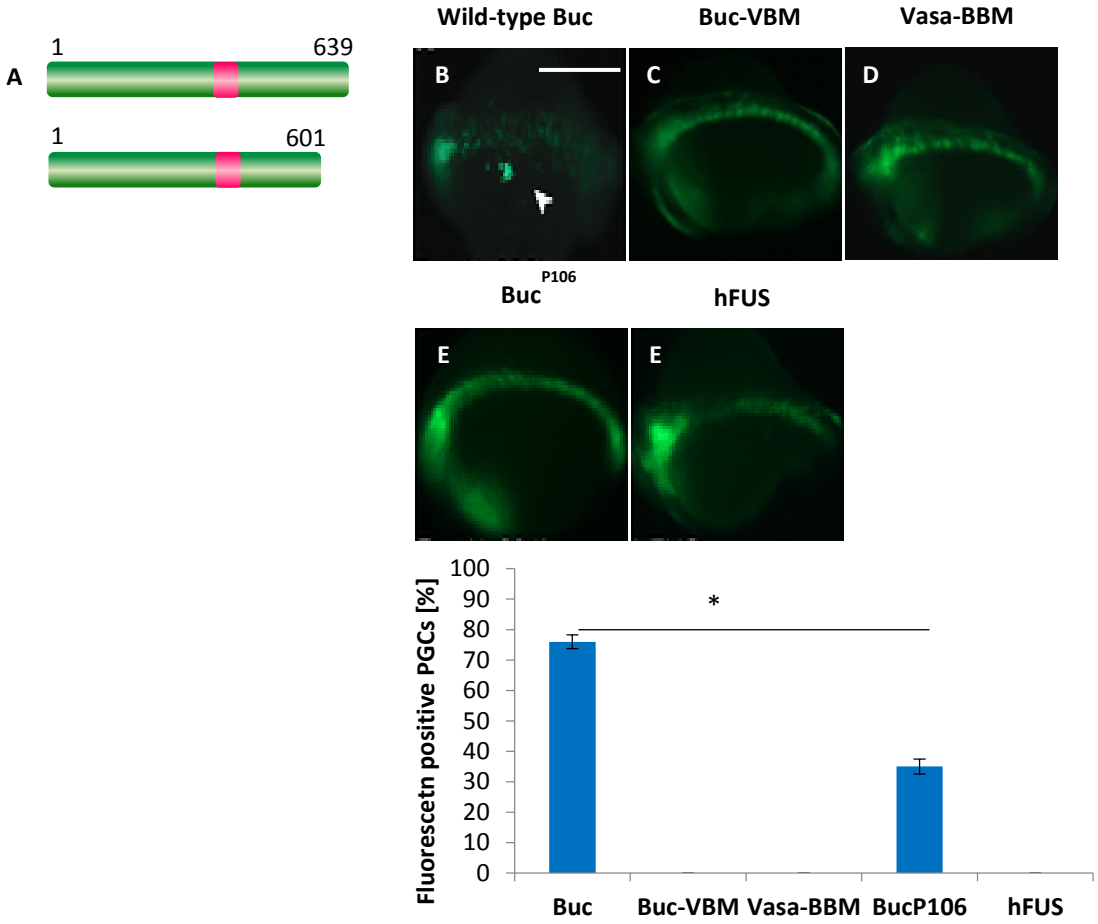

Figure 35: Buc-Vasa binding motifs and its intrinsically disordered regions are not sufficient for germ cell formation.

(A) A cartoon representing wild-type Buc (top) and mutant BucP^{106} (bottom). Reporter RNA, nanos3-3'-UTR GFP and all the other RNAs are injected into a somatic cell (corner cell) of a 16-cell stage embryo. (B) Wild-type Buc (amino acid 1-639) induced ectopic germ cells (76.6±2.3%; n = 60) (C) Buc-VBM (amino acid 363-400; 0±0%, n = 26), (D) Vasa-BBM (amino acid 600-625; 0±0%, n = 35), (E) mutant BucP^{106} (amino acid 1-601; 35.9±2.6%; n = 60) and (F) hFUS did not induce ectopic germ cells. (F) Quantification of fluorescent positive PGCs. The data represent three independent experiments. The Y-axis shows the percentage of fluorescent positive PGCs containing embryos and the X-axis indicates the injected constructs. Error bars represent standard deviation of the mean. Test statistics: Student's t-test. * $P < 0.05$. Scale bar 100 µm. Note that, I performed the experiments related to figure 35B,E and F and published in (Krishnakumar et al., 2018).

2.12. Buc-VBM and Vasa-BBM act as dominant negative proteins during germ cell specification

Unexpectedly, the injection of mutant Bucp106 (aa1-601) with the VBM does not induce the formation of germ cells (Fig. 35). This result raises the hypothesis that a second interaction of Buc might be required to specify germ cells in addition to having IDRs and Buc and Vasa binding motifs. As a result of this hypothesis, I further speculated that the Buc-VBM acts as a dominant negative protein by inhibiting endogenous Vasa and thus PGC specification. To test this, I injected mRNA of Buc-VBM into one-cell embryos of Buc-GFP transgenic fish. Compared to un-injected controls, I observed a reduction in the number of germ cells in embryos injected with Buc-VBM (Figure 36B and C)

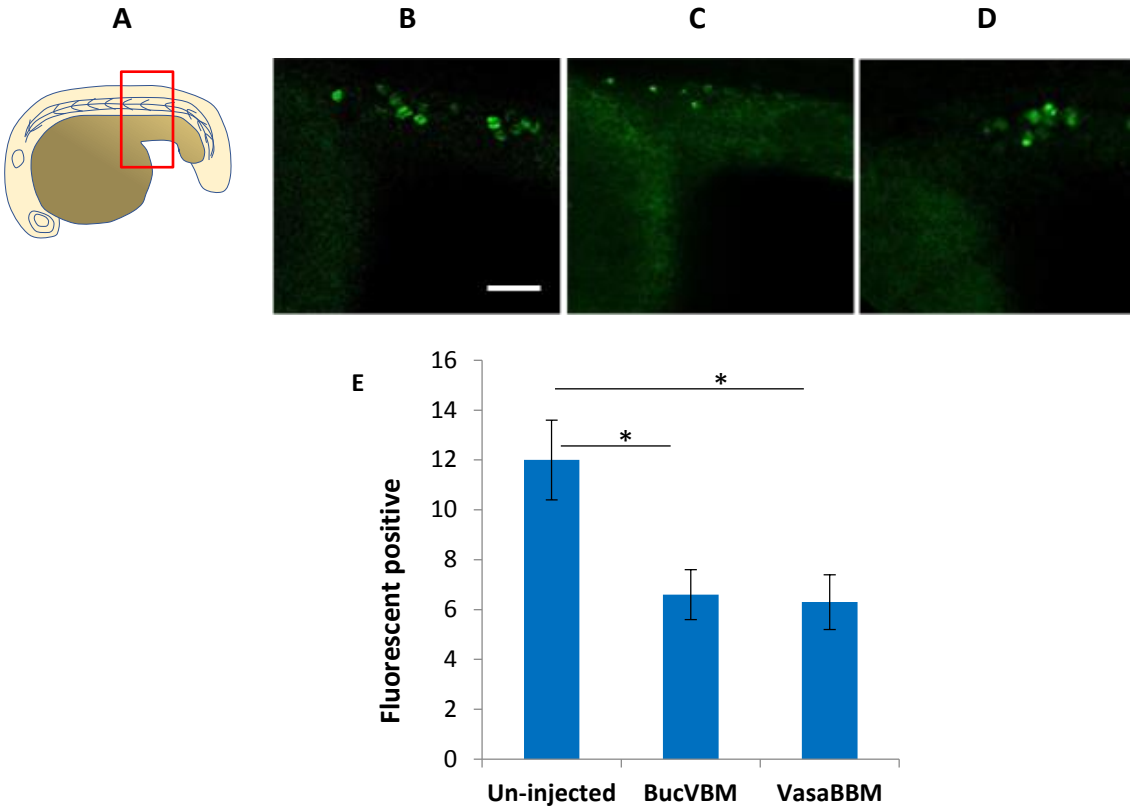

Figure 36: Buc-GFP larvae showed less germ cell after injection of Buc-VBM and Vasa-BBM into Buc-GFP embryos.

(A) A cartoon represents the lateral view of 15-18-somite stage zebrafish larvae, animal to the left. Imaging area boxed in red. (B) Un-injected Buc-GFP embryos showing germ cells (12±1.6, n=15). (C) Injection of Buc-VBM showed reduction of germ cell formation (6±1.0, n=18). (D) Injection of Vasa-BBM showed reduction of germ cell formation (6.3±1.1, n=16). (E) Quantification of number of germ cells. The data presented are averaged from three independent experiments. Therefore, Y-axis represents average germ cell count and X-axis represents injected constructs, Buc-VBM and Vasa-BBM. Error bars represent standard deviation of the mean. Test statistic: Student's t-test. * $P < 0.05$. Scale bar 50 µm

The reduced number of germ cells suggests a dominant-negative effect, which can be explained by an additional molecular interaction, which is required during germ cell specification. In this model, Buc-VBM can interact with endogenous Vasa, but this dimer is not able to bind to a third molecule, which renders the complex inactive. This model predicts that Vasa-BBM would also generate an inactive complex together with endogenous Buc and eventually lead to a reduced number of germ cells. To verify this hypothesis, I overexpressed Vasa-BBM, which should bind to endogenous Buc and form inactive complexes. Indeed, Vasa-BBM overexpression in Buc-eGFP transgenic embryos also showed a reduction of germ cells supporting the hypothesis that Buc-VBM acts as a dominant-negative molecule (Figure 36D). Taken together, these data show that both binding motifs lack another necessary interaction essential for germ cell specification.

2.13. RNA activates zebrafish Vasa helicase activity

Recently, it was shown that Oskar binds to *nanos* RNA (Jeske et al., 2015) *in vivo*. We previously showed that full length Buc but not a Buc deletion mutant with amino acids 1-362 interacts with *nanos3* - 3' UTR (Krishnakumar et al. 2018) *in vivo*. These data suggest that the C-terminal region of Buc has a potential RNA interaction motif. Moreover, binding of an RNA molecule is necessary to complete the closed conformation of ATPase active site in Vasa to increase the ATPase activity (Jankowsky, 2011). Therefore, I analyzed the ATPase activity of Vasa in the presence of RNA.

After incubation of 50 µM ssRNA (polyA$_{(8)}$) with Vasa, I observed higher ATPase activity compared to the control without RNA (Figure 37, red vs. green line). As Buc-VBM stimulates the Vasa ATPase activity, I examined ATPase activity in the presence of Buc-VBM together with ssRNA. Fascinatingly, ATPase activity was even stronger in the presence of Buc-VBM and ssRNA compared to the Vasa helicase core with ssRNA (Figure 37, black vs. red line). This result suggests that RNA enhances the activity of the Buc-Vasa complex. Moreover, the interaction with RNA provides an explanation for the reduction of germ cells upon

overexpression of Buc-VBM and Vasa-BBM, because these peptides might not interact with RNA *in vivo*.

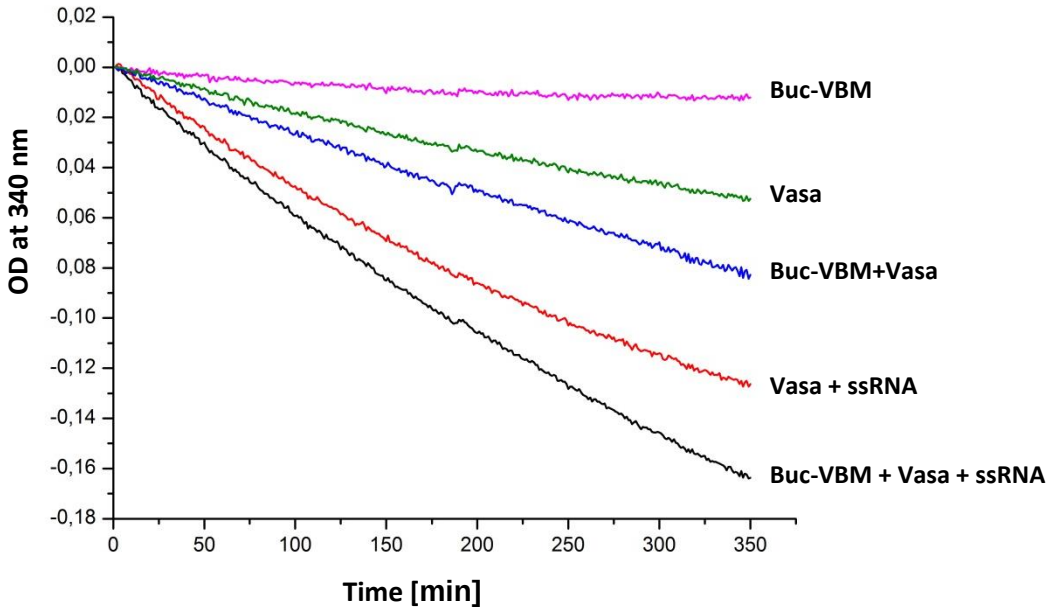

Figure 37: RNA enhances ATPase activity of Vasa.

Buc-VBM activates Vasa helicase activity. Y-axis denotes the reduction of NADH absorption, which is directly proportional to the rate of ATP hydrolysis. The absorbance was measured at 340 nm. X-axis denotes the incubation time in minutes. The data presented are averaged from three independent experiments. Incubation of 100 µM Buc-VBM with 2.5 mM ATP showed mild ATPase activity (pink line). Incubation of 5 µM Vasa with 2.5 mM ATP demonstrated relatively higher ATPase activity (green line). Incubation of 5 µM Vasa with 50 µM ssRNA showed enhanced ATPase activity (red line) compared to 5 µM Vasa with 100 µM Buc-VBM (blue line). Vasa ATPase activity was further enhanced in the presence of ssRNA and Buc-VBM (black line).

2.14. Amino acid D379 in Buc is required for interaction with Vasa

My results in Figure 24 showed that BucΔVBM and VasaΔBBM do not interact *in vivo* with wild-type Vasa and Buc, respectively. Nevertheless, these deletion constructs might not fold into their functional structure without these interaction motifs. Thus, point mutations in the interface of the Buc and Vasa binding site would allow a more meaningful conclusion whether Buc and Vasa interaction is required for germ cell specification. However, there is no structural information available for the Buc-VBM and Vasa interaction. As the Oskar eLOTUS domain interacts with *Drosophila* Vasa RecA-like C-terminal domain, I aligned the peptide sequence of Buc-VBM and Oskar eLOTUS domain to check whether there are any

conserved residues between these two peptides. The alignment revealed three amino acids of Buc-VBM, Aspartate (D379), Glutamate (E386), and Serine (S389), which are conserved between two sequences (Figure 38A).

When I compared the position of these three residues with the predicted secondary structures for Buc-VBM, I discovered that D379 is part of the loop region connecting the two predicted α-helices, while E386 and S389 are part of the second α-helix (Figure 38B).

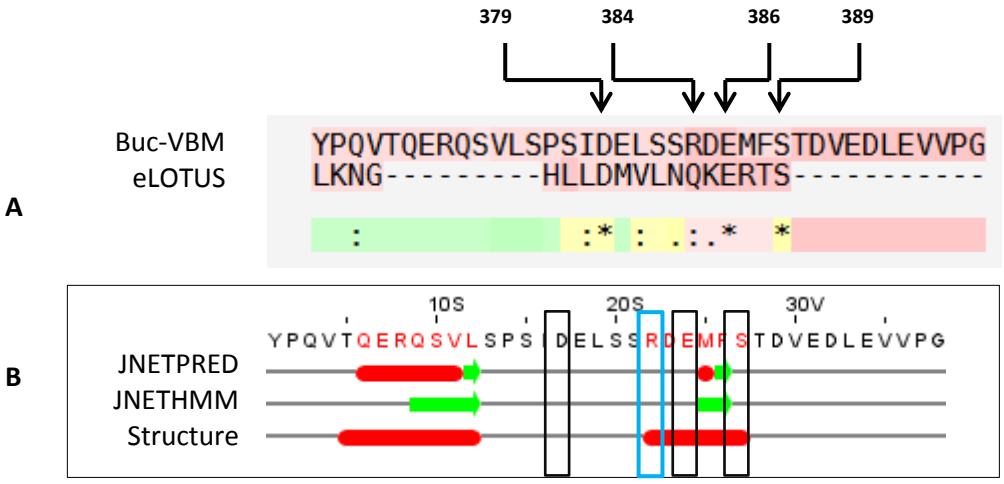

Figure 38: Alignment of Buc-VBM with Oskar eLOTUS domain.

A) Alignment of Buc-VBM and eLOTUS domain revealed that D379, E384 and S386 are conserved between two sequences (black stars and positions of the amino acids are labeled on top of the sequence). In the alignment, an * (asterisk) indicates positions with a fully conserved residue. A ':' (colon) denotes conservation based on strongly similar properties - scoring > 0.5 in the PAM 250 matrix. A '.' (dot) denotes conservation based on weakly similar properties - scoring =< 0.5 in the PAM 250 matrix. (B) Representation of the three amino acids D379, E386 and S389 in JPred secondary structure prediction (black boxes) and a non-conserved amino acid R384 (light blue box) that I used as a control during Buc-VBM mutation experiments.

To study the role of these three amino acids for the interaction with Vasa in BiFC assay, I attempted to create point mutations for D379L (Aspartate to Leucine), E386L (Glutamate to Leucine) and S389A (Serine to Alanine) in in full-length Buc. Unfortunately, the site directed mutagenesis failed in many attempts, so I generated these changes in Buc-VBM. As a control, I mutated a non-conserved amino R384G (Arginine to Glycine). Then I fused the Venus-VC fragment to the C-terminus of each mutant construct to examine their activitiy in

the BiFC assay. After co-injection of D379L, E386L and S389A together with wild-type Vasa, I observed that these mutants Buc showed a reduced fluorescence in the BiFC assay compared to wild-type Buc or Buc R384G (Figure 39).

Among the three mutants, BucD379L had the weakest activity compared to BucE386L and BucS389A (Figure 39). These results suggest that D379 may be a key residue in Buc-VBM for the interaction with Vasa. It seems that the predicted loop region of the Buc-VBM contributes in forming the Buc-Vasa binding interface.

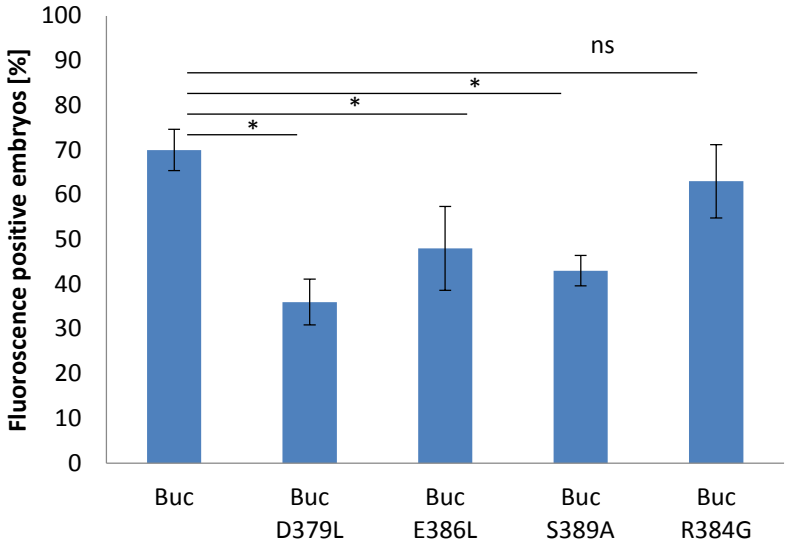

Figure 39: Buc D379L mutation reduces the interaction with Vasa.

The data presented are averaged fluorescent positive embryos from three independent experiments. Therefore, Y-axis represents the average fluorescent positive embryos. X-axis represents the injected mutant Buc constructs. Test statistics: Student's t-test, * P <0.05. Buc mutants including Buc D379L (36±5.1, n= 86), E386L (48±9.4, n= 77), and S389A (43±3.4, n= 50), showed reduction of fluorescent positive embryos compared to wild-type Buc (70±4.6, n= 69) and R382G (63±8.2, n= 63). Test statistics: Student's t-test, * P <0.05.

2.15. Homology model predicts three residues in the Vasa-BBM potentially forming an interface during interaction with Buc

I used the predicted Vasa model as a template to investigate key amino acid residues important to interact with Buc. The predicted Vasa model reveals that the Vasa-BBM consists of one α-helix and a ß-sheet with a flexible loop between them (Figure 40). Surface

representation revealed that three amino acids, S607, S608, I609, of the flexible loop are exposed on the protein surface (Figure 40B). This suggests that these amino acids have a great probability to interact with Buc-VBM.

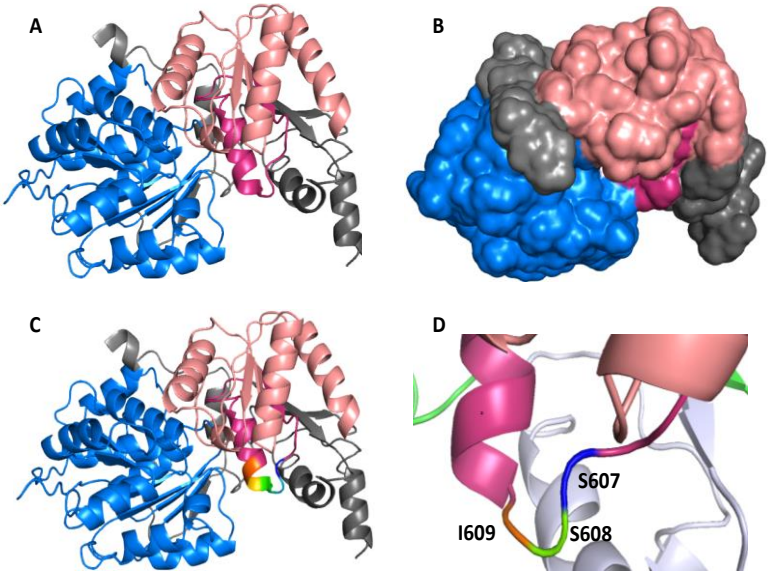

Figure 40: Secondary Structure of Vasa-BBM with exposed amino acids.

(A) Homology model predicted for zebrafish Vasa with RecA like N-terminal domain (blue), RecA like C-terminal domain (light rose) and flanking amino acids (grey). The Vasa-BBM is shown in dark pink. (B) Surface representation of predicted Vasa model showing the exposed region of Vasa-BBM (dark pink). (C) Model highlighting the exposed amino acids in rainbow colors magnified in D. (D) Magnification of exposed amino acids, S607 (blue), S608 (green) and I609 (orange).

In silico mutagenesis analysis using the PyMol tool (The PyMOL Molecular Graphics System, Version 2.2.3 Schrödinger, LLC, Sengoku *et al.*, 2006) identified that mutating S607A (Serine to Alanine), S608A (Serine to Alanine), and I609Q (Isoleucine to Glutamine) greatly disturbs the structural stability of the flexible loop. This makes these residues primary candidates to address their function to maintain the Vasa-Buc binding-interface. After generation of these mutations in full-length Vasa, I injected mRNA of these variants to perform a BiFC-assay with Buc. While VasaS607A and VasaS608 showed a strongly reduced binding with Buc, VasaI609Q mutant completely lost its interaction with Buc (Figure 41).

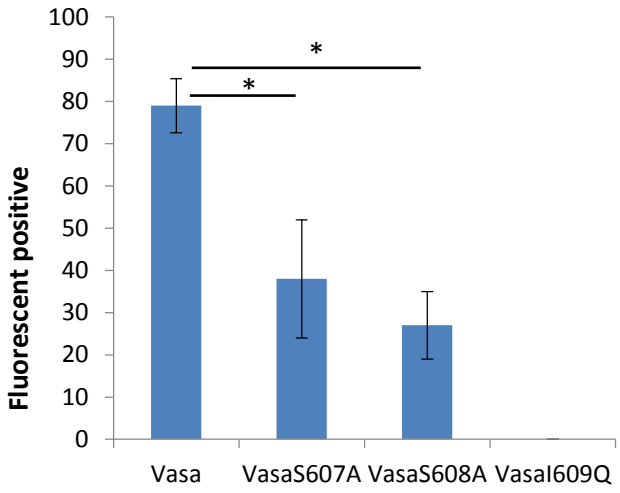

Figure 41: VasaI609Q is critical for interaction with Buc.

The data presented are averaged fluorescent positive embryos from three independent experiments. Therefore, Y-axis represents the average fluorescent positive embryos. X-axis represents the injected mutant Vasa constructs. Test statistics: Student's t-test, * P <0.05. Compared to wild-type Vasa (79±6.4, n = 64), Vasa S607A (38±14.0, n = 55) and Vasa S608A (27±8.0 n = 33) showed a reduced number of fluorescence. Fascinatingly, Vasa I609Q (0±0, n = 61) did not show fluorescent embryos at 3 hpf.

To analyze whether the VasaI609Q decreases the stability, I generated a fusion of this Vasa variants with GFP. Overexpression of the same amount of RNA (200 ng/ µl) of these Vasa variants shows similar expression levels *in vivo* as wild-type Vasa-GFP (Figure 42C and D). These data are consistent with the conclusion that Vasa I609 is not required for the stability of Vasa, but is a critical amino acid for the binding to Buc.

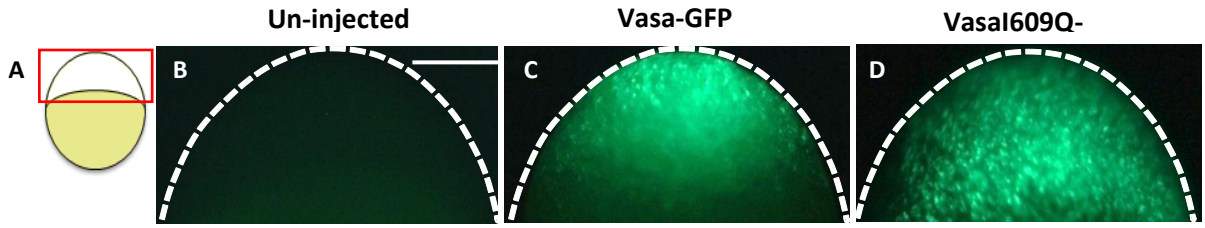

Figure 42: The I609Q mutation does not reduce stability of Vasa *in vivo*.

(A) A cartoon illustrates the lateral view of embryos at 3 hpf, animal to the top. Confocal imaging area boxed in red. This region is outlined with a white dashed line in panel (B-D). (B) VasaI609 showed a similar fluorescent signal in the blastodisc as Vasa-GFP when compared to an un-injected control. Scale bar 200 µm.

2.16. Vasa mutant for ATPase activity induces ectopic germ cells

I discovered that Vasa directly bind to Buc and that this interaction stimulates the ATPase activity of Vasa *in vivo*. It has previously been shown that the T546A mutant of *Drosophila* Vasa abolishes the ATPase activity (Sengoku et al., 2006). However, this variant was only tested *in vitro*. Moreover, in the year 2006 only RNA was known to stimulate the ATPase activity of Vasa, but it was not discovered yet, that Oskar is required to induce full ATPase activity (Jeske et al., 2017; Sengoku et al., 2006). Further, mutants of *Drosophila* Vasa of the residues F504E and F508E do not bind to eLOTUS domain of Oskar losing the ability to be activated (Jeske et al., 2017). Taken together, none of these publications addressed whether the ATPase activity is required for germ cell specification *in vivo*.

To investigate whether the ATPase activity of Vasa is required for germ cell specification, I generated a similar T546A variant of zebrafish Vasa, whose ATPase activity is abolished. Sequence alignment of zebrafish Vasa and *Drosophila* Vasa indicated that *Drosophila* Vasa Threonine 546 (T546) is conserved in zebrafish Vasa as T585 (Figure 43A). I mutated T585A (Threonine to Alanine) and injected into a corner somatic cell in 16-cell stage of embryo. Interestingly, I observed that zebrafish mutant Vasa T585A induced ectopic germ cells comparable to wild-type Vasa (Figure 43B and C), suggesting that germ cell induction by Vasa is independent of its ATPase activity.

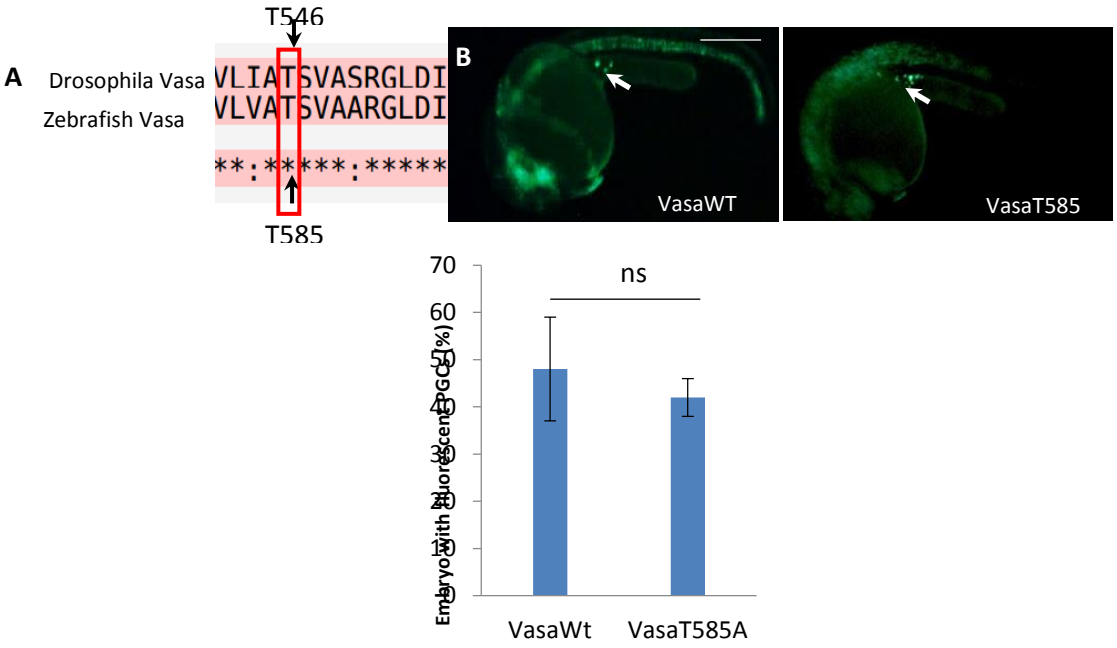

Figure 43: Vasa helicase activity is not required for germ cell induction.

(A) Illustrates partial pair-wise sequence alignment of *Drosophila* Vasa (amino acid 542-555) and zebrafish Vasa (amino acid 581-594). The conserved *Drosophila* Vasa T546 and zebrafish Vasa T585 are highlighted by a red rectangle and the corresponding amino acid position is labelled on the sequence. Full sequence alignment is attached in appendix II (B) After 24 hpf, both wild-type Vasa and VasaT585A induced ectopic fluorescent germ cells (white arrow). (C) Quantification of fluorescent germ cells after injection of wild-type Vasa and VasaT585A into a somatic cell at 16-cell stage embryos. The data presented are averaged germ cells from three independent experiments. Therefore, Y-axis represents average fluorescent PGCs and X-axis represents injected constructs. Error bars represent Standard deviation of the mean. Test statistics: Student's t-test. * $P < 0.05$.

3. Discussion

Buc has been recently identified as the first vertebrate protein that organizes *in vivo* the aggregation of germ plasm. Mutants show that Buc is necessary for germ plasm formation and mRNA injections demonstrate that it is sufficient for the formation of primordial germ cells (Bontems et al., 2009). Zebrafish Buc is specific to vertebrates, but its amino acid sequence encodes a completely novel protein without any known motifs or domains (Bontems et al., 2009). Although Buc is the first vertebrate protein, which has this fascinating activity of inducing germ cells *in vivo*, its amino acid sequence did not provide any biochemical mechanism, by which it exerts this important function.

Instead of initiating a laborious biochemical approach with Buc, which is also hampered by the insolubility of recombinant protein, we developed an "evolutionary" approach to address the biochemical function of Buc. We recently demonstrated that Buc has an equivalent biological function with the *Drosophila* germ plasm organizer Oskar *i.e.* both proteins specify the development of primordial germ cells in zebrafish (Krishnakumar et al., 2018). This is quite remarkable, because Buc and Oskar do not show any sequence homology and an Oskar homolog is not present in the zebrafish genome (Krishnakumar et al., 2018). This publication described for the first time two proteins with equivalent biological function *in vivo* in the absence of sequence similarity.

To explain this novel phenomenon at the biochemical level, we proposed that Buc and Oskar share a conserved interactome. The evolutionary conserved RNA helicase Vasa has been recognized as a critical component because its interaction is conserved between Buc and Oskar (Jeske et al., 2017, 2015; Krishnakumar et al., 2018). Although, structural and functional details are available for Oskar binding to Vasa, no study investigated the consequence of zebrafish Buc and Vasa interaction during germ cell specification. Thus, the aim of my thesis was to characterize the Buc-Vasa complex and investigate the consequence of their interaction for germ cell specification.

3.1. Buc directly binds with Vasa

The amino acid composition of Buc predicts an intrinsically disordered protein (IDP). Thus, after expression of recombinant Buc protein in *Escherichia coli*, Buc was found in the insoluble pellet, but not in the soluble fraction. It seems that recombinant Buc protein is highly aggregated in the pellet fraction, because IDPs have a higher tendency to form hydrogen bonds and many electrostatic interactions via charged amino acids (Linding et al., 2004). Hence, recombinant Buc is not available to examine its structural features and biochemical functions. I therefore chose an alternative approach. There, I isolate a small motif, which interacts with Vasa, which then allows me to study the structural features and biochemical functions of the Buc - Vasa interaction.

Previously, it has been shown that Buc interacts with Vasa both *in vitro* and *in vivo* (Krishnakumar et al., 2018) using co-immunoprecipitation and the BiFC assay. Co-immunoprecipitation can also be performed using *in vitro* translated protein in a cell free system or by extraction of cell lysates. However, these samples are complex as they also contain other proteins in addition to the protein to be examined. Thus, co-immunoprecipitation cannot discriminate whether an interaction is direct or not. In the BiFC assay, reconstitution of fluorophore is dependent on their close proximity of two complementary fragments (Kerppola, 2006a, 2008). Therefore, the fluorescent signal detected by the BiFC assay does not reflect whether two proteins interact directly or not. Pull-down assay with recombinant and purified protein is one of the best alternative approaches to show the direct interaction of two proteins. Thus, pulling-down recombinant GST tagged Buc-VBM with Vasa confirmed that Buc directly binds to Vasa *in vitro* validating the *in vivo* BiFC results. However, addition of excess amount of Vasa while increasing its concentration did not show strong band for Vasa after Coomassie staining. This suggests that the interaction between Buc and Vasa is weak or transient. We discovered Buc interacts with *nanos* mRNA (Krishnakumar et al., 2018) and I observed a strong ATPase activity of Vasa in the presence of Buc-VBM and ssRNA. Thus, I speculate that the interaction between Buc and Vasa probably stabilize in the presence of RNA. Nonetheless, the possibility exists that a contamination of the same molecular weight as Vasa is present in the Coomassie stained gel, which might mediate the interaction between Vasa and Buc. Although this possibility is very

unlikely, one way to test it, would be to cut the Vasa band and sequence the isolated protein by mass-spectrometry. A contaminating protein would then appear by additional sequences.

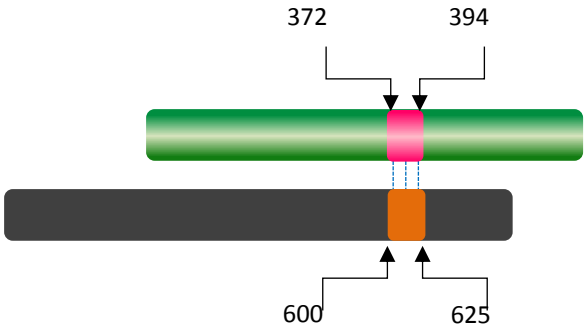

Figure 44: The novel binding motifs in Buc and Vasa.

Full-length of Buc colored in green while Vasa is colored in dark grey. The isolated novel Buc-Vasa binding motif (amino acid 372-394) boxed in pink and Vasa-Buc binding motif (amino acid 600-625) boxed in orange. The direct binding of Buc and Vasa shows in dashed line in blue.

3.2. The novel interaction motifs in Buc and Vasa

Based on the BiFC assay, I isolated two novel interaction motifs, Buc-VBM (amino acid 372-394) and Vasa-BBM (amino acid 600-625) (Figure 44). The amino acid 372-394 in Buc identifies a highly conserved motif in all Buc orthologs (Figure 45). However, for the first time I discovered that this region is responsible to interact with Vasa. Therefore, this conservation actually suggests that other vertebrates with a conserved Buc protein in their genome also use the interaction with Vasa to specify germ cells.

Using structural predictions and mutagenesis experiments, I discovered that the D379 in Buc-VBM is critical for the interaction with Vasa. As I could not generate a D379L mutation in full-length Buc, it was not possible to study the activity of this point mutation in the germ cell induction assay. A loss of germ cell inducing activity of the D379L mutant would suggest that direct binding of Buc to Vasa is central to induce germ cell development. This model is also consistent with the widespread evolutionary conservation of Vasa as a canonical germline marker (Gustafson & Wessel, 2010; Juliano et al., 2010). Most importantly, the identification of D379 as a candidate residue in Buc, which is critical for the interaction with Vasa opens new avenues to investigate germ cell development in vertebrates. For instance, it is now theoretically possible to examine the endogenous role of the Buc-Vasa interaction by using CRISPR-Cas9 mediated mutagenesis in zebrafish. Such an experiment would allow

to confirm *in vivo* whether Buc is indeed an activator of the Vasa's ATPase activity the context of an entire vertebrate. Similarly, the Vasa-BBM was previously not recognized as an interaction surface for other proteins. Furthermore, Vasa I609Q completely reduced its interaction with Buc. This result suggests that compared to the other direct Buc binding protein such as Rbpms2 (Hermes) (Heim et al., 2014), binding of direct binding of Buc to Vasa is key to induce germ cell development.

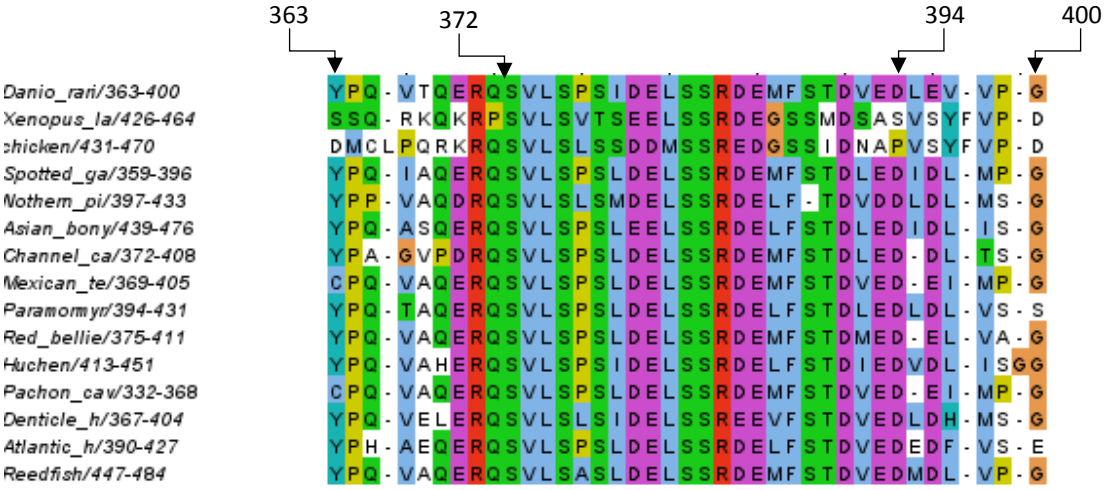

Figure 45: The Buc-VBM is highly conserved among vertebrates.

Alignment of Buc orthologs revealed that the Buc-VBM (amino acid 363-400: labelled on the top of the sequence) is conserved highly conserved among Buc orthologs. Amino acids are colored based on the ClustalX color code. Hydrophobic amino acids are [Alanine (A), Isoleucine (I), Leucine (L), Methionine (M), Phenylalanine (F), Tryptophan (W), Valine (V)] colored in blue. Positively charge amino acids [(Lysine (K) and Arginine(R)] are colored in red. Negatively charge amino acids [(Aspartic acid (D) and Glutamic acid (E)] are colored in magenta. Polar amino acids (Asparagine (N), Glutamine (Q), Serine (S) and Threonine (T)] colored in green. Aromatic amino acids (Histidine (H) and Tyrosine (Y)] colored in cyan. Cystine colored in pink. Glycine colored in orange. Proline colored in yellow

3.3. Buc and Oskar share structural similarities

Previously, we showed the functional equivalence between Buc and *Drosophila* Oskar protein despite no sequence similarity between these two proteins (Krishnakumar et al., 2018). Functional equivalence could be explained by convergent or divergent evolution. In the convergence model, two proteins might have evolved independently to adopt the same function but originate from two independent ancestors. These two genes start their evolution with different genetic mechanisms and selection constraints, but during further

evolution develop a conserved and common interactome to induce germ cells in two different species. In the divergent model, both proteins might have evolved different sequences from a common ancestor, but maintained a conserved interactome for germ cell specification. The conservation of the common interactome is a response to a similar evolutionary pressure to maintain fertility (Wake et al., 2011; Cusanovich et al., 2014).

Do my results support the convergent or the divergent evolution model of germ plasm organizers? The crystal structure solved for the *Drosophila* Oskar LOTUS-Vasa complex revealed that the α2 helix of the Drosophila Vasa RecA like C-terminal domain interfaces with α2 helix and α5 helix of the LOTUS domain (Jeske et al., 2017). The α2 helix of the LOTUS domain is one of the trihelical bundle helices of the winged HTH core while the α5 helix is found in the C-terminal region of the LOTUS domain (Figure 29). Remarkably, the crystal structure of the LOTUS domain did not show any secondary structure for the C-terminal region of LOTUS domain suggesting that it is disordered. However, the α5 helix in the LOTUS domain forms as soon as it binds to Vasa suggesting that the secondary structure of the C-terminal extension is induced, when it interacts with Vasa (Figure 30) (Jeske et al., 2017).

To support the stated hypothesis, that Buc and Oskar would share structural identity during their interaction with Vasa, I performed *in sillico* secondary structure prediction for Buc-VBM as an alternative approach to crystallization. I used CFSSP, PEP2D and Jnet, which are the three predominantly used algorithms in structural biology to predict protein secondary structures. In addition, I performed CD-spectroscopy to measure secondary structures of the Buc-VBM in the presence and absence of the crowding agent Trifluroethanol (TFE). Together, *in silico* predictions and CD-spectroscopy data revealed that Buc-VBM has a disordered state with a high probability to form α-helices in increasing concentrations of crowding agents. Therefore, the Buc-Vasa complex shares some structural identity during their interaction just like the *Drosophila* Oskar-Vasa complex (Figure 46).

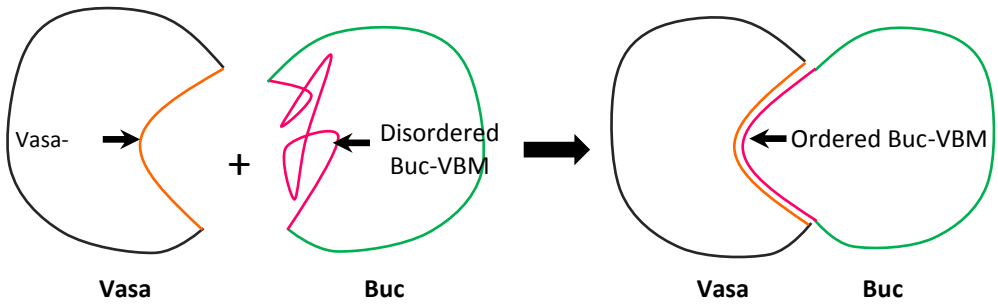

Figure 46: Buc-VBM adopts secondary structure from its disordered state.

. (A) Representation of Vasa and Buc interaction. The Vasa-BBM is colored in orange. Rest of the Vasa sequence colored in dark grey. The disordered Buc-VBM is colored in pink. Rest of the Buc sequence is colored in green (B) The disordered Buc-VBM adopts ordered structures after interaction with Vasa-BBM.

Indeed, my data showed that amino acids in the predicted helix of Buc (E386 and S389) or in the turn stabilizing the helix (D379) are critical in Buc to interact with Vasa. Remarkably, I609 in Vasa seems to be a key residue for the interaction with Buc. These findings raise a number of open questions *e.g.* is there a conserved residue like I609 in *Drosophila* Vasa? Which residues in Buc and zebrafish Vasa are indeed involved in stabilizing the contact between the two proteins. However, in depth understating of Buc and Vasa interaction is difficult due to lack of structural data. Therefore, co-crystallization of recombinant Buc-VBM together with Vasa would provide better insight to understand the Buc and Vasa interaction.

During my thesis, I tried to co-crystalize the Buc-Vasa complex. There, I initially performed pre-crystallization tests to find out the appropriate protein concentration of Buc-VBM (amino acid 363-400) and Vasa (amino acid 227-670) for crystallization screening. After setting up the protein crystallization screen, I could not get crystals for the Buc-VBM and Vasa complex. Thereafter, started to optimize the crystallization screen changing various parameters such as buffer condition, protein concentration, addition of additives, pH and temperature. However, I did not observe any crystal growth after those optimizations. Nevertheless, one way to optimize the co-crystallization is based on an alternative optimization strategy, which is known as the seeding method. For this, I plan to use crystal particles of the DEAH helicase, ctPrp22 (Hamann et al., 2019) due to evolutionary conservation of DEAD and DEAH-box helicase. Therefore, I expect that addition of crystal particles of ctPrp22 crystals into the crystallising solution of Buc-VBM-Vasa complex could probably facilitate crystal growth.

3.4. Helicase activity of DEAD box protein is modulated by protein cofactors

It has been shown that certain RNA binding proteins act as cofactors to stimulate helicase activity of DEAD box helicases (Rogers et al., 2001). For example, eukaryotic translation initiation factor, eIF4B stimulates the helicase activities of eIF4A and eIF4F while eIF4H also stimulates the helicase activity of eIF4A (Rogers et al., 2001). In addition, yeast cytoplasmic nucleoporin, Gle1 bound to a small molecule, inositol hexakisphosphate (IP6), stimulates the ATPase activity of Dbp5p at the nuclear pore during mRNA export (Bolger & Wente, 2011).

Moreover, G-patch domain containing proteins have been extensively recognized as cofactors, which stimulate ATPase activity of DEAH RNA helicases (Sloan & Bohnsack, 2018). For instance, G-patch protein Pfa1p stimulates ATPase activity of the DEAH helicase, Prp43p during yeast ribosome biogenesis (Lebaron et al., 2009). Further, Spp2 acts as a cofactor to accelerate the ATPase activity of Prp2, a DEAH helicase during remodelling the spliceosome complex (Warkocki et al., 2015). These data show that protein cofactors are required to modulate helicase activity of DEAD/H helicases.

3.5. The Oskar LOTUS domain and Buc-VBM stimulate the helicase activity of Vasa

Remarkably, it has been shown that the Oskar LOTUS domain stimulates the ATPase activity of *Drosophila* Vasa upon their interaction albeit Oskar does not belong to any protein family of the known putative helicase regulating cofactors like the mentioned G-patch proteins (Jeske et al., 2017). This study in *Drosophila* therefore reports for the first-time the active form of Vasa since its discovery (Schupbach & Wieschaus, 1986). Consistent with this finding, I demonstrated that Buc-VBM indeed activates zebrafish Vasa ATPase activity *in vitro*. This discovery assigns the first biochemical function to Buc as a novel cofactor, which stimulates the ATPase activity of zebrafish Vasa.

This result also solves an open question about the role of Vasa in germline development. In some organisms like *Drosophila*, the Vasa protein is restricted to the germline. By contrast, in other species like zebrafish, Vasa is ubiquitous and then gets restricted to the germline during later embryogenesis. According to my data, the expression of Vasa is not a molecular marker for the prospective germline, but rather its activity. Unfortunately, the product of "active" Vasa is not known. Instead, my data suggest that the expression or localization of the Vasa activator like Buc or Oskar is currently the best molecular marker to predict the future germ cells of the embryo. Unfortunately, Buc and Oskar seem to be restricted to a few species and change their amino acid sequence rapidly, which makes the identification of homologous proteins in other species difficult (Krishnakumar & Dosch, 2018).

3.6. Post-translational modification of Vasa and Buc is important for germ line development

Arginine methylation has been identified as an important post-translational modification (PTM) involved in various biological functions such as RNA processing, protein-protein interactions, DNA repair and gene regulation (Zhu et al., 2019). It has been shown that Vasa undergoes both asymmetric (aDMA) and symmetric dimethylation (sDMA) of arginine by protein methyltransferases (PRMTs) and that this methylation is conserved across phyla (Kirino et al., 2010; Vourekas et al., 2010).

It has been recently reported that in prmt5−/− zebrafish the sDMA of Vasa is disrupted, which resulted in defects in germ cell development during early embryonic development in addition to failure of gonad differentiation in adult zebrafish (Zhu et al., 2019). The defect in germ cell development could be caused by reduced or inhibited interaction between Buc and Vasa as prmt5−/− zebrafish disrupt the sDMA of Vasa. Further, it has been shown that RNA binding protein are the major targets of PRMTs (Pahlich et al., 2006).

As zebrafish Vasa indeed is an RNA binding protein, disruption of sDMA of Vasa would probably have an effect on RNA metabolism, such as mRNA transcription, splicing, transport, translation, and turnover. With my data I showed that Buc stimulates zebrafish Vasa helicase

activity. Therefore, I believe, that regulation of RNA metabolism involve in germ cell specification pathway is taking place upon Vasa activation by Buc. As a consequence, disruption of sDMA of Vasa probably inhibit its downstream functions related to RNA metabolism, thus, defect in germ cell development.

Moreover, recently it has been shown that the C-terminal region of Buc is a target of sDMAs, which is essential for interaction with Tdrd6a (Roovers et al., 2018). The interaction with Tdrd6a is critical to regulate the solubility, accumulation and mobility of Buc within the germ plasm thereby maintaining liquid-liquid phase separation of germ plasm and eventually PGC formation during early embryogenesis (Roovers et al., 2018).

3.7. Importance of C-terminal region of Buc during germ cell specification

Previously I showed that mutant $BucP^{106}$ (amino acid 1-601), which lacks the terminal 38 amino acids and Buc-VBM (amino acid 372-394) do not induce ectopic germ cells in germ cell induction assay. Moreover, we showed that Buc interacts with *nanos3* mRNA (Krishnakumar et al., 2018). Physiochemical properties revealed that the terminal 38 amino acids are positively charge as the region is rich in arginine and Lysine. Therefore, we speculated that this region is has a high potential to interact with RNA. Therefore, I hypothesized that in the first step, Buc interacts with RNA. Then Buc binds to Vasa through their Buc-Vasa binding motifs. Thereafter, Buc presents the interacted RNA molecule to Vasa as Vasa involves in RNA processing. Further, the RNA processing will be regulated through triggering Vasa helicase activity stimulated by Buc (Figure 47). My results revealed indeed helicase activity of Vasa is higher in the presence Buc-VBM and RNA (Figure 37) supporting the above hypothesis. Therefore, mapping the RNA binding motif in Buc will provide more details to understand the role of Buc in germ cell specification.

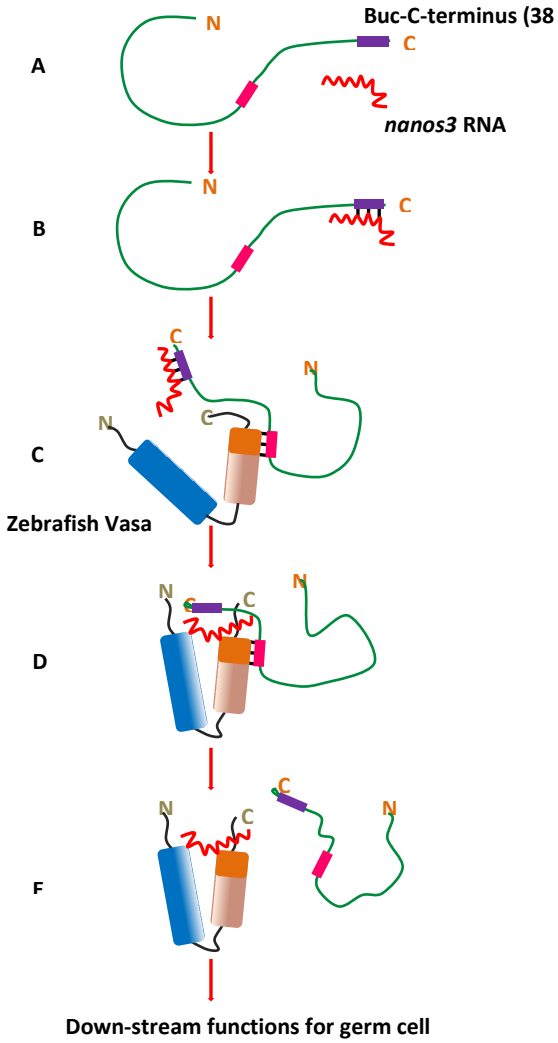

Figure 47: Hypothetical model illustrating potential role of Buc, Vasa, RNA germ cell specification.

(A) Buc protein shown as green line. The Buc-VBM boxed in pink and the terminal 38 amino acids boxed in purple. *nanos3* RNA shown in red wavy line. The N-and C-terminus of Buc denoted as 'N' and 'C' in orange color. (B) *nanos3* RNA binds to the C-terminal region of Buc. (C) Vasa protein with its open conformation. The RecA like N-terminal domain of Vasa boxed in blue while RecA like C-terminal domain boxed in rose. The N-and C-terminus of Vasa denoted as 'N' and 'C' in light brown color. Buc carries *nanos3* RNA and bind to Vasa through the Buc-VBM (pink) in Buc and Vasa-BBM (orange) in Vasa. (D) Buc presents the *nanos3* RNA to Vasa and Vasa complete its closed conformation. (E) Buc released from the Vasa and Vasa perform its downstream functions to promote germ cell specification.

Considering the interaction of RNA and Tdrd6a with Buc, I speculate that these two interactions probably play a role to establish the specificity of Buc and Vasa interaction during germ cell specification. Because, the mutant $BucP^{106}$ lacks the terminal 38 amino acids. According to the hypothesis, now Buc^{p106} cannot interact with RNA or Tdrd6a. As a result, $BucP^{106}$ lacks its specificity for Vasa, even though $BucP^{106}$ has the Vasa binding motif,

thus resulting in defects in germ cell specification (Figure 48). Further, the defect in PGC formation in tdrd6a $^{-/-}$ mutants has been explained by the insufficient accumulation of germ plasm mRNP granules in the absence of Tdrd6a (Roovers et al., 2018). Therefore, Tdrd6a may have other function in addition to regulating Buc-Vasa interaction specificity.

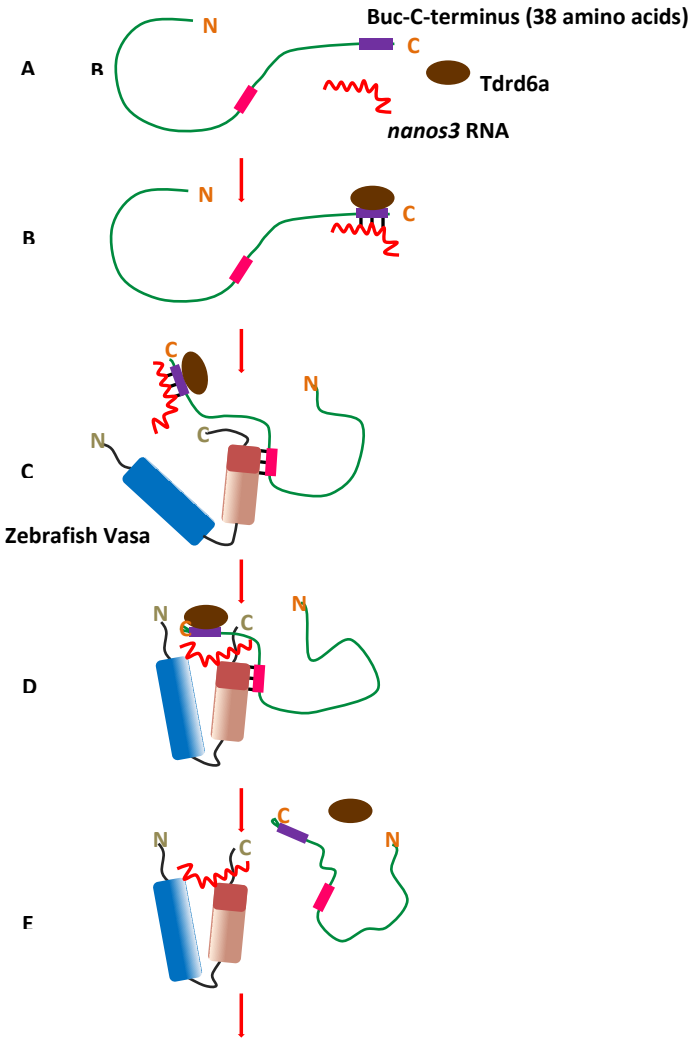

Figure 48: Hypothetical model illustrating potential role of Buc, Vasa, RNA and Tdrd6a during germ cell specification.

(A) Buc protein shown as green line. The Buc-VBM boxed in pink and the terminal 38 amino acids boxed in purple. *nanos3* RNA shown in red wavy line and Tdrd6a shown in brown oval. The N-and C-terminus of Buc denoted as 'N' and 'C' (B) Tdrd6a and *nanos3* RNA binds to the C-terminal region of Buc. (C) Vasa protein with its open conformation. The RecA like N-terminal domain of vasa boxed in blue while RecA like C-terminal domain boxed in rose. The N-and C-terminus of Vasa denoted as 'N' and 'C' in light brown color. Buc carries *nanos3* RNA and Tdrd6a and bind to Vasa through the Buc-VBM and Vasa-BBM. (D) Buc presents the *nanos3* RNA to Vasa and Vasa complete its closed conformation. (E) Buc and Tdrd6a are released from the Vasa and Vasa perform its downstream functions.

3.8. Is the helicase activity of Vasa necessary for germ cell formation?

I found that Buc-VBM stimulates Vasa helicase activity. Surprisingly, I showed that a Vasa mutant for helicase activity, Vasa T585A induced ectopic germ cells. This finding contradicts the conclusion that germ cell formation requires Vasa's helicase activity. For this conclusion I would first need not to confirm that VasaT585A's has no helicase activity in *in vitro* assays as performed in Figure 34. Therefore, first, I would need to verify that the Vasa T585A mutation participates in ATP hydrolysis in zebrafish even though it looks conserved with *Drosophila* T546, which was already shown to abolish Vasa's ATPase activity (Sengoku et al., 2006). Interestingly, the Vasa mutant for helicase activity has never been used *in vivo* to examine its function in the germline. The reason might be that the helicase activity is not required for germ cell specification.

Alternatively, recently two mutations, K295N located in the flanking sequence upstream to the RecA like N-terminal domain and E400Q mutation in conserved DEAD motifs located in the RecA like N-terminal domain in *Drosophila* Vasa, have been show to interfere with helicase activity (Durdevic & Ephrussi, 2019; Xiol et al., 2014). I found that these two amino acids are indeed conserved as K326N and E435Q in the RecA like N-terminal domain of zebrafish Vasa. These mutations in Vasa need to be studied first by *in vitro* ATPase assay followed by germ cell induction assay in zebrafish to investigate importance of helicase activity during germ cell specification.

3.9. Investigate the hierarchy of germ cell specification pathway

The investigation of zebrafish germ cell specification pathway after fertilization is technically challenging. For example, it is impossible to investigate protein function after fertilization by genetics, bsince all proteins are produced maternally during oogenesis. One can therefore not mutate an allele in a way, that it loses the maternal contribution of Buc and Vasa during early embryogenesis. Therefore, it needs an alternative approach to remove endogenous protein. It has been reported that endogenous protein can be achieved by using deGradFP (Caussinus et al., 2012) or Trim-away system (Clift et al., 2018).

deGradFP system contains a Ubquitin binding element and a GFP nanobody. After GFP nanobody binds to GFP moiety of GFP-tagged protein, the protein complex is targeted to ubiquitin-proteasome pathway for protein degradation (Caussinus et al., 2012) Buc-GFP transgenic fish which were generated in the *buc* mutant background can be used in dGradFP system. To do so, dGradFP mRNA can be injected into one-cell stage Buc-GFP embryos and depletion of Buc can be monitored by checking the GFP signal. If there is no GFP signal after 24 hpf compared to uninjected embryos, it means Buc was degraded and no germ cells have been formed. To confirm no detectable germ cells, embryos can be fixed and stained for germ cell markers, such as Vasa.

Nevertheless, until now no Vasa-GFP transgenic fish line has been generated which rescues the vasa mutant phenotype similar to the Buc-GFP line (cite Riemer). Therefore, the trim-away system provides a great opportunity to degrade maternally provided Vasa during early embryogenesis. The Trim-Away system is based on an E3 ubiquitin ligase called tripartite motif-containing protein 21 (TRIM21). TRIM21 is known to bind antibody-bound pathogens through the Fc domain of bound antibody and then to target them to the ubiquitin-proteasome pathway for protein degradation (Clift et al., 2018). To perform the trim-away experiment, anti-Vasa antibody would be injected into one-cell stage embryos. After 24 hpf, embryos can be fixed and stained with Buc antibody to check germ cell formation. If germ cells are detected after depletion of Vasa and no germ cells are detected after depleting Buc, it would suggest that Buc is upstream to Vasa and it is necessary for germ cell formation (Figure 48). Nontheless, my results propose for the first time that Buc acts as a novel regulator of Vasa activity thereby integrating this novel protein into known pathways of germline development.

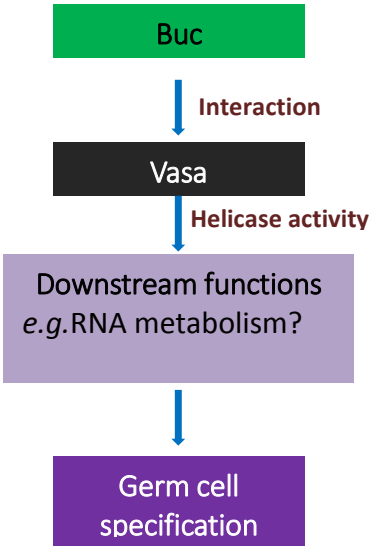

Figure 49: Hypothetical hierarchy of germ cell specification.

According to the data, Buc binds with Vasa. Then Buc stimulates Vasa's helicase activity. The helicase activity regulates the downstream functions such as RNA processing during germ cell specification.

4. Materials and Methods

4.1. Zebrafish handling and maintenance

Zebrafish (*Danio rerio*) were used as a model organism. Experiments were performed using AB*TLF zebrafish (wild-type) and Buc-GFP transgenic zebrafish line (Stephan 2015). All the fish were maintained and fed according to the standard protocol (Westerfield, 2000).

4.2. Manipulation of zebrafish embryos

4.2.1. Microinjection

Pulled 1.0 mm OD injection needles with a micropipette puller device with following settings, heat =515, pull= 228, vel = 80, time= 250. Agarose (1.5% in 1X E3 medium; (5 mM NaCl, 0.17 mM KCl, 0.33 mM CaCl2, 0.33 mM MgSO4, 0.00001 % methylene blue)) plates were prepared placing a mold with wedge-shaped troughs to make grooves in the plates, which facilitates holding embryos during microinjection. Capped sense RNA were diluted in nuclease-free water and 0.025 - 0.05% phenol red and 0.1 M KCl. Calibrated the needles in which it injects approximately 0.5 nl of working solution. One-cell stage embryos were injected with 1 nl of diluted RNA with indicated RNA concentration.

4.2.2. Dechorionation

Embryos were manually dechorionated using dumont (#5) watchmaker forceps for imaging purpose. For co-immunoprecipitation experiments, embryos were enzymatically dechorionated using pronase (stock [30 mg/ml] ; Roche, Mannheim) to a final concentration 3 mg/ml in 1X E3 medium. After 5-10 minutes incubation, floating chorions were decanted and embryos were washed three times with 1X E3 medium. Then, embryos were transferred using fire polished Pasteur pipette.

4.2.3. Deyolking

Approximately 200 dechorionated embryos were transferred into 1 ml of cold ½ Ginzburg Fish Ringer deyolking buffer (55 mM NaCl, 2.7 mM CaCl2, 1.8 mM KCl, 1.25 mM NaHCO3). The embryos were triturated using 200 µl pipette tip once and released them back into the buffer slowly. After embryos were shaken for 5 min at 1100 rpm at 4 ^{o}C to dissolve the yolk. Embryonic cells were pelleted at 1100 rpm for 2 minute and discarded the supernatant. Re-suspended the pellet using 1 ml of wash buffer (110 mM NaCl, 3.5 mM KCl, 2.7 mM $CaCl_2$, 10 mM Tris/Cl pH8.5) and sample was shaken for 1 min at 1100 rpm. Cells were pelleted at 1100 rpm for 1 minute and discarded the supernatant. Two additional wash steps were performed as described.

4.2.4. Preparation of embryo lysates

Deyolked embryonic cell pellets were re-suspended in 2X SDS loading buffer (100 mM Tris (pH 6.8), 20 % glycerol, 4 % SDS, 200 mM β-mercaptoethanol, 0.02 % bromophenol blue). Then samples were incubated at 95 °C for 5 minutes. Allowed to samples to cool down at room temperature. After that samples were centrifuged at 13 000 rpm for 10 minutes to remove contaminants. Supernatant was transferred and used for SDS-polyacrylamide gel electrophoresis.

4.3. Plasmid vectors and constructs

4.3.1. Plasmid vectors for In-Fusion cloning

pCS2+ multipurpose mammalian expression vector was used to clone BiFC, GFP-fusion and mCherry-fusion protein constructs.

4.3.2. Plasmid vectors for Gateway cloning

Gateway entry clones were generated by using pDONR221 vector while expression clones were generated by using pCSDest or pGCS vectors, which are originated from pCS-vector backbone.

Table 2: Cloned vector and expression construct

Plasmid	Vector	Insert	Stratergy
Buc-VBM experiments			
pCS2+ BucWT	PCS2+	buc full-length	(Bontems et al., 2009)
pCS2+ BucWT-VC	PCS2+	buc full-length	pCS2+VC empty vector used to clone the construct. In-Fusion cloning primers were designed selecting BamHI and XbaI sites from the pCS2+VC vector and the vector was linearized using the same restriction enzymes. Buc 1-639 sequence was amplified with using pCS2+ BucWT as a template. PCR products were recombined into the linearized vector in a standard In-Fusion reaction.
pCS2+ VC-BucWT	PCS2+	buc full-length	pCS2+VC empty vector used to clone the construct. In-Fusion cloning primers were designed selecting BamHI and XbaI sites from the pCS2+VC vector and the vector was linearized using the same restriction enzymes. Buc 1-639 sequence was amplified with using pCS2+ BucWT as a template. PCR products were recombined into the linearized vector in a standard In-Fusion reaction.
pCS2+ Buc (1-362aa)-VC	PCS2+	buc 1-362aa	pCS2+VC empty vector used to clone the construct. In-Fusion cloning primers were designed selecting BamHI and XbaI sites from the pCS2+VC vector and the vector was linearized using the same restriction enzymes. Buc 1-362 sequence was amplified with using pCS2+ BucWT as a template. PCR products were recombined into the linearized vector in a standard In-Fusion reaction.

Plasmid	Vector	Insert	Stratergy
pCS2+ Buc (363-639aa)-VC	PCS2+	buc 363-639 aa	pCS2+VC empty vector used to clone thie construct. In-Fusion cloning primers were designed selecting BamHI and XbaI sites from the pCS2+VC vector and the vector was linearized using the same restriction enzymes. Buc 363-639 sequence was amplified with using pCS2+ BucWT as a template. PCR products were recombined into the linearized vector in a standard In-Fusion reaction.
pDONR Buc(363-400aa)	pDONR	buc 363-400 aa	Designed gateway *attB1*FW and *attB2*RV primers. Buc 363-400 sequence was amplified using pCS2+ BucWT as a template. PCR products were recombined into pDONR221 vector in a standard gateway BP cloning reaction.
pCSDest_Buc(363-400aa)-VC	pCSDest		Generated donor vector was recombined into pCSDest-C-VC vector.
pDONR Buc(401-639aa)	pDONR	buc 401-639 aa	Designed gateway *attB1*FW and *attB2*RV primers. Buc 400 -639 sequence was amplified using pCS2+ BucWT as a template. PCR products were recombined into pDONR221 vector in a standard gateway BP cloning reaction..
pCSDest_Buc(401-639)-VC	pCSDest		Generated donor vector was recombined into pCSDest-C-VC vector.
pDONR Buc(372-394aa)	pDONR	buc 372-394 aa	Designed gateway *attB1*FW and *attB2*RV primers. Buc 372-394 sequence was amplified using pCS2+ BucWT as a template. PCR products were recombined into pDONR221 vector in a standard gateway BP cloning reaction.
pCSDest_Buc(372-394)-VC	pCSDest		Generated donor vector was recombined into pCSDest-C-VC vector

Plasmid	Vector	Insert	Stratergy
pCS2+ BucDetla(372-394aa)-VC	pCS2+	buc Δ372-394 aa	pCS2+VC empty vector used to clone this construct. In-Fusion cloning primers were designed selecting BamHI and XbaI sites in addition to the gene specific overlap PCR primers. The vector was linearized using the same restriction enzymes. Buc 1-371 and 395-639 sequences were amplified using pCS2+ BucWT as a template. Purified these PCR products were then mixed in a standard overlap extension PCR reaction to generate final construct. The final PCR product was recombined into the linearized vector in a standard In-Fusion reaction
pCS2+ BucDetla(372-394aa)-GFP	pCS2+	buc Δ372-394 aa	pCS2+GFP (stop)vector used to clone this construct. In-Fusion cloning primers were designed selecting BamHI and XbaI sites from the pCS2+GFP vector and the vector was linearized using the same restriction enzymes. Buc Δ372-394 sequence was amplified using pCS2+ BucDetla (372-394aa)-VC as a template. PCR products was recombined into the linearized vector in a standard In-Fusion reaction.
Buc mutant			
pCSDest BucD379L-VC	pCSDest	buc 363-400 aa	Designed primers with 15-20 bp of complementary sequence on either side of the desired mutation. Complete pCSDest Buc(363-400)-VC vector was amplified in standard site directed mutagenesis PCR reaction. Template plasmid was removed by DpnI restriction enzyme digestion and 5 µl of PCR sample was transformed into XL1-Blue cells and plated. Screened colonies for positive mutation.
pCSDest BucE386L-VC	pCSDest	buc 363-400 aa	Designed primers with 15-20 bp of complementary sequence on either side of the desired mutation. Complete pCSDest Buc(363-400)-VC vector was amplified in standard site directed mutagenesis PCR reaction. Template plasmid was removed by DpnI restriction enzyme digestion and 5 µl of PCR sample was transformed into XL1-Blue cells and plated. Screened colonies for positive mutation.

Plasmid	Vector	Insert	Stratergy
pCSDest BucS389A-VC	pCSDest	buc 363-400 aa	Designed primers with 15-20 bp of complementary sequence on either side of the desired mutation. Complete pCSDest Buc(363-400)-VC vector was amplified in standard site directed mutagenesis PCR reaction. Template plasmid was removed by DpnI restriction enzyme digestion and 5 µl of PCR sample was transformed into XL1-Blue cells and plated. Screened colonies for positive mutation.
pCSDest BucR384G-VC	pCSDest	buc 363-400 aa	Designed primers with 15-20 bp of complementary sequence on either side of the desired mutation. Complete pCSDest Buc(363-400)-VC vector was amplified in standard site directed mutagenesis PCR reaction. Template plasmid was removed by DpnI restriction enzyme digestion and 5 µl of PCR sample was transformed into XL1-Blue cells and plated. Screened colonies for positive mutation.
Vasa-BBM experiments			
pCSDest VasaWT	pCS2+	Vasa 1-715 aa	(Krishnakumar et al., 2018)
pCS2+ Vasa-VN	pCS2+	Vasa 1-715 aa	pCS2+VN empty vector used to clone the construct. In-Fusion cloning primers were designed selecting BamHI and XbaI sites from the pCS2+VN vector and the vector was linearized using the same restriction enzymes. Vasa 1-715 sequence was amplified using pCSDest VasaWT as a template. PCR products were recombined into the linearized vector in a standard In-Fusion reaction.
pCS2+ VN-Vasa		Vasa 1-715 aa	pCS2+VN empty vector used to clone the construct. In-Fusion cloning primers were designed selecting BamHI and XbaI sites from the pCS2+VN vector and the vector was linearized using the same restriction enzymes. Vasa 1-715 sequence was amplified with using pCSDest VasaWT as a template. PCR products were recombined into the linearized vector in a standard In-Fusion reaction.

Plasmid	Vector	Insert	Stratergy
pCS2+ Vasa(1-277aa)-VN		Vasa 1-277 aa	pCS2+VN empty vector used to clone the construct. In-Fusion cloning primers were designed selecting BamHI and XbaI sites from the pCS2+VN vector and the vector was linearized using the same restriction enzymes. Vasa 1-277 sequence was amplified using pCSDest VasaWT as a template. PCR products was recombined into the linearized vector in a standard In-Fusion reaction.
pCS2+ Vasa(278-715aa)-VN	pCS2+	Vasa 278-715 aa	pCS2+VN empty vector used to clone the construct. In-Fusion cloning primers were designed selecting BamHI and XbaI sites from the pCS2+VN vector and the vector was linearized using the same restriction enzymes. Vasa 278-715 sequence was primers using pCSDest VasaWT as a template. PCR products were recombined into the linearized vector in a standard In-Fusion reaction.
pDONR Vasa(278-495aa)	pDONR	Vasa 278-495 aa	Designed gateway *attB1* FW and *attB2* RV primers. Vasa 278-495 sequence was amplified using pCS2+ pCSDest VasaWT as a template. PCR products were recombined into pDONR221 vector in a standard gateway BP cloning reaction.
pCSDest Vasa(278-495aa)-VN	pCSDest		Generated donor vector was recombined into pCSDest-C-VN vector.
pDONR Vasa(496-715aa)	pDONR	Vasa 496-715 aa	Designed gateway *attB1* FW and *attB2* RV primers. Vasa 496-715 sequence was amplified using pCS2+ pCSDest VasaWT as a template. PCR products were recombined into pDONR221 vector in a standard gateway BP cloning reaction.
pCSDest Vasa(496-715aa)-VN	pCSDest		Generated donor vector was recombined into pCSDest-C-VN vector.

Plasmid	Vector	Insert	Stratergy
pDONR Vasa(496-623aa)	pDONR	Vasa 496-623 aa	Designed gateway *attB1* FW and *attB2* RV primers. Vasa 496-623 sequence was amplified using pCS2+ pCSDest VasaWT as a template. PCR products were recombined into pDONR221 vector in a standard gateway BP cloning reaction.
pCSDest Vasa(496-623aa)-VN	pCSDest		Generated donor vector was recombined into pCSDest-C-VN vector.
pDONR Vasa(624-715aa)	pDONR	Vasa 624-715 aa	Designed gateway *attB1* FW and *attB2* RV primers. Vasa 624-715 sequence was amplified using pCS2+ pCSDest VasaWT as a template. PCR products were recombined into pDONR221 vector in a standard gateway BP cloning reaction.
pDONR Vasa(545-715aa)	pDONR	Vasa 545-715 aa	Designed gateway *attB1* FW and *attB2* RV primers. Vasa 545-715 sequence was amplified using pCS2+ pCSDest VasaWT as a template. PCR products were recombined into pDONR221 vector in a standard gateway BP cloning reaction.
pCSDest Vasa(545-715aa)-VN	pCSDest		Generated donor vector was recombined into pCSDest-C-VN vector.
pDONR Vasa(496-665aa)	pDONR	Vasa 496-665 aa	Designed gateway *attB1* FW and *attB2* RV primers. Vasa 496-665 sequence was amplified using pCS2+ pCSDest VasaWT as a template. PCR products were recombined into pDONR221 vector in a standard gateway BP cloning reaction.
pCSDest Vasa(496-665aa)-VN	pCSDest		Generated donor vector was recombined into pCSDest-C-VN vector.
pDONR Vasa(600-715aa)	pDONR	Vasa 600-715 aa	Designed gateway *attB1* FW and *attB2* RV primers. Vasa 600-715 sequence was amplified using pCS2+ pCSDest VasaWT as a template. PCR products were recombined into pDONR221 vector in a standard gateway BP cloning reaction.
pCSDest Vasa(600-715aa)-VN	pCSDest		Generated donor vector was recombined into pCSDest-C-VN vector.

Plasmid	Vector	Insert	Stratergy
pDONR Vasa(545-615aa)	pDONR	Vasa 545-615 aa	Designed gateway *attB1* FW and *attB2* RV primers. Vasa 545-615 sequence was amplified using pCS2+ pCSDest VasaWT as a template. PCR products were recombined into pDONR221 vector in a standard gateway BP cloning reaction.
pCSDest Vasa(545-615aa)-VN	pCSDest		Generated donor vector was recombined into pCSDest-C-VN vector.
pDONR Vasa(600-655aa)	pDONR	Vasa 600-655 aa	Designed gateway *attB1* FW and *attB2* RV primers. Vasa 600-655 sequence was amplified using pCS2+ pCSDest VasaWT as a template. PCR products were recombined into pDONR221 vector in a standard gateway BP cloning reaction.
pCSDest Vasa(600-655aa)-VN	pCSDest		Generated donor vector was recombined into pCSDest-C-VN vector.
pDONR Vasa(600-645aa)	pDONR	Vasa 600-645 aa	Designed gateway *attB1* FW and *attB2* RV primers. Vasa 600-645 sequence was amplified using pCS2+ pCSDest VasaWT as a template. PCR products were recombined into pDONR221 vector in a standard gateway BP cloning reaction.
pCSDest Vasa(595-645aa)-VN	pCSDest		Generated donor vector was recombined into pCSDest-C-VN vector.
pDONR Vasa(600-635aa)	pDONR	Vasa 600-635 aa	Designed gateway *attB1* FW and *attB2* RV primers. Vasa 600-635 sequence was amplified using pCS2+ pCSDest VasaWT as a template. PCR products were recombined into pDONR221 vector in a standard gateway BP cloning reaction.
pCSDest Vasa(595-635aa)-VN	pCSDest		Generated donor vector was recombined into pCSDest-C-VN vector.
pDONR Vasa(600-625aa)	pDONR	Vasa 600-625 aa	Designed gateway *attB1* FW and *attB2* RV primers. Vasa 600-625 sequence was amplified using pCS2+ pCSDest VasaWT as a template. PCR products were recombined into pDONR221 vector in a standard gateway BP cloning reaction.

Plasmid	Vector	Insert	Stratergy
pCSDest Vasa(600-625aa)-VN	pCSDest		Generated donor vector was recombined into pCSDest-C-VN vector.
pCS2+ VasaDetla(600-625)-VN	pCS2+	Vasa Δ600-655 aa	pCS2+VC empty vector used to clone this construct. In-Fusion cloning primers were designed selecting BamHI and XbaI sites in addition to the gene specific overlap PCR primers. The vector was linearized using the same restriction enzymes. Vasa 1-599 and 626-715 sequences were amplified using pCSDest VasaWT as a template. Purified these PCR products were then mixed in a standard overlap extension PCR reaction to generate final construct. The final PCR product was recombined into the linearized vector in a standard In-Fusion reaction
pCS2+ VasaDetla(600-625)-GFP	pCS2+		pCS2+GFP (stop) vector used to clone this construct. In-Fusion cloning primers were designed selecting BamHI and XbaI sites from the pCS2+GFP vector and the vector was linearized using the same restriction enzymes. Vasa delta 600-625 sequence was amplified with listed primers using pCS2+ VasaDetla (600-625aa)-VC as a template. PCR products was recombined into the linearized vector in a standard In-Fusion reaction.
Vasa mutant			
pCS2+Vasa S607A-VN	pCS2+	vasa 1-715 aa	Designed primers with 15-20 bp of complementary sequence on either side of the S607A mutation using pCS2+Vasa-VN vector. Complete vector was amplified in standard site directed mutagenesis PCR reaction. Incubated the PCR sample with DpnI restriction enzyme to remove template plasmid. Then 5 µl of PCR sample was transformed into XL1-Blue cells and plated.

Plasmid	Vector	Insert	Stratergy
pCS2+Vasa S608A-VN	pCS2+	vasa 1-715 aa	Designed primers with 15-20 bp of complementary sequence on either side of the S608A mutation using pCS2+Vasa-VN vector. Complete vector was amplified in standard site directed mutagenesis PCR reaction. Incubated the PCR sample with DpnI restriction enzyme to remove template plasmid. Then 5 µl of PCR sample was transformed into XL1-Blue cells and plated.
pDONR VasaI609Q	pCS2+	vasa 1-715 aa	Designed primers with 15-20 bp of complementary sequence on either side of the I609Q mutation using pDONR Vasa vector. Complete vector was amplified in standard site directed mutagenesis PCR reaction. Incubated the PCR sample with DpnI restriction enzyme to remove template plasmid. Then 5 µl of PCR sample was transformed into XL1-Blue cells and plated.
pCSDest VasaI609Q-VN	pCSDest		Generated donor vector was recombined into pCSDest-C-VN vector.
Recombinant protein expression vectors			
pGEX GST-Buc (363-400aa)	pGEX	buc 363-400 aa	pGEX GST empty vector used to clone this construct. In-Fusion cloning primers were designed selecting EcoRI site. The vector was linearized using the same restriction enzyme. Buc 363-400 sequences were amplified using pCS2+ BucWT as a template. The PCR products were recombined into the linearized vector in a standard In-Fusion reaction
pGEX GST-Vasa(227-670aa)	pGEX	vasa 227-670 aa	pGEX GST empty vector used to clone this construct. In-Fusion cloning primers were designed selecting BamHI site. The vector was linearized using the same restriction enzyme. Vasa 227-670 sequence was amplified using pCSDest VasaWT as a template. The PCR products were recombined into the linearized vector in a standard In-Fusion reaction

Plasmid	Vector	Insert	Stratergy
Gateway adopted destination vectors			
pCSDest C-VC	pCSDest		pCDest empty vector used to clone the construct. In-Fusion cloning primers were designed selecting XhoI site. The vector was linearized using the same restriction enzymes. The Venus C-terminus(VC) sequences were amplified using pCS2+ VC as a template. The PCR products were recombined into the linearized vector in a standard In-Fusion reaction
pCSDest C-VN	pCSDest		pCDest empty vector used to clone the construct. In-Fusion cloning primers were designed selecting XhoI site. The vector was linearized using the same restriction enzymes. The Venus N-terminus(VN) sequences were amplified using pCS2+ VN as a template. The PCR products were recombined into the linearized vector in a standard In-Fusion reaction
pCSDest N-VC	pCSDest		pCDest empty vector used to clone this construct. In-Fusion cloning primers were designed selecting ClaI site. The vector was linearized using the same restriction enzymes. The Venus C-terminus(VC) sequences were amplified using pCS2+ VC as a template. The PCR products were recombined into the linearized vector in a standard In-Fusion reaction
pCSDest N-VN	pCSDest		pCDest empty vector used to clone this construct. In-Fusion cloning primers were designed selecting ClaI site. The vector was linearized using the same restriction enzymes. The Venus N-terminus(VN) sequences were amplified using pCS2+ VN as a template. The PCR products were recombined into the linearized vector in a standard In-Fusion reaction

Table 3: Primers used for gateway cloning and In-Fusion cloning

Primer Name	Sequence (5' – 3' direction	Cloning purpose
BiFC-Buc-VC Forward	ATCTCCCGGGGGATCC**ATGGAAGGAATAAATAACAATTCA**	pCS2+ plasmid
BiFC-Buc-VC Reverse	TGTCCATGGTGGATCC**GTATCTTGAGCCTCTTTTCTTCA**	pCS2+ plasmid
BiFC-VC-Buc Forward	CAAGACCGGTTCTAGA**ATGGAAGGAATAAATAACAATT**	pCS2+ plasmid
BiFC-VC-Buc Reverse	AGTCAGGCCTTCTAGTTA**GTATCTTGAGCCTCTTTTCT**	pCS2+ plasmid
Buc (1-362) aa FW	ATCTCCCGGGGGATCC**ATGGAAGGAATAAATAACAATT**	pCS2+ plasmid
Buc (1-362) aa RV	TGTCCATGGTGGATCC**GTAGCTGTAGGAATAAGCACT**	pCS2+ plasmid
Buc (363-639) aa FW	ATCTCCCGGGGGATCCATG**TACCCACAAGTGACCC**	pCS2+ plasmid
Buc (363-639)aa RV	TGTCCATGGTGGATCC**GTATCTTGAGCCTCTTTTCTT**	pCS2+ plasmid
pDONR Buc(401-639)FW	GGGGACAAGTTTGTACAAAAAAGCAGGCTTA**ATGCATGTTTATGTTGGTGGTGGT**	pCS2+ plasmid
pDONR Buc(401-639)RV	GGGGACCACTTTGTACAAGAAAGCTGGGTT**GTATCTTGAGCCTCTTTTCTTCATAGAACCT**	pCS2+ plasmid
Buc Delta(372-394)aa overlap FW	CTCGAAGTTGTTCCAGGGCATGTTTATGTTGGTGGTGGTAGGC	pCS2+ plasmid
Buc Delta(372-394)aa overlap RV	ACTCTGGCGCTCTTGGGTCACTTGTGGGTAGTAGCTG	pCS2+ plasmid
Buc D379L FW	GTCTTAAGTCCATCCATACTTGAGCTCTCCTCCAGAGAT	SDM into pCDsest plasmid
Buc D379L RV	ATCTCTGGAGGAGAGCTCAAGTATGGATGGACTTAAGAC	SDM into pCDsest plasmid

Primer Name	Sequence (5’ – 3’ direction	Cloning purpose
Buc E386L FW	GAGCTCTCCTCCAGAGATCTAATGTTCTCCACTGATGTA	SDM into pCDsest plasmid
Buc E386L RV	TACATCAGTGGAGAACATTAGATCTCTGGAGGAGAGCTC	SDM into pCDsest plasmid
Buc S389A_1 FW	TCCAGAGATGAAATGTTCGCCACTGATGTAGAGGATCTC	SDM into pCDsest plasmid
Buc S389A_1 RV	GAGATCCTCTACATCAGTGGCGAACATTTCATCTCTGGA	SDM into pCDsest plasmid
Buc R384G FW	CATAGATGAGCTCTCCTCCGGAGATGAAATGTTCTCCACTG	SDM into pCDsest plasmid
Buc R384G RV	CAGTGGAGAACATTTCATCTCCGGAGGAGAGCTCATCTATG	SDM into pCDsest plasmid
BiFC- Vasa-VN FW	ATCTCCCGGGGGATCC**ATGGATGACTGGGAGGAAG**	pCS2+ plasmid
BiFC- Vasa-VN RV	TCACCATGGTGGATCC**TTCCCATTCCTCATCGTCT**	pCS2+ plasmid
BiFC-VN-Vasa FW	GGCCACCGGTTCTAGA**ATGGATGACTGGGAGGAAG**	pCS2+ plasmid
BiFC-VN-Vasa RV	AGTCAGGCCTTCTAG**TTATTCCCATTCCTCATCGTC**	pCS2+ plasmid
BiFC Vasa(1-277)aa FW	ATCTCCCGGGGGATCC**ATGGATGACTGGGAGGA**	pCS2+ plasmid
BiFC Vasa(1-277)aa RV	TCACCATGGTGGATCC**AGTCATAATTGCTTTTGGA**	pCS2+ plasmid
BiFC Vasa(278-715)aa FW	ATCTCCCGGGGGATCC**ATGTTTGAGGAAGCAGG**	pCS2+ plasmid
BiFC Vasa(278-715)aa RV	TCACCATGGTGGATCC**TTCCCATTCCTCATCG**	pCS2+ plasmid
pDONR vasa(278-495)aa FW	GGGGACAAGTTTGTACAAAAAAGCAGGCTTA**ATGTTTGAGGAAGCAGGACTTTGT**	pDONR plasmid
pDONR vasa(278-495)aa RV	GGGGACCACTTTGTACAAGAAAGCTGGGTT**CACACCAACAGCAAGGAAAATA**	pDONR plasmid

Primer Name	Sequence (5’ – 3’ direction	Cloning purpose
pDONR Vasa(496-715)aa FW	GGGGACAAGTTTGTACAAAAAAGCAGGCTTA**ATGG TGGGTGGAGCATGCAGT**	pDONR plasmid
pDONR Vasa(1-715)aa NS RV	GGGGACCACTTTGTACAAGAAAGCTGGGTT**TTCCC ATTCCTCATCGTCTGCAG**	pDONR plasmid
pDONR Vasa(496-715)aa FW	GGGGACAAGTTTGTACAAAAAAGCAGGCTTA**ATGG TGGGTGGAGCATGCAGT**	pDONR plasmid
pDONR Vasa(496-623)aa RV	GGGGACCACTTTGTACAAGAAAGCTGGGTT**CCCAC AGCGTCCAGTTCT**	pDONR plasmid
pDONR Vasa (624-715)aa FW	GGGGACAAGTTTGTACAAAAAAGCAGGCTTA**ATGG GGAACACCGGTCG**	pDONR plasmid
pDONR Vasa(545-715)aa FW	GGGGACAAGTTTGTACAAAAAAGCAGGCTTA**ATGA CATTTCTCTGTCAAGAGAAGATCTCAAC**	pDONR plasmid
pDONR Vasa(496-665)aa RV	GGGGACCACTTTGTACAAGAAAGCTGGGTT**GAAGG CAACTTCCTCCAGCC**	pDONR plasmid
pDONR Vasa(600-655)aa FW	GGGGACAAGTTTGTACAAAAAAGCAGGCTTA**ATGG TTGTGAATTTTGACATGCCC**	pDONR plasmid
pDONR Vasa(545-715)aa FW	GGGGACAAGTTTGTACAAAAAAGCAGGCTTA**ATGA CATTTCTCTGTCAAGAGAAGATCTCAAC**	pDONR plasmid
pDONR Vasa(545-615)aa RV	GGGGACCACTTTGTACAAGAAAGCTGGGTT**ATGGA CATACTCATCGATGCTGC**	pDONR plasmid
pDONR Vasa(545-655)aa RV	GGGGACCACTTTGTACAAGAAAGCTGGGTT**AACTA CTTGTTGGGCCCCTGAAAG**	pDONR plasmid
pDONR Vasa(600-645)aa RV	GGGGACCACTTTGTACAAGAAAGCTGGGTT**GACCA GGGAGCGAGCTAATG**	pDONR plasmid
pDONR Vasa(600-635)aa RV	GGGGACCACTTTGTACAAGAAAGCTGGGTT**TGGGT TAAAAAAGGACACGGCG**	pDONR plasmid
pDONR Vasa(600-625)aa RV	GGGGACCACTTTGTACAAGAAAGCTGGGTT**GTTCC CACAGCGTCCAGTTCT**	pDONR plasmid

Primer Name	Sequence (5’ – 3’ direction	Cloning purpose
Vasa Delata(600-625) Overlap FW	GAGCAAGTCCAGCATGTT**GGTCGCGCCGTGTCCTTTTTTAAC**	pCS2+ plasmid
Vasa Delata(600-625) Overlap RV	AAAGGACACGGCGCGACC**AACATGCTGGACTTGCTCAATATCCAG**	pCS2+ plasmid
pCSDesVasa_S607A_FW	GTGAATTTTGACATGCCCGCCAGCATCGATGAGTATGTCCATC	SDM into pCSDest plasmid
pCSDesVasa_S607A_RV	GATGGACATACTCATCGATGCTGGCGGGCATGTCAAAATTCAC	SDM into pCSDest plasmid
pCSDesVasa_S608A_FW	TGAATTTTGACATGCCCAGCGCCATCGATGAGTATGTCCATCG	SDM into pCSDest plasmid
pCSDesVasa_S608A_RV	CGATGGACATACTCATCGATGGCGCTGGGCATGTCAAAATTCA	SDM into pCSDest plasmid
pDONR Vasa(1-715)aa FW	GGGGACAAGTTTGTACAAAAAAGCAGGCTTA**ATGGATGACTGGGAGGAAGATCAG**	pDONR plasmid
pCSDesVasa_I609Q_FW	GAATTTTGACATGCCCAGCAGCCAGGATGAGTATGTCCATCGCATAG	SDM into pCSDest plasmid
pCSDesVasa_I609Q _RV	CTATGCGATGGACATACTCATCCTGGCTGCTGGGCATGTCAAAATTC	SDM into pCSDest plasmid
pGEX_Inf Buc(363-400)aa FW	GGGATCCCCGGAATT**CTACCCACAAGTGACCCAAGAGC**	pGEX plasmid
pGEX_Inf Buc(363-400)aa RV	GTCGACCCGGGAATT**TTACCCTGGAACAACTTCGAGATCC**	pGEX plasmid
pGEX Vasa 227-660aa FW	GGGGCCCCTGGGATC**AAATGCAGGACCCAAGGTTGTTTATG**	pGEX plasmid
pGEX Vasa 227-670aa RV	GGAATTCCGGGGATC**CTATGTTGTCCCATGAGCACTGAAG**	pGEX plasmid

4.4. Molecular biology methods

4.4.1. Polymerase chain reaction (PCR)

Target DNA fragments were amplified in a standard PCR reaction (Mullis et al., 1986) as shown in table 3 and 4.

Table 4: Standard PCR reaction

Reagent	Volume	Final concentration
5X Phusion HF buffer (New England BioLabs, Ipswich, USA)	10.0 µl	1X
Forward primer (10 µM) (Sigma Aldrich, Hannover)	2.5 µl	0.5 µM
Reverse primer (10 µM) (Sigma Aldrich, Hannover)	2.5 µl	0.5 µM
dNTPs (5mM) (Thermo Scientific, USA)	2.0 µl	200 µM
Template DNA	variable	< 250ng
Phusion DNA polymerase (New England BioLabs, USA)	1.0 µl	
Nuclease free water	to 50 µl	

Table 5: Standard PCR cycle condition

Step	Temperature	Time
Initial denaturation	98 °C	3.00 min
35-40 cycles	98 °C	0.15 sec
	depending on primer T_m	0.15sec
	72 °C	15-30 sec/kb
Final extension	72 °C	10 min
Hold	20 °C	

4.4.2. Agarose gel electrophoresis

DNA or RNA were resolved in an agarose gel with horizontal electric field (Sharp et al., 1973). Based on the expected DNA or RNA fragment size, Prepared 0.5 – 1% agarose gel in 1X TBE buffer 1x TBE buffer (90 mM Tris (pH 8.0), 90 mM boric acid, 2 mM EDTA) with 0.5 µg/ml ethidium bromide to visualize nucleic acids. Before loading on gel, DNA samples were mixed with 10X loading buffer (50 % glycerol, 0.4 % bromophenol blue) and RNA samples were mixed with gel loading buffer II (Life Technologies, Carlsbad, USA). Electrophoresis performed using 1X TBE buffer at 75-100 V. The 1 kb Plus DNA ladder (Life Technologies, Carlsbad, USA) was used to determine expected size of DNA or RNA fragments. Gels were documented using ChemiDoc gel documentation system (Bio-Rad, Munich).

4.4.3. Purification of DNA

DNA was purified from agarose gel or directly from PCR mixture itself using Gel and PCR clean-up kit according to the manufacturer's instructions. Concentration of purified DNA was determined with the NanoDrop 2000c spectrophotometer (Thermo Scientific, Wilmington, USA).

4.4.4. Plasmid DNA preparation

Pre-transformed Plasmid DNA was isolated from bacteria culture using the NucleoBond Xtra Midi Kit (Macherey and Nagel, Dueren) according to the manufacturer's instructions. The DNA concentration was was measured with the NanoDrop 2000c spectrophotometer (Thermo Scientific, Wilmington, USA).

4.4.5. Gateway cloning

The gateway cloning (Life Technologies, Carlsbad, USA) is developed based on the site-specific recombination strategy used by bacteria phage λ to integrate its DNA in the *E. coli* chromosome. There, specific recombination sites called *att*P in phage and *att*B in *E. coli* integrate each other to generate *att*L and *att*R sites that flank the integrated phage DNA.

First, designed forward and reverse primers containing *att*B site followed by gene specific sequence (Table 2). The a*tt*B-PCR products were recombined into an *att*P-site containing pDONR 221 vector in a standard gateway BP recombination reaction to generate gateway donor vectors (Table 5). Generated donor vector was recombined into appropriate destination vectors in standard gateway LR recombination reaction to generate expression clones (Table 6).

Table 6: Gateway BP recombination reaction

Reaction Component	**Sample**	**Negative control**	**Positive control**
*att*B-PCR products (50-150 ng/µl)	1-7 µl	1-7 µl	
pDONR 221 vector (150 ng/µl)	1.0 µl	1.0 µl	2.0 µl
pEXP7-tet positive control (50 ng/µl)	---	----	2.0 µl
5X BP Clonase II Reaction Buffer	2.0 µl	**2.0 µl H_20**	2.0 µl
Nuclease free water	to 10.0 µl	to 10.0 µl	4.0 µl
Gently mix and spin the reaction mixture. Then incubate overnight at 25 ^{0}C.			

Table 7: Gateway LR recombination reaction

Reaction Component	**Sample**	**Negative control**	**Positive control**
pDONR Vector (50-150 ng/µl)	1-7 µl	1-7 µl	
Destination Vector (150 ng/µl)*	1.0 µl	1.0 µl	2.0 µl
pENTR-gus positive control (50 ng/µl)	---	----	2.0 µl
5X LR Clonase II Reaction Buffer	2.0 µl	**2.0 µl H20**	2.0 µl
Nuclease free water	to 10.0 µl	to 10.0 µl	4.0 µl
Gently mix and spin the reaction mixture, then incubate overnight at 25 ^{0}C.			

4.4.6. In-Fusion cloning

This is also based on site-specific recombination of gene of interest into a target vector. In-Fusion cloning primers were designed selecting one or two restriction enzymes from destination vector. In each case, both forward and reverse primers were containing 15 bp overhangs in addition to the gene specific sequence. The destination vector was linearized using the same restriction enzymes used for the primer designing. PCR products was recombined into the linearized vector in a standard In-Fusion reaction as shown in table 7.

Table 8: In-Fusion cloning reaction

Reaction Component	**Sample**	**Negative control**	**Positive control**
PCR products (100 -200 ng/µl)	1-7 µl	1-7 µl	2 µl of 2 kb control insert
Linearized vector (50-100 ng/µl)	1.0 µl	1.0 µl	1 µl of pUC19 control vector
5X In-Fusion HD enzyme premix	2.0 µl	**2.0 µl H_20**	2.0 µl
Nuclease free water	to 10.0 µl	to 10.0 µl	4.0 µl
Gently mix and spin the reaction mixture. Then incubate at 50 °C for 15 minutes.			

4.4.7. Chemical transformation for gateway cloning

Thawed and gently mixed DH5α competent cells to ensure even distribution and aliquot 50 µl of the competent cells into a 1.5 ml microcentrifuge tube. Added 2.5 µl of the BP recombination reaction mixture to the cells and gently pipette the cells for even distribution of the reaction mixture. The cells were incubated on ice for 30 minutes followed by heat-shock the competent cells for 45-60 seconds at 42 ^{o}C. Then cells were immediately transferred onto ice and kept for 2-3 minutes. After adding 450 µl S.O.C medium (0.5% Yeast Extract, 2% Tryptone, 10 mM NaCl, 2.5 mM KCl, 10 mM MgCl2, 10 mM MgSO4, 20 mM Glucose) cells were incubated for one hour at 37 ^{o}C while horizontal shaking by 220 rpm. Spreaded 250 µl of transformation reaction on a 1.5% LB-agar plate containing kanamycin (for BP recombination reaction) or ampicillin (LR recombination reaction) as a selection antibiotic and incubated the plates overnight at 37 ^{o}C.

4.4.8. Chemical transformation for In-Fusion cloning

Performed same procedure described in section with few exception. Stellar™ competent cells were used instead of DH5α competent cells. Plated 50-100 µl of sample on 1.5% LB-agar plate containing ampicillin as a selection antibiotic and incubated the plates overnight at 37 ^{o}C.

4.4.9. *In vitro* transcription

Capped sense RNA was synthesized using the SP6 mMessage mMachine kit as described by the manufacturer (Life Technologies, Carlsbad, USA). A standard reaction was prepared as shown in the table.8. Synthesized RNA was purified with Illustra Probe Quant G-50 columns as described by the manufacturer (GE Healthcare, Little Chalfont, UK). The RNA concentration was determined with the NanoDrop 2000c spectrophotometer (Thermo Scientific, Wilmington, USA) and RNA integrity was determined by agarose gel electrophoresis

Table 9: *In vitro* transcription reaction set up

Reaction component	**Volume**
2X NTP/ CAP	10.0 µl
10X reaction buffer	2.0 µl
Linearized plasmid DNA	100-1000 ng
SP6 RNA polymerase	2.0 µl
Nuclease free water	To 20 µl
Gently mix the sample tube and spin the tube. **After incubate the sample at 42 ^{O}C for 2-3 hours**	
After 3 hours add 2 µl of TURBO DNase and incubate the sample for 15 min at 37 ^{o}C.	

4.4.10. SDS- polyacrylamide gel electrophoresis

Zebrafish embryo cell lysate or *in vitro* translated proteins were resolved using SDS-polyacrylamide gel electrophoresis. Protein samples were mixed with 2x SDS loading buffer (100 mM Tris (pH 6.8), 20 % glycerol, 4 % SDS, 200 mM β-mercaptoethanol, 0.02 % bromophenol blue), incubated for 5 min at 95 ^{o}C. Samples were loaded on 10 - 15% SDS gel based on the molecular weight of the target protein and the Page Ruler prestained protein ladder (Thermo Scientific, Wilmington, USA) was separately loaded to determine the approximate molecular weight of the proteins. Vertical electrophoresis performed in 1x Laemmli buffer (25 mM Tris, 250 mM glycine, 0.01 % SDS) at a constant voltage of 80 V. After the dye front reached the seperating gel, the voltage was increased to 120 V. Subsequently the gel was stained with Coomassie blue (section) or used the gel for western blotting.

4.4.11. Coomassie staining

After SDS-gel electrophoresis, the gels were washed with dH_2O. Thereafter, gels were incubated in Coomassie staining solution (50 % methanol, 10 % glacial acetic acid, 0.1 % Coomassie Brilliant Blue) for 30 min to 1 h at room temperature. The stained gels were washed three times with dH_2O and incubated in a destaining solution (40 % methanol, 10 % glacial acetic acid) over night at room temperature.

4.4.12. Western blot

After SDS-PAGE, proteins were transferred to a nitrocellulose membrane using semi-dry blotting. The nitrocellulose membrane and whatman papers were soaked in blotting buffer (39 mM glycine, 48 mM Tris, 0.037 % SDS, 20 % methanol). Stacked three whatman papers and placed the nitrocellulose membrane on top of the whatman papers. Protein gel placed on the nitrocellulose membrane followed by stacking another whatman papers. The proteins were transferred for one hour at 250 mA and 25 V. After, membrane was blocked using 5% skim milk in TBS (10 mM Tris (pH 8.0), 150 mM NaCl). The membrane incubated for one hour at 4 ^{o}C. Then, the membrane was incubated overnight at 4 ^{o}C with diluted antibodies in 5%

skim milk +TBST (10 mM Tris (pH 8.0), 150 mM NaCl, 0.05 % Tween20). The membrane was washed 3 x 5 min in TBST and incubated with fluorescent coupled secondary antibody for one hour at room temperature. The membrane was washed 3 x 5 min with TBST and fluorescent signal was detected using Odyssey CLx Infrared Imaging system (Li-Cor, Lincoln, USA) and analyzed with the Image Studio Software (Li-Cor, Lincoln, USA).

4.4.13. Live-cell imaging

Embryos were manually dechorionated and mounted on 1.5 % agarose coated dishes filled with 1x E3 medium and imaged by stereo microscope SteREO Lumar.V12 (Carl Zeiss Microscopy, Jena), (Chapter 2.2.2). Images were processed using the software Axio Vision Rel. 4.8 (Carl Zeiss Microscopy, Jena). For imaging with LSM80, dechorionated embryos were placed on a Fluorodish (WPI, Sarasota, USA) with 1x E3. Images were analyzed using the ZEN 2011 software (Carl Zeiss Microscopy, Jena).

4.4.14. Recombinant protein expression of Buc-VBM

The Buc-VBM encoding amino acids 363-400 was amplified by PCR. The PCR product was cloned into pGEX-6p1 vector, which contains GST fusion tag using EcoRI restriction enzyme. The GST fusion protein was recombinantly expressed in BL21 (DE3) cells. The protein expression was induced by adding IPTG to 0.5 mM final concentration and incubated overnight at 16 ^{o} C while shaking at 200 rpm. Cells were harvested, resuspended and in lysis buffer disrupted using a microfluidizer (Microfluidics) in 50 mM Tris/HCl (pH 7.8), 500 mM NaCl, 5% (v/v) glycerol and 10 mM ethylenediaminetetraacetic acid (EDTA) + 1 protease inhibitor cOmplete ULTRA tablet/ 50 ml buffer). The lysate was clarified by ultracentrifugation at 30 000 g and 4 ^{o} C for 30 minutes. The clarified lysate loaded on Glutathion Sepharose column (GE healthcare) at room temperature. The protein was subsequently eluted with 30 mM reduced glutathione. The GST-tag was proteolytically cleaved by adding PreScission Protease (1 µl (2 units) 100 µg of fusion protein) in to the eluated protein and incubated overnight at 4 ^{o} C. The tag was removed using a Superdex 75 gel-fltration column coupled to a Glutathione Sepharose column in 20 mM Tris/HCl (pH 7.8),

200 mM NaCl, 5% glycerol and 2 mM $MgCl_2$. The protein was concentrated Amicon Ultra centrifugal concentrator (Merck) and flash frozen in liquid nitrogen.

4.4.15. Recombinant protein expression of Vasa (227-670) aa

The Vasa encoding amino acids 227 -670 was amplified by PCR. The PCR product was cloned into pGEX-6p1 vector, which contains GST fusion tag using BamHI restriction enzyme. The GST fusion protein was recombinantly expressed in BL21 (DE3) cells. The protein expression was induced adding IPTG to 0.5 mM final concentration together with Ethanol added 4% (V/V) , K_2HPO_4 to 30 mM final concentration and incubated overnight at 16 ^{o} C while shaking at 200 rpm. Cells were harvested, resuspended and in lysis buffer disrupted using a microfluidizer (Microfluidics) in 50 mM Tris/HCl (pH 7.8), 500 mM NaCl, 5% (v/v) glycerol and 10 mM ethylenediaminetetraacetic acid (EDTA) + 1 protease inhibitor cOmplete ULTRA tablet/ 50 ml buffer). The lysate was clarified by ultracentrifugation at 30 000 g and 4 ^{o} C for 30 minutes. The clarified lysate loaded on Glutathion Sepharose column (GE healthcare) at room temperature. Potentially bound nucleic acids were removed washing the lysate with was buffer supplemented with 2 M LiCl. The protein was subsequently eluted with 30 mM reduced glutathione. The GST-tag was proteolytically cleaved by adding PreScission Protease (1 µl (2 units) 100 µg of fusion protein) in to the eluated protein and incubated overnight at 4 ^{o} C. The tag was removed using a Superdex 75 gel-fltration column coupled to a Glutathione Sepharose column in 20 mM Tris/HCl (pH 7.8), 200 mM NaCl, 5% glycerol and 2 mM $MgCl_2$. The protein was concentrated Amicon Ultra centrifugal concentrator (Merck) and flash frozen in liquid nitrogen.

4.4.16. ATPase assay

The ATPase activity of Vasa was measured with a nicotinamide adenine dinucleotide (NADH) dependent coupled enzymatic assay (Kiianitsa et al., 2003) The assay detects the reduction of the NADH absorption at 340 nm as a direct effect of the ATP consumption over time with a VICTOR Nivo Multimode Microplate Reader (PerkinElmer). The ATPase activity of Vasa was determined by mixing 5 µM Vasa with and without 100 µM of Buc-VBM together with 2.5 mM, 250 nM NADH, 500 nM phosphoenolpyruvate, 6–8.3 U ml-1 pyruvate kinase and 9–14 U ml-1 lactic dehydrogenase. RNA stimulated ATPase activity of Vasa was performed by adding 50 µM ssRNA ($polyA_{(8)}$) into 5 µM Vasa with and without 100 µM of Buc-VBM with other common components listed. All reactions were performed in triplicates of 150 µl in each at 25° C.

4.4.17. Circular dichroism (CD) spectroscopy

CD-spectra for Buc-VBM (amino acid 363-400) was performed using a Chirascan CD spectrometer (Applied Photophysics) at far-UV spectra (185–260 nm). Initially, protein buffer was exchanged to a buffer containing 20 mM Na-phosphate buffer to favor the CD-spectra. Measurements were recorded at room temperature using 0.1 mg/ ml Buc-VBM protein concentration. The CD data are presented as molar ellipticity ($[\theta]deg \times cm^2/dmol$ and plotted using QtiPlot (v.0.9.8.9).

4.5. Bioinformatics methods

4.5.1. Pairwise sequence alignment

Sequences were pairwise aligned using Needleman-Wunsch algorithm (https://www.ebi.ac.uk/Tools/psa/emboss_needle/) .

4.5.2. Multiple sequence alignments

Multiple sequence alignment was performed using T-Coffee multiple sequence alignment server (https://www.ebi.ac.uk/Tools/msa/tcoffee/) (Notredame et al., 2000).

4.5.3. Aligns protein sequences using structural information

Protein sequences were aligned using T-Coffee Expresso server (http://tcoffee.crg.cat/apps/tcoffee/do:expresso) (Di Tommaso et al., 2011).

4.5.4. *In silico* protein modeling

PyMol Ve 2.3 was used to visualize and structural arrangement and alignment of predicted protein models.

5. References

Anne, J. (2010). Arginine methylation of SmB is required for Drosophila germ cell development. *Development*. 137 (17). p.pp. 2819–2828.

Ashok Kumar, T. (2013). CFSSP: Chou and Fasman Secondary Structure Prediction server. *Wide Spectrum*. 1 (9). p.pp. 15–19.

Bayer, P., Arndt, A., Metzger, S., Mahajan, R., Melchior, F., Jaenicke, R. & Becker, J. (1998). Structure determination of the small ubiquitin-related modifier SUMO-1. *Journal of Molecular Biology*. 280 (2). p.pp. 275–286.

Bolger, T.A. & Wente, S.R. (2011). Gle1 is a multifunctional DEAD-box protein regulator that modulates Ded1 in translation initiation. *Journal of Biological Chemistry*. 286 (46). p.pp. 39750–39759.

Bontems, F., Stein, A., Marlow, F., Lyautey, J., Gupta, T., Mullins, M.C. & Dosch, R. (2009). Bucky Ball Organizes Germ Plasm Assembly in Zebrafish. *Current Biology*. [Online]. 19 (5). p.pp. 414–422. Available from: http://dx.doi.org/10.1016/j.cub.2009.01.038.

Boswell, R.E. & Mahowald, A.P. (1985). tudor, a gene required for assembly of the germ plasm in Drosophila melanogaster. *Cell*. 43 (1). p.pp. 97–104.

Braat, A.K., Zandbergen, T., Van De Water, S., Goos, H.J.T.H. & Zivkovic, D. (1999). Characterization of zebrafish primordial germ cells: Morphology and early distribution of vasa RNA. *Developmental Dynamics*. 216 (2). p.pp. 153–167.

Breitwieser, W., Markussen, F.H., Horstmann, H. & Ephrussi, A. (1996). Oskar protein interaction with vasa represents an essential step in polar granule

assembly. *Genes and Development*. 10 (17). p.pp. 2179–2188.

Buehr, M.L. & Blackler, A.W. (1970). Sterility and partial sterility in the South African clawed toad following the pricking of the egg. *Journal of Embryology and Experimental Morphology*. 23 (2). p.pp. 375–384.

Carr, R. M., Oranu, A., & Khungar, V. (2016). piRNA Biogenesis in Drosophila Melanogaster. *Physiology & behavior*. 176 (1). p.pp. 139–148.

Caruthers, J.M. & McKay, D.B. (2002). Helicase structure and mechanism. *Current Opinion in Structural Biology*. 12 (1). p.pp. 123–133.

Caussinus, E., Kanca, O. & Affolter, M. (2012). Fluorescent fusion protein knockout mediated by anti-GFP nanobody. *Nature Structural and Molecular Biology*. 19 (1). p.pp. 117–122.

Cieri, D., Vicario, M., Giacomello, M., Vallese, F., Filadi, R., Wagner, T., Pozzan, T., Pizzo, P., Scorrano, L., Brini, M. & Calì, T. (2018). SPLICS: A split green fluorescent protein-based contact site sensor for narrow and wide heterotypic organelle juxtaposition. *Cell Death and Differentiation*. 25 (6). p.pp. 1131–1145.

Clift, D., So, C., McEwan, W.A., James, L.C. & Schuh, M. (2018). Acute and rapid degradation of endogenous proteins by Trim-Away. *Nature Protocols*. [Online]. 13 (10). p.pp. 2149–2175. Available from: http://dx.doi.org/10.1038/s41596-018-0028-3.

Cole, C., Barber, J.D. & Barton, G.J. (2008). The Jpred 3 secondary structure prediction server. *Nucleic acids research*. 36 (Web Server issue). p.pp. 197–201.

Cusanovich, D.A., Pavlovic, B., Pritchard, J.K. & Gilad, Y. (2014). The Functional Consequences of Variation in Transcription Factor Binding. *PLOS Genetics*. 10 (3).

Dahanukar, A., Walker, J.A. & Wharton, R.P. (1999). Smaug, a novel RNA-binding protein that operates a translational switch in Drosophila. *Molecular Cell*. 4 (2). p.pp. 209–218.

Dosch, R. (2015). Next generation mothers: Maternal control of germline development in zebrafish. *Critical Reviews in Biochemistry and Molecular Biology*. 50 (1). p.pp. 54–68.

Dosch, R., Wagner, D.S., Mintzer, K.A., Runke, G., Wiemelt, A.P. & Mullins, M.C. (2004). Maternal control of vertebrate development before the midblastula transition: Mutants from the zebrafish I. *Developmental Cell*. 6 (6). p.pp. 771–780.

Drozdetskiy, A., Cole, C., Procter, J. & Barton, G.J. (2015). JPred4: A protein secondary structure prediction server. *Nucleic Acids Research*. 43 (W1). p.pp. W389–W394.

Dudgeon, C.L., Coulton, L., Bone, R., Ovenden, J.R. & Thomas, S. (2017). Switch from sexual to parthenogenetic reproduction in a zebra shark. *Scientific Reports*. 7 (January). p.pp. 1–8.

Durdevic, Z. & Ephrussi, A. (2019). Germ cell lineage homeostasis in drosophila requires the vasa RNA helicase. *Genetics*. 213 (3). p.pp. 911–922.

Ephrussi, Anne; Lehmann, R. (1992). Induction of germ cell fate by oskar. *Nature*. 358 (July). p.pp. 387–392.

Ephrussi, A., Dickinson, L.K. & Lehmann, R. (1991). Oskar Organizes the Germ Plasm and Directs Localization of the Posterior Determinant Nanos. *Cell*. 66 (1). p.pp. 37–50.

Extavour, C.G. & Akam, M. (2003). Mechanisms of germ cell specification across the metazoans: Epigenesis and preformation. *Development*. 130 (24). p.pp. 5869–5884.

Florence L. Marlow and Mary C. Mullins (2008). Bucky ball functions in Balbiani body assembly and animal- vegetal polarity in the oocyte and follicle cell layer in zebrafish. *Developmental Biology*. 321 (1). p.pp. 40–50.

Gustafson, E.A. & Wessel, G.M. (2010). Vasa genes: Emerging roles in the germ line and in multipotent cells. *BioEssays*. 32 (7). p.pp. 626–637.

Hamann, F., Enders, M. & Ficner, R. (2019). Structural basis for RNA translocation by DEAH-box ATPases. *Nucleic Acids Research*. 47 (8). p.pp. 4349–4362.

Hashimoto, Y., Maegawa, S., Nagai, T., Yamaha, E., Suzuki, H., Yasuda, K. & Inoue, K. (2004). Localized maternal factors are required for zebrafish germ cell formation. *Developmental Biology*. 268 (1). p.pp. 152–161.

Heim, A.E., Hartung, O., Rothhämel, S., Ferreira, E., Jenny, A. & Marlow, F.L. (2014). Oocyte polarity requires a Bucky ball-dependent feedback amplification loop. *Development (Cambridge)*. 141 (4). p.pp. 842–854.

Hickford, D.E., Frankenberg, S., Pask, A.J., Shaw, G. & Renfree, M.B. (2011). DDX4 (VASA) Is Conserved in Germ Cell Development in Marsupials and Monotremes1. *Biology of Reproduction*. 85 (4). p.pp. 733–743.

Ikenishi, K., Kotani, M. & Tanabe, K. (1974). Ultrastructural changes associated with UV irradiation in the 'germinal plasm' of Xenopus laevis. *Developmental Biology*. 36 (1). p.pp. 155–168.

Ikenishi, K., Sakiko, N. & Okuda, T. (1986). Direct Evidence for the Presence of Germ Cell Determinant in Vegetal Pole Cytoplasm of Xenopus laevis and in a Subcellular Fraction of It: (Xenopus laevis/germ cell determinant/germ plasm/PGC induction). *Development, Growth & Differentiation*. 28 (6). p.pp. 563–568.

Illmensee, K. & Mahowald, A.P. (1974). Transplantation of posterior polar plasm in Drosophila. Induction of germ cells at the anterior pole of the egg. *Proceedings of the National Academy of Sciences of the United States of America*. 71 (4). p.pp. 1016–1020.

Jankowsky, E. (2011). RNA helicases at work: Binding and rearranging. *Trends in Biochemical Sciences*. [Online]. 36 (1). p.pp. 19–29. Available from: http://dx.doi.org/10.1016/j.tibs.2010.07.008.

Jensen, L.J., Ussery, D.W. & Brunak, S. (2003). Functionality of system components: Conservation of protein function in protein feature space. *Genome Research*. 13 (11). p.pp. 2444–2449.

Jeske, M., Bordi, M., Glatt, S., Müller, S., Rybin, V., Müller, C.W. & Ephrussi, A. (2015). The crystal structure of the Drosophila germline inducer Oskar identifies two domains with distinct Vasa Helicase- and RNA-binding activities. *Cell Reports*. 12 (4). p.pp. 587–598.

Jeske, M., Müller, C.W. & Ephrussi, A. (2017). The LOTUS domain is a conserved DEAD-box RNA helicase regulator essential for the recruitment of Vasa to the germ plasm and nuage. *Genes and Development*. 31 (9). p.pp. 939–952.

Johnstone, O. & Lasko, P. (2004). Interaction with eIF5B is essential for Vasa function during development. *Development*. 131 (17). p.pp. 4167–4178.

Jostes, S. & Schorle, H. (2018). Signals and transcription factors for specification of human germ cells. *Stem Cell Investigation*. 5 (3). p.pp. 1–5.

Juliano, C.E., Swartz, S.Z. & Wessel, G.M. (2010). A conserved germline multipotency program. *Development*. 137 (24). p.pp. 4113–4126.

Kaczka, P., Winiewska, M., Zhukov, I., Rempoła, B., Bolewska, K., Łozinski, T., Ejchart, A., Poznańska, A., Wierzchowski, K.L. & Poznański, J. (2014). The TFE‐induced transient native‐like structure of the intrinsically disordered σ_4^704 domain of Escherichia coli RNA polymerase. *European Biophysics Journal*. 43 (12). p.pp. 581–594.

Kerppola, T.K. (2008). Bimolecular fluorescence complementation (BiFC) analysis as a probe of protein interactions in living cells. *Annu Rev Biophys*. 37. p.pp. 465–87.

Kerppola, T.K. (2006). Design and implementation of bimolecular fluorescence complementation (BiFC) assays for the visualization of protein interactions in living cells. *Nature Protocols*. 1 (3). p.pp. 1278–1286.

Kerppola, T.K. (2006). Visualization of molecular interactions by fluorescence complementation. *Nature Reviews Molecular Cell Biology*. 7 (6). p.pp. 449–456.

Kiianitsa, K., Solinger, J.A. & Heyer, W.D. (2003). NADH-coupled microplate photometric assay for kinetic studies of ATP-hydrolyzing enzymes with low and high specific activities. *Analytical Biochemistry*. 321 (2). p.pp. 266–271.

Kim-Ha, J., Smith, J.L. & Macdonald, P.M. (1991). oskar mRNA is localized to the posterior pole of the Drosophila oocyte. *Cell*. 66 (1). p.pp. 23–35.

Kirino, Y., Vourekas, A., Kim, N., De Lima Alves, F., Rappsilber, J., Klein, P.S., Jongens, T.A. & Mourelatos, Z. (2010). Arginine methylation of vasa protein is conserved across phyla. *Journal of Biological Chemistry*. 285 (11). p.pp. 8148–8154.

Kloc, M., Bilinski, S. & Etkin, L.D. (2004). The Balbiani Body and Germ Cell Determinants: 150 Years Later. *Current Topics in Developmental Biology*. 59. p.pp. 1–36.

Kloc, M., Jedrzejowska, I., Tworzydlo, W. & Bilinski, S.M. (2014). Balbiani body, nuage and sponge bodies - The germ plasm pathway players. *Arthropod Structure and Development*. [Online]. 43 (4). p.pp. 341–348. Available from: http://dx.doi.org/10.1016/j.asd.2013.12.003.

Köprunner, M., Thisse, C., Thisse, B. & Raz, E. (2001). A zebrafish nanos-related gene is essential for the development of primordial germ cells. *Genes and Development*. 15 (21). p.pp. 2877–2885.

Krishnakumar, P. & Dosch, R. (2018). Germ Cell Specification: The Evolution of a Recipe to Make Germ Cells. In: *Germ Cell*. pp. 1–22.

Krishnakumar, P., Riemer, S., Perera, R., Lingner, T., Goloborodko, A., Khalifa, H., Bontems, F., Kaufholz, F., El-Brolosy, M.A. & Dosch, R. (2018). Functional equivalence of germ plasm organizers. *PLoS Genetics*. 14 (11). p.pp. 1–29.

Kwan, K.M., Fujimoto, E., Grabher, C., Mangum, B.D., Hardy, M.E., Campbell, D.S., Parant, J.M., Yost, H.J., Kanki, J.P. & Chien, C. Bin (2007). The Tol2kit: A multisite gateway-based construction Kit for Tol2 transposon transgenesis constructs. *Developmental Dynamics*. 236 (11). p.pp. 3088–3099.

Lasko, P.F. & Ashburner, M. (1988). The product of the Drosophila gene vasa is very similar to eukaryotic initiation factor-4A. *Nature*. 335 (6191). p.pp. 611–617.

Laureto, P.P. De, Donadi, M., Scaramella, E., Frare, E. & Fontana, A. (2001). Trifluoroethanol-assisted protein folding: fragment 53-103 of bovine α-lactalbumin. *Biosystems*. 1548. p.pp. 29–37.

Lavial, F., Acloque, H., Bachelard, E., Nieto, M.A., Samarut, J. & Pain, B. (2009). Ectopic expression of Cvh (Chicken Vasa homologue) mediates the reprogramming of chicken embryonic stem cells to a germ cell fate. *Developmental Biology*. [Online]. 330 (1). p.pp. 73–82. Available from: http://dx.doi.org/10.1016/j.ydbio.2009.03.012.

Lebaron, S., Papin, C., Capeyrou, R., Chen, Y.L., Froment, C., Monsarrat, B., Caizergues-Ferrer, M., Grigoriev, M. & Henry, Y. (2009). The ATPase and helicase activities of Prp43p are stimulated by the G-patch protein Pfa1p during yeast ribosome biogenesis. *EMBO Journal*. 28 (24). p.pp. 3808–3819.

Lehmann, R. & Nüsslein-Volhard, C. (1986). Abdominal segmentation, pole cell formation, and embryonic polarity require the localized activity of oskar, a maternal gene in drosophila. *Cell*. 47 (1). p.pp. 141–152.

Liang, L., Diehl-Jones, W. & Lasko, P. (1994). Localization of vasa protein to the Drosophila pole plasm is independent of its RNA-binding and helicase activities. *Development*. 120 (5). p.pp. 1201–1211.

Linder, P. (2006). Dead-box proteins: A family affair - Active and passive players in RNP-remodeling. *Nucleic Acids Research*. 34 (15). p.pp. 4168–4180.

Linder, P. & Jankowsky, E. (2011). From unwinding to clamping - the DEAD box RNA helicase family. *Nature Reviews Molecular Cell Biology*. [Online]. 12 (8). p.pp. 505–516. Available from: http://dx.doi.org/10.1038/nrm3154.

Linder, P. & Lasko, P. (2006). Bent out of Shape: RNA Unwinding by the DEAD-Box Helicase Vasa. *Cell*. 125 (2). p.pp. 219–221.

Linding, R., Schymkowitz, J., Rousseau, F., Diella, F. & Serrano, L. (2004). A comparative study of the relationship between protein structure and β-aggregation in globular and intrinsically disordered proteins. *Journal of Molecular Biology*. 342 (1). p.pp. 345–353.

Liu, N., Han, H. & Lasko, P. (2009). Vasa promotes Drosophila germline stem cell differentiation by activating mei-P26 translation by directly interacting with a (U)-rich motif in its 3' UTR. *Genes and Development*. 23 (23). p.pp. 2742–2752.

Marlow, F. (2015). Primordial Germ Cell Specification and Migration. *F1000Research*. 4 (0). p.pp. 1–14.

Marlow, F.L. (2010). *Maternal Control of Development in Vertebrates*.

Miles, L.B. & Verkade, H. (2014). TA-cloning vectors for rapid and cheap cloning of zebrafish transgenesis constructs. *Zebrafish*. 11 (3). p.pp. 281–282.

Miller, K.E., Kim, Y., Huh, W., Park, H., Developmental, C. & Program, B. (2016). *Bimolecular fluorescence complementation (BiFC) analysis: advances and recent applications for genome-wide interaction studies*. 427 (11). p.pp. 2039–2055.

Nakamura, S., Hira, S., Fujiwara, M., Miyagata, N., Tsuji, T., Kondo, A., Kimura, H., Shinozuka, Y., Hayashi, M., Kobayashi, S. & Mukai, M. (2019). A truncated form of a transcription factor Mamo activates vasa in Drosophila embryos. *Communications Biology*. [Online]. 2 (1). p.pp. 1–13. Available from: http://dx.doi.org/10.1038/s42003-019-0663-4.

Nakamura, T. & Extavour, C.G. (2016). The transcriptional repressor Blimp-1 acts downstream of BMP signaling to generate primordial germ cells in the cricket gryllus bimaculatus. *Development (Cambridge)*. 143 (2). p.pp. 255–263.

Norma J. Greenfield (2012). Using circular dichroism spectra to estimate protein secondary structure. *ProQuest Dissertations and Theses*. 1 (6). p.p. 218.

Notredame, C., Higgins, D.G. & Heringa, J. (2000). T-coffee: A novel method for fast and accurate multiple sequence alignment. *Journal of Molecular Biology*. 302 (1). p.pp. 205–217.

O.H. Kaufman and F.L. Marlow (2017). Methods to study maternal regulation of germ cell specification in zebrafish. *Physiology & behavior*. 176 (5). p.pp. 139–148.

Pahlich, S., Zakaryan, R.P. & Gehring, H. (2006). Protein arginine methylation: Cellular functions and methods of analysis. *Biochimica et Biophysica Acta - Proteins and Proteomics*. 1764 (12). p.pp. 1890–1903.

Pek, J.W., Patil, V.S. & Kai, T. (2012). piRNA pathway and the potential processing site, the nuage, in the Drosophila germline. *Development Growth and Differentiation*. 54 (1). p.pp. 66–77.

Popovic, M., Bialecka, M., Gomes Fernandes, M., Taelman, J., Van Der Jeught, M., De Sutter, P., Heindryckx, B. & De Sousa Lopes, S.M.C. (2019). Human blastocyst outgrowths recapitulate primordial germ cell specification events. *Molecular Human Reproduction*. 25 (9). p.pp. 519–526.

Raz, E. (2003). Primordial germ-cell development: The zebrafish perspective. *Nature Reviews Genetics*. 4 (9). p.pp. 690–700.

Raz, E. (2000). The function and regulation of vasa-like genes in germ-cell development. *Genome biology*. 1 (3). p.pp. 1–6.

Riemer, S., Bontems, F., Krishnakumar, P., Gömann, J. & Dosch, R. (2015). A functional Bucky ball-GFP transgene visualizes germ plasm in living zebrafish. *Gene Expression Patterns*. [Online]. 18 (1–2). p.pp. 44–52. Available from: http://dx.doi.org/10.1016/j.gep.2015.05.003.

Rogers, G.W., Richter, N.J., Lima, W.F. & Merrick, W.C. (2001). Modulation of the Helicase Activity of eIF4A by eIF4B, eIF4H, and eIF4F. *Journal of Biological Chemistry*. 276 (33). p.pp. 30914–30922.

Roovers, E.F., Kaaij, L.J.T., Redl, S., Bronkhorst, A.W., Wiebrands, K., de Jesus Domingues, A.M., Huang, H.Y., Han, C.T., Riemer, S., Dosch, R., Salvenmoser, W., Grün, D., Butter, F., van Oudenaarden, A. & Ketting, R.F. (2018). Tdrd6a Regulates the Aggregation of Buc into Functional Subcellular Compartments that Drive Germ Cell Specification. *Developmental Cell*. 46 (3). p.pp. 285-301.e9.

Roy, A., Kucukural, A. & Zhang, Y. (2010). I-TASSER: A unified platform for automated protein structure and function prediction. *Nature Protocols*. 5 (4). p.pp. 725–738.

Saitou, M. & Yamaji, M. (2010). Germ cell specification in mice: Signaling, transcription regulation, and epigenetic consequences. *Reproduction*. 139 (6). p.pp. 931–942.

Santos, A.C. & Lehmann, R. (2004). Germ cell specification and migration in Drosophila and beyond. *Current Biology*. 14 (14). p.pp. 578–589.

Schupbach, T. & Wieschaus, E. (1986). Germline autonomy of maternal-effect mutations altering the embryonic body pattern of Drosophila. *Developmental Biology*. 113 (2). p.pp. 443–448.

Schüpbach, T. & Wieschaus, E. (1986). Maternal-effect mutations altering the anterior-posterior pattern of the Drosophila embryo. *Roux's Archives of Developmental Biology*. 195 (5). p.pp. 302–317.

Sengoku, T., Nureki, O., Nakamura, A., Kobayashi, S. & Yokoyama, S. (2006). Structural Basis for RNA Unwinding by the DEAD-Box Protein Drosophila Vasa. *Cell*. 125 (2). p.pp. 287–300.

Singh, H., Singh, S. & Singh Raghava, G.P. (2019). Peptide Secondary Structure Prediction using Evolutionary Information. *bioRxiv*. [Online]. p.p. 558791. Available from: http://biorxiv.org/content/early/2019/02/22/558791.abstract.

Sloan, K.E. & Bohnsack, M.T. (2018). Unravelling the Mechanisms of RNA Helicase Regulation. *Trends in Biochemical Sciences*. [Online]. 43 (4). p.pp. 237–250. Available from: https://doi.org/10.1016/j.tibs.2018.02.001.

Smith, J.L., Wilson, J.E. & Macdonald, P.M. (1992). Overexpression of oskar directs ectopic activation of nanos and presumptive pole cell formation in Drosophila embryos. *Cell*. 70 (5). p.pp. 849–859.

Smith, L.D. (1966). The role of a 'germinal plasm' in the formation of primordial germ cells in Rana pipiens. *Developmental Biology*. 14 (2). p.pp. 330–347.

St Johnston, D., Beuchle, D. & Nüsslein-Volhard, C. (1991). staufen, a gene required to localize maternal RNAs in the Drosophila egg. *Cell*. 66 (1). p.pp. 51–63.

Styhler, S., Nakamura, A., Swan, A., Suter, B. & Lasko, P. (1998). vasa is required for GURKEN accumulation in the oocyte, and is involved in oocyte differentiation and germline cyst development. *Development*. 125 (9). p.pp. 1569–1578.

Tada, H., Mochii, M., Orii, H. & Watanabe, K. (2012). Ectopic formation of primordial germ cells by transplantation of the germ plasm: Direct evidence for germ cell determinant in Xenopus. *Developmental Biology*. [Online]. 371 (1). p.pp. 86–93. Available from: http://dx.doi.org/10.1016/j.ydbio.2012.08.014.

Tanabe, K. & Kotani, M. (1974). Relationship between the amount of the 'germinal plasm' and the number of primordial germ cells in Xenopus laevis. *Journal of Embryology and Experimental Morphology*. 31 (1). p.pp. 89–98.

Tomancak, P., Guichet, A., Zavorszky, P. & Ephrussi, A. (1998). Oocyte polarity depends on regulation of gurken by Vasa. *Development*. 125 (9). p.pp. 1723–1732.

Di Tommaso, P., Moretti, S., Xenarios, I., Orobitg, M., Montanyola, A., Chang, J.M., Taly, J.F. & Notredame, C. (2011). T-Coffee: A web server for the multiple sequence alignment of protein and RNA sequences using structural information and homology extension. *Nucleic Acids Research*. 39 (SUPPL. 2). p.pp. 13–17.

Vanzo, N.F. & Ephrussi, A. (2002). Oskar anchoring restricts pole plasm formation to the posterior of the Drosophila oocyte. *Development*. 129 (15). p.pp. 3705–3714.

Villefranc, J.A., Amigo, J. & Lawson, N.D. (2007). Gateway compatible vectors for analysis of gene function in the zebrafish. *Developmental Dynamics*. 236 (11). p.pp. 3077–3087.

Vourekas, A., Kirino, Y. & Mourelatos, Z. (2010). Elective affinities: A Tudor-Aubergine tale of germline partnership. *Genes and Development*. 24 (18). p.pp. 1963–1966.

Wagner, D.S., Dosch, R., Mintzer, K.A., Wiemelt, A.P. & Mullins, M.C. (2004). Maternal control of development at the midblastula transition and beyond: Mutants from the zebrafish II. *Developmental Cell*. 6 (6). p.pp. 781–790.

Wakahara, M. (1977). Partial characterization of 'primordial germ cell forming activity' localized in vegetal pole cytoplasm in anuran eggs. *Journal of Embryology and Experimental Morphology*. Vol. 39. p.pp. 221–233.

Wake, D.B., Wake, M.H. & Specht, C.D. (2011). Homoplasy: From detecting pattern to determining process and mechanism of evolution. *Science*. 331 (6020). p.pp. 1032–1035.

Walgers, R., Lee, T.C. & Cammers-Goodwin, A. (1998). An indirect chaotropic mechanism for the stabilization of helix conformation of peptides in

aqueous trifluoroethanol and hexafluoro-2- propanol. *Journal of the American Chemical Society*. 120 (20). p.pp. 5073–5079.

Warkocki, Z., Schneider, C., Mozaffari-Jovin, S., Schmitzová, J., Höbartner, C., Fabrizio, P. & Lührmann, R. (2015). The G-patch protein Spp2 couples the spliceosome-stimulated ATpase activity of the deah-box protein Prp2 to catalytic activation of the spliceosome. *Genes and Development*. 29 (1). p.pp. 94–107.

Xiol, J., Spinelli, P., Laussmann, M.A., Homolka, D., Yang, Z., Cora, E., Couté, Y., Conn, S., Kadlec, J., Sachidanandam, R., Kaksonen, M., Cusack, S., Ephrussi, A. & Pillai, R.S. (2014). RNA clamping by Vasa assembles a piRNA amplifier complex on transposon transcripts. *Cell*. 157 (7). p.pp. 1698–1711.

Yoon, C., Kawakami, K. & Hopkins, N. (1997). Zebrafish vasa homologue RNA is localized to the cleavage planes of 2- and 4-cell-stage embryos and is expressed in the primordial germ cells. *Development*. 124 (16). p.pp. 3157–3165.

Zhu, J., Zhang, D., Liu, X., Yu, G., Cai, X., Xu, C., Rong, F., Ouyang, G., Wang, J. & Xiao, W. (2019). Zebrafish prmt5 arginine methyltransferase is essential for germ cell development. *Development (Cambridge)*. 146 (20).

6. List of Figures

7. List of Tables

8. Appendix I-

8.1. Pairwise sequence Alignment of *Drosophila* Vasa and zebrafish Vasa

MSA

The multiple sequence alignment result as produced by T-coffee.

```
T-COFFEE, Version_11.00.d625267 (2016-01-11 15:25:41 - Revision d625267 - Build 507
Cedric Notredame
SCORE=99
*
 BAD AVG GOOD
*
Dm_Vasa    :  99
zf_Vasa    :  99
cons       :   9

Dm_Vasa    ------------------------------MSDDWDDEPIVDTRGARGGDWSDDEDTAKSFSGEAEGDGV
zf_Vasa    MDDWEEDQSPVVSCSSGFGLGSNGSDGGFKSFYTGGAGNDKSNSEGTEGSSWKMTGDSFRGRGGRGGSRGGR

cons                                      :.. .::   .     ..    .:.     .  .. .*

Dm_Vasa    GGSGGEGGGYQGGNRDVFGRIGGGRGGGAGGYRGGNRDGGGFHGGRREGERDFRGGEGGFRGGQGGSRGGQG
zf_Vasa    GGFSGFKSEIDENGSDGGWNGGESRGKGRGGFRGGFRSGSRDENDENGNDDGWKGGESRGRGRGGFGGGFRG

cons       ** .*  .  : .. *   . * .** * **:*** *.*.  ..... .: .::***.  **  * . * :*

Dm_Vasa    GSRGGQGGFRGGEGGFRGRLYENEDGDERRGRLDREERGGERRGRLDREERGGERGERGDGGFARRRRNEDD
zf_Vasa    GFRDGGNEDTGRRGFGRENNENGNDEGEGRGRGRGGFRGGFRDGGGDESGKRGFGRGGFRGRNEEVFSKVTT

cons       * *.* .   * .*  * .  :.:* .* ***     *** * *  *.. : *      *   .   :

Dm_Vasa    INNNNNIVEDVERKREFYIPPEPSNDAIEIFSSGIASGIHFSKYNNIPVKVTGSDVPQPIQHFTSADLRDII
zf_Vasa    ADKLDQEGSENAGPKVVYVPPPPPEEESSIFSH-YATGINFDKYDDILVDVSGSNPPKAIMTFEEAGLCDSL

cons        :: ::  .:    : .*:** *.::  .***  *:**:*.**::* *.*:**: *:.*  * .*.* * :

Dm_Vasa    IDNVNKSGYKIPTPIQKCSIPVISSGRDLMACAQTGSGKTAAFLLPILSKLLEDPHELELG-------RPQV
zf_Vasa    SKNVSKSGYVKPTPVQKHGIPIISAGRDLMACAQTGSGKTAAFLLPILQRFMTDG---VAASKFSEIQEPEA

cons       .**.****  ***:** .**:**:**********************.::: *    .       .*:.

Dm_Vasa    VIVSPTRELAIQIFNEARKFAFESYLKIGIVYGG--TS--FRHQNECITRGCHVVIATPGRLLDFVDRTFIT
zf_Vasa    IIVAPTRELINQIYLEARKFAYGTCVRPVVVYGGINTGYTIRE----VLKGCNVLCATPGRLHDLIGRGKIG

cons       :**:*****  **: ******: : ::  :****  *.  :*.    : :**:*: ****** *::.*  *

Dm_Vasa    FEDTRFVVLDEADRMLDMGFSEDMRRIMTHVTMR--PEHQTLMFSATFPEEIQRMAGEFLK-NYVFVAIGIV
zf_Vasa    LSKVRYLVLDEADRMLDMGFEPEMRKLVASPGMPSKEERQTLMFSATYPEDIQRMAADFLKVDYIFLAVGVV

cons       :...*::**************. :**::::   *   *:********:**:*****.:*** :*:*:*:*:*

Dm_Vasa    GGACSDVKQTIYEVNKYAKRSKLIEILSE--QADGTIVFVETKRGADFLASFLSEKEFPTTSIHGDRLQSQR
zf_Vasa    GGACSDVEQTIVQVDQYSKRDQLLELLRATGNE-RTMVFVETKRSADFIATFLCQEKISTTSIHGDREQRER

cons       *******:*** :*::*:**.:*:*:*   :  *:*******.***:*:**.:::::.******** * :*

Dm_Vasa    EQALRDFKNGSMKVLIATSVASRGLDIKNIKHVINYDMPSKIDDYVHRIGRTGRVGNNGRATSFFDPEKDRA
zf_Vasa    EKALSDFRLGQCPVLVATSVAARGLDIEQVQHVVNFDMPSSIDEYVHRIGRTGRCGNTGRAVSFFNPESDTP

cons       *:** **: *.  **:*****:*****::::**:*:****.**:********** **.***.***:**.* .

Dm_Vasa    IAADLVKILEGSGQTVPDFLRTCGAGGDGGYSNQNFGGVDVRGRGNYVGDATNVEEEEQWD-----------
zf_Vasa    LARSLVKVLSGAQQVVPKWLEEVAFSAHGTTGFNPRGKVFASTDSRKGGSFKSDEPPPSQTSAPSAAAAADD

cons       :* .***:*.*: *.**.:*.  . ...*  . :  * * .   ..  *. .. *   .

Dm_Vasa    ----
zf_Vasa    EEWE

cons
```

9. Appendix II-

9.1. Data file for ATPase assay p55

Time	Vasa	Buc+Vasa	Buc only
1	0	0	0
2	-0.00167	0.002667	0.003
3	-0.002	0.002	0
4	-0.00133	0.002667	0.001
5	-0.00133	0.002	0.001
6	-0.00133	0.001667	0
7	-0.004	0.001	0
8	-0.004	-0.00133	0
9	-0.001	-0.00133	0
10	-0.00167	-0.004	-0.001
11	-0.004	-0.00567	-0.001
12	-0.00333	-0.00533	0
13	-0.00367	-0.006	0
14	-0.005	-0.009	-0.001
15	-0.004	-0.008	-0.001
16	-0.00567	-0.00867	-0.001
17	-0.00467	-0.00867	-0.001
18	-0.006	-0.01067	-0.001
19	-0.006	-0.00933	-0.001
20	-0.008	-0.011	-0.001
21	-0.00633	-0.01133	-0.003
22	-0.00767	-0.01267	-0.003
23	-0.00567	-0.011	-0.001
24	-0.00767	-0.014	-0.001
25	-0.00833	-0.01367	-0.001
26	-0.00833	-0.016	-0.003
27	-0.01033	-0.01633	-0.001
28	-0.00867	-0.01533	-0.002
29	-0.01067	-0.017	-0.001
30	-0.01	-0.017	-0.003
31	-0.01033	-0.01833	-0.004
32	-0.00967	-0.01767	-0.003
33	-0.01	-0.01767	-0.002
34	-0.012	-0.01867	-0.004
35	-0.01133	-0.019	-0.003
36	-0.01133	-0.02067	-0.005
37	-0.01167	-0.02167	-0.004
38	-0.012	-0.021	-0.003

39	-0.01467	-0.022	-0.005
40	-0.012	-0.02033	-0.005
41	-0.01233	-0.02167	-0.005
42	-0.01433	-0.02433	-0.005
43	-0.013	-0.024	-0.003
44	-0.01433	-0.024	-0.005
45	-0.015	-0.02567	-0.005
46	-0.01467	-0.02467	-0.005
47	-0.01767	-0.02767	-0.005
48	-0.01667	-0.02733	-0.005
49	-0.01433	-0.02667	-0.006
50	-0.01733	-0.02833	-0.008
51	-0.01767	-0.02967	-0.005
52	-0.01833	-0.03033	-0.007
53	-0.01867	-0.03033	-0.006
54	-0.018	-0.03	-0.005
55	-0.019	-0.03133	-0.008
56	-0.01867	-0.033	-0.005
57	-0.01933	-0.03233	-0.006
58	-0.01967	-0.03333	-0.007
59	-0.02033	-0.03267	-0.007
60	-0.019	-0.034	-0.007
61	-0.01967	-0.03467	-0.007
62	-0.02133	-0.03433	-0.007
63	-0.02267	-0.03633	-0.007
64	-0.02	-0.03567	-0.006
65	-0.02067	-0.036	-0.008
66	-0.024	-0.038	-0.008
67	-0.02167	-0.037	-0.008
68	-0.02367	-0.03967	-0.009
69	-0.024	-0.03967	-0.008
70	-0.02267	-0.03967	-0.008
71	-0.02333	-0.04067	-0.009
72	-0.024	-0.04167	-0.009
73	-0.02433	-0.041	-0.008
74	-0.02433	-0.04233	-0.01
75	-0.02567	-0.042	-0.009
76	-0.025	-0.04267	-0.01
77	-0.025	-0.043	-0.01
78	-0.02667	-0.045	-0.008
79	-0.026	-0.045	-0.012
80	-0.02633	-0.04533	-0.008
81	-0.028	-0.04533	-0.011
82	-0.02733	-0.047	-0.01
83	-0.02867	-0.04767	-0.01

84	-0.02867	-0.04767	-0.01
85	-0.029	-0.04933	-0.011
86	-0.02667	-0.04733	-0.011
87	-0.02833	-0.04833	-0.01
88	-0.03067	-0.05	-0.011
89	-0.031	-0.05067	-0.009
90	-0.03067	-0.051	-0.01
91	-0.03133	-0.052	-0.008
92	-0.03033	-0.05233	-0.013
93	-0.031	-0.05233	-0.009
94	-0.031	-0.05333	-0.011
95	-0.03033	-0.05267	-0.012
96	-0.03233	-0.056	-0.011
97	-0.03133	-0.05467	-0.008
98	-0.033	-0.056	-0.012
99	-0.03233	-0.05533	-0.011
100	-0.032	-0.055	-0.012
101	-0.034	-0.05567	-0.012
102	-0.034	-0.058	-0.011
103	-0.035	-0.059	-0.011
104	-0.03267	-0.05967	-0.011
105	-0.03667	-0.06033	-0.013
106	-0.036	-0.06033	-0.011
107	-0.03533	-0.05933	-0.012
108	-0.03467	-0.06133	-0.011
109	-0.03733	-0.06233	-0.013
110	-0.03667	-0.06267	-0.012
111	-0.037	-0.06233	-0.011
112	-0.03833	-0.065	-0.013
113	-0.038	-0.065	-0.011
114	-0.03833	-0.06533	-0.012
115	-0.03567	-0.06433	-0.013
116	-0.03967	-0.065	-0.013
117	-0.03867	-0.066	-0.015
118	-0.039	-0.066	-0.013
119	-0.04067	-0.06733	-0.014
120	-0.04	-0.06767	-0.015
121	-0.04033	-0.068	-0.013
122	-0.04133	-0.07	-0.013
123	-0.04167	-0.06967	-0.014
124	-0.04133	-0.07	-0.015
125	-0.04167	-0.071	-0.014
126	-0.04133	-0.072	-0.013
127	-0.04167	-0.07133	-0.015
128	-0.04267	-0.07167	-0.015

129	-0.04367	-0.07267	-0.015
130	-0.04267	-0.07233	-0.016
131	-0.042	-0.074	-0.015
132	-0.04267	-0.074	-0.014
133	-0.04433	-0.07433	-0.015
134	-0.044	-0.07533	-0.015
135	-0.044	-0.075	-0.014
136	-0.04333	-0.07533	-0.015
137	-0.043	-0.07633	-0.015
138	-0.04533	-0.07733	-0.015
139	-0.04533	-0.07767	-0.016
140	-0.04533	-0.07767	-0.016
141	-0.047	-0.07867	-0.015
142	-0.04633	-0.08	-0.015
143	-0.047	-0.081	-0.015
144	-0.04833	-0.081	-0.015
145	-0.047	-0.08067	-0.016
146	-0.048	-0.082	-0.015
147	-0.047	-0.08233	-0.018
148	-0.04767	-0.08267	-0.016
149	-0.04867	-0.084	-0.015
150	-0.048	-0.08333	-0.016
151	-0.04733	-0.08433	-0.015
152	-0.04967	-0.08533	-0.015
153	-0.04967	-0.08467	-0.015
154	-0.049	-0.08433	-0.017
155	-0.05	-0.08633	-0.018
156	-0.05067	-0.08833	-0.017
157	-0.052	-0.088	-0.019
158	-0.05033	-0.08767	-0.018
159	-0.05167	-0.089	-0.017
160	-0.05167	-0.09033	-0.018
161	-0.05133	-0.08833	-0.017
162	-0.053	-0.09133	-0.014
163	-0.05433	-0.09133	-0.017
164	-0.052	-0.09167	-0.018
165	-0.05267	-0.092	-0.016
166	-0.054	-0.09233	-0.017
167	-0.05367	-0.093	-0.016
168	-0.055	-0.094	-0.018
169	-0.05633	-0.09333	-0.017
170	-0.056	-0.095	-0.017
171	-0.05567	-0.09467	-0.018
172	-0.056	-0.095	-0.017
173	-0.05633	-0.097	-0.017

174	-0.056	-0.09633	-0.018
175	-0.05767	-0.098	-0.018
176	-0.057	-0.097	-0.019
177	-0.05733	-0.09833	-0.018
178	-0.05833	-0.09767	-0.018
179	-0.05633	-0.09733	-0.019
180	-0.057	-0.099	-0.019
181	-0.05767	-0.09967	-0.018
182	-0.05933	-0.10167	-0.019
183	-0.057	-0.10033	-0.017
184	-0.058	-0.10167	-0.018
185	-0.05933	-0.102	-0.019
186	-0.061	-0.10333	-0.019
187	-0.05933	-0.103	-0.019
188	-0.05967	-0.10333	-0.019
189	-0.061	-0.10533	-0.018
190	-0.06233	-0.10467	-0.018
191	-0.061	-0.10533	-0.019
192	-0.062	-0.10633	-0.018
193	-0.062	-0.107	-0.019
194	-0.05967	-0.10633	-0.02
195	-0.06367	-0.10767	-0.019
196	-0.064	-0.10767	-0.019
197	-0.064	-0.10867	-0.02
198	-0.06367	-0.10967	-0.019
199	-0.066	-0.11133	-0.018
200	-0.065	-0.11167	-0.02
201	-0.06533	-0.11067	-0.019
202	-0.06567	-0.112	-0.02
203	-0.06567	-0.11167	-0.019
204	-0.06633	-0.11233	-0.02
205	-0.06433	-0.11167	-0.02
206	-0.06633	-0.114	-0.02
207	-0.06733	-0.11333	-0.02
208	-0.06733	-0.11533	-0.02
209	-0.06767	-0.11533	-0.021
210	-0.068	-0.11467	-0.021
211	-0.06967	-0.11667	-0.02
212	-0.07033	-0.11633	-0.021
213	-0.06733	-0.11733	-0.02
214	-0.06767	-0.117	-0.021
215	-0.07067	-0.11767	-0.021
216	-0.071	-0.119	-0.021
217	-0.07	-0.11733	-0.022
218	-0.07033	-0.11933	-0.021

219	-0.069	-0.11933	-0.021
220	-0.06867	-0.12	-0.022
221	-0.07333	-0.12233	-0.022
222	-0.07133	-0.12167	-0.022
223	-0.07233	-0.122	-0.021
224	-0.07333	-0.12267	-0.022
225	-0.072	-0.12333	-0.022
226	-0.07333	-0.12367	-0.021
227	-0.07267	-0.12333	-0.022
228	-0.07233	-0.124	-0.021
229	-0.073	-0.125	-0.022
230	-0.07467	-0.12567	-0.022
231	-0.075	-0.12567	-0.024
232	-0.075	-0.12633	-0.022
233	-0.07433	-0.12767	-0.023
234	-0.076	-0.12767	-0.023
235	-0.075	-0.12733	-0.02
236	-0.07567	-0.12767	-0.022
237	-0.07633	-0.129	-0.022
238	-0.076	-0.13033	-0.024
239	-0.07733	-0.13067	-0.021
240	-0.07833	-0.13067	-0.024
241	-0.07967	-0.13267	-0.023
242	-0.07833	-0.13167	-0.023
243	-0.07867	-0.13333	-0.022
244	-0.07833	-0.13367	-0.025
245	-0.079	-0.13333	-0.023
246	-0.07767	-0.13367	-0.024
247	-0.07933	-0.135	-0.025
248	-0.08033	-0.13533	-0.025
249	-0.082	-0.13567	-0.025
250	-0.081	-0.137	-0.022
251	-0.08133	-0.13733	-0.026
252	-0.08167	-0.13733	-0.024
253	-0.08167	-0.138	-0.025
254	-0.081	-0.137	-0.026
255	-0.08367	-0.139	-0.025
256	-0.082	-0.13967	-0.025
257	-0.08267	-0.14	-0.023
258	-0.08167	-0.13867	-0.025
259	-0.084	-0.14033	-0.024
260	-0.08533	-0.14167	-0.027
261	-0.08367	-0.141	-0.025
262	-0.08567	-0.14167	-0.025
263	-0.08667	-0.144	-0.026

264	-0.08567	-0.14367	-0.024
265	-0.08567	-0.14433	-0.026
266	-0.086	-0.14433	-0.025
267	-0.086	-0.145	-0.025
268	-0.086	-0.144	-0.026
269	-0.08633	-0.14533	-0.025
270	-0.088	-0.14733	-0.025
271	-0.08833	-0.147	-0.025
272	-0.08833	-0.14733	-0.025
273	-0.08833	-0.148	-0.025
274	-0.09033	-0.149	-0.025
275	-0.08867	-0.14833	-0.027
276	-0.08967	-0.14967	-0.025
277	-0.091	-0.15	-0.026
278	-0.08967	-0.15067	-0.026
279	-0.09133	-0.15133	-0.025
280	-0.09133	-0.15167	-0.026
281	-0.093	-0.15267	-0.026
282	-0.091	-0.152	-0.028
283	-0.09367	-0.154	-0.027
284	-0.093	-0.15367	-0.028
285	-0.094	-0.15433	-0.027
286	-0.092	-0.15433	-0.025
287	-0.09433	-0.15567	-0.027
288	-0.094	-0.15633	-0.026
289	-0.09433	-0.157	-0.027
290	-0.09367	-0.156	-0.027
291	-0.093	-0.15667	-0.027
292	-0.09633	-0.15867	-0.025
293	-0.09633	-0.15933	-0.026
294	-0.098	-0.15967	-0.027
295	-0.09567	-0.15933	-0.026
296	-0.097	-0.15933	-0.026
297	-0.09633	-0.16033	-0.029
298	-0.09633	-0.16033	-0.027
299	-0.09867	-0.162	-0.028
300	-0.09567	-0.162	-0.027
301	-0.09833	-0.16367	-0.028
302	-0.098	-0.16333	-0.026
303	-0.099	-0.16267	-0.027
304	-0.098	-0.16333	-0.029
305	-0.10133	-0.16367	-0.029
306	-0.098	-0.164	-0.027
307	-0.10133	-0.16467	-0.027
308	-0.10067	-0.167	-0.028

309	-0.1	-0.16633	-0.029
310	-0.10033	-0.16633	-0.027
311	-0.101	-0.16767	-0.03
312	-0.101	-0.168	-0.029

10. Appendix III

10.1. Data for ATPase assay p55

Time (min)	Buc+Vasa+RNA	Buc+Vasa	Vasa+RNA	Buc	Vasa
1	0	0	0	0	0
2	3.33E+01	1.00E-03	-6.67E+01	0	6.67E+01
3	-0,00133	0,00133	-0,00133	0	-3.33E+01
4	-3.33E+01	1.00E-03	-3.33E+01	0	-3.33E+01
5	-0,00233	-6.67E+01	-6.67E+01	0	-3.33E+01
6	-0,00267	-0,002	-0,00133	-3.33E+01	-6.67E+01
7	-0,00333	-0,00167	-0,00233	-6.67E+01	-3.33E+01
8	-0,00433	-0,00167	-0,002	-1.00E-03	-0,00167
9	-0,005	-0,00267	-0,00133	-1.00E-03	-1.00E-03
10	-0,00533	-0,00267	-0,002	-3.33E+01	-0,00167
11	-0,007	-0,004	-0,003	-0,00133	-0,00167
12	-0,00833	-0,005	-0,00333	-0,00133	-0,00267
13	-0,00733	-0,00467	-0,00167	-6.67E+01	-1.00E-03
14	-0,00833	-0,005	-0,002	-0,00133	-0,00233
15	-0,00867	-0,00567	-0,00433	-0,00167	-0,00267
16	-0,01167	-0,00733	-0,00467	-0,00167	-0,00367
17	-0,01133	-0,00733	-0,00433	-0,00167	-0,00267
18	-0,01233	-0,00833	-0,00433	-0,00233	-0,00333
19	-0,012	-0,008	-0,005	-0,00133	-0,003
20	-0,01233	-0,00833	-0,004	-3.33E+01	-0,00267
21	-0,01433	-0,00933	-0,00567	-0,00267	-0,00467
22	-0,013	-0,00933	-0,00467	-1.00E-03	-0,00333
23	-0,016	-0,01033	-0,00533	-0,00267	-0,00433
24	-0,016	-0,01267	-0,00633	-0,00133	-0,00467
25	-0,01667	-0,01267	-0,00667	-0,00333	-0,00467
26	-0,01667	-0,011	-0,00567	-0,00233	-0,004
27	-0,01633	-0,012	-0,006	-0,00233	-0,00367
28	-0,01733	-0,013	-0,00733	-0,00167	-0,00467
29	-0,018	-0,014	-0,00633	-0,00233	-0,005
30	-0,01933	-0,01467	-0,00667	-0,003	-0,005

31	-0,02	-0,01433	-0,008	-0,00233	-0,00533
32	-0,02033	-0,016	-0,008	-0,00267	-0,00533
33	-0,02067	-0,01533	-0,008	-0,00267	-0,00533
34	-0,021	-0,016	-0,00733	-0,00233	-0,00567
35	-0,02267	-0,01833	-0,00967	-0,00367	-0,00667
36	-0,02167	-0,01733	-0,00867	-0,00233	-0,006
37	-0,023	-0,01833	-0,009	-0,00333	-0,00767
38	-0,02433	-0,018	-0,00967	-0,00267	-0,00633
39	-0,02567	-0,02033	-0,01067	-0,00433	-0,00767
40	-0,02533	-0,01967	-0,01	-0,003	-0,00667
41	-0,02633	-0,02067	-0,01067	-0,00367	-0,007
42	-0,02567	-0,02	-0,01033	-0,003	-0,007
43	-0,027	-0,02067	-0,01067	-0,00367	-0,00833
44	-0,026	-0,02067	-0,01	-0,003	-0,00667
45	-0,028	-0,02167	-0,011	-0,003	-0,00767
46	-0,028	-0,02267	-0,012	-0,00233	-0,008
47	-0,02833	-0,023	-0,011	-0,00333	-0,008
48	-0,03067	-0,024	-0,01233	-0,00367	-0,009
49	-0,03033	-0,02333	-0,013	-0,003	-0,00867
50	-0,03	-0,02367	-0,01233	-0,00333	-0,00833
51	-0,03167	-0,02533	-0,013	-0,003	-0,009
52	-0,03267	-0,02567	-0,014	-0,003	-0,00933
53	-0,034	-0,02733	-0,015	-0,006	-0,01067
54	-0,03333	-0,02667	-0,01467	-0,00467	-0,01
55	-0,03467	-0,02733	-0,01433	-0,00367	-0,01067
56	-0,035	-0,02833	-0,015	-0,00533	-0,00933
57	-0,03533	-0,029	-0,01533	-0,00567	-0,01067
58	-0,036	-0,02833	-0,015	-0,004	-0,01067
59	-0,03667	-0,02967	-0,016	-0,00467	-0,011
60	-0,037	-0,03	-0,01533	-0,00467	-0,011
61	-0,03633	-0,02867	-0,01567	-0,00433	-0,01033
62	-0,03733	-0,03	-0,015	-0,004	-0,01033
63	-0,03833	-0,03067	-0,016	-0,00367	-0,01067
64	-0,04033	-0,033	-0,018	-0,005	-0,013
65	-0,04	-0,033	-0,017	-0,005	-0,01267
66	-0,04133	-0,033	-0,01867	-0,005	-0,013
67	-0,04067	-0,03267	-0,01733	-0,00367	-0,01167
68	-0,04167	-0,03333	-0,019	-0,005	-0,01167
69	-0,042	-0,03367	-0,01767	-0,004	-0,01233
70	-0,04333	-0,03467	-0,01833	-0,005	-0,013
71	-0,04333	-0,03367	-0,019	-0,00533	-0,013
72	-0,04433	-0,03633	-0,019	-0,00567	-0,015
73	-0,04433	-0,03567	-0,01933	-0,00567	-0,013
74	-0,044	-0,03533	-0,01933	-0,00433	-0,01233
75	-0,04567	-0,036	-0,01933	-0,00533	-0,013

76	-0,04633	-0,03733	-0,021	-0,00533	-0,014
77	-0,04633	-0,037	-0,02033	-0,00533	-0,01533
78	-0,04567	-0,03767	-0,02067	-0,00433	-0,014
79	-0,047	-0,03867	-0,02033	-0,00533	-0,01433
80	-0,04833	-0,03933	-0,022	-0,00533	-0,01533
81	-0,049	-0,04	-0,02167	-0,00567	-0,01567
82	-0,04933	-0,03967	-0,022	-0,006	-0,01567
83	-0,05033	-0,04033	-0,02167	-0,00633	-0,016
84	-0,05033	-0,04067	-0,02167	-0,00533	-0,015
85	-0,05067	-0,041	-0,02267	-0,00533	-0,01533
86	-0,052	-0,04167	-0,024	-0,00567	-0,01567
87	-0,052	-0,04233	-0,02333	-0,006	-0,01533
88	-0,05233	-0,04333	-0,02333	-0,006	-0,01667
89	-0,05333	-0,04167	-0,023	-0,00533	-0,016
90	-0,054	-0,04333	-0,02333	-0,006	-0,01633
91	-0,054	-0,04433	-0,02467	-0,00533	-0,01733
92	-0,05367	-0,04433	-0,02333	-0,00533	-0,01567
93	-0,05433	-0,04367	-0,024	-0,00533	-0,016
94	-0,056	-0,045	-0,025	-0,00567	-0,01733
95	-0,056	-0,046	-0,02467	-0,00567	-0,01733
96	-0,05533	-0,04567	-0,024	-0,006	-0,01633
97	-0,05767	-0,04667	-0,026	-0,00633	-0,01767
98	-0,058	-0,04733	-0,02633	-0,007	-0,01867
99	-0,059	-0,04767	-0,027	-0,007	-0,01833
100	-0,05933	-0,04733	-0,02667	-0,006	-0,01867
101	-0,059	-0,04867	-0,02533	-0,00633	-0,018
102	-0,06	-0,04867	-0,02767	-0,006	-0,01867
103	-0,05967	-0,04833	-0,02767	-0,007	-0,01933
104	-0,061	-0,04967	-0,026	-0,006	-0,01767
105	-0,06233	-0,05	-0,027	-0,00633	-0,01867
106	-0,06167	-0,05	-0,02733	-0,00633	-0,018
107	-0,06433	-0,05233	-0,02833	-0,007	-0,02
108	-0,063	-0,05133	-0,02733	-0,00633	-0,01967
109	-0,064	-0,05233	-0,02967	-0,008	-0,02067
110	-0,064	-0,05267	-0,02967	-0,00733	-0,02
111	-0,06467	-0,05267	-0,029	-0,00667	-0,02
112	-0,06567	-0,05167	-0,029	-0,00667	-0,01967
113	-0,065	-0,05267	-0,02867	-0,00667	-0,01933
114	-0,06567	-0,05367	-0,02933	-0,007	-0,02
115	-0,067	-0,05433	-0,029	-0,006	-0,02
116	-0,06833	-0,05467	-0,03	-0,00733	-0,02133
117	-0,06667	-0,05467	-0,031	-0,007	-0,021
118	-0,06833	-0,05533	-0,02933	-0,00733	-0,021
119	-0,06867	-0,05567	-0,03033	-0,007	-0,02167
120	-0,06867	-0,05567	-0,03067	-0,006	-0,02033

121	-0,06933	-0,05633	-0,03167	-0,007	-0,021
122	-0,06967	-0,05633	-0,032	-0,007	-0,02067
123	-0,06933	-0,05667	-0,03133	-0,007	-0,021
124	-0,07067	-0,05767	-0,031	-0,00667	-0,021
125	-0,07267	-0,05867	-0,033	-0,00733	-0,02233
126	-0,07133	-0,05833	-0,032	-0,00667	-0,02133
127	-0,07233	-0,059	-0,032	-0,00733	-0,02167
128	-0,07267	-0,05967	-0,032	-0,008	-0,02167
129	-0,074	-0,06067	-0,03467	-0,00767	-0,02333
130	-0,075	-0,06067	-0,034	-0,008	-0,02267
131	-0,074	-0,06033	-0,03333	-0,00667	-0,02233
132	-0,07467	-0,06133	-0,03367	-0,007	-0,02333
133	-0,07667	-0,063	-0,03533	-0,00767	-0,02367
134	-0,077	-0,06233	-0,03467	-0,008	-0,02367
135	-0,07633	-0,06267	-0,035	-0,00733	-0,02333
136	-0,077	-0,06233	-0,035	-0,00767	-0,024
137	-0,07733	-0,06167	-0,03433	-0,007	-0,02433
138	-0,078	-0,063	-0,035	-0,00733	-0,025
139	-0,07933	-0,065	-0,03733	-0,009	-0,02567
140	-0,078	-0,06367	-0,03567	-0,00733	-0,02367
141	-0,079	-0,06433	-0,03667	-0,00633	-0,024
142	-0,08	-0,06533	-0,037	-0,008	-0,02467
143	-0,08	-0,06533	-0,03633	-0,00833	-0,02433
144	-0,082	-0,066	-0,03733	-0,00833	-0,02533
145	-0,08233	-0,06633	-0,03767	-0,00867	-0,02567
146	-0,08267	-0,06633	-0,03767	-0,00833	-0,02567
147	-0,083	-0,06733	-0,03867	-0,00833	-0,02633
148	-0,083	-0,06767	-0,03833	-0,008	-0,02567
149	-0,08467	-0,06833	-0,04	-0,00933	-0,02667
150	-0,085	-0,06933	-0,03933	-0,01033	-0,027
151	-0,084	-0,067	-0,038	-0,008	-0,026
152	-0,08567	-0,06967	-0,03933	-0,00933	-0,027
153	-0,08533	-0,06967	-0,04	-0,00767	-0,027
154	-0,08633	-0,07	-0,04033	-0,00867	-0,02767
155	-0,08767	-0,07067	-0,04067	-0,009	-0,028
156	-0,08733	-0,071	-0,041	-0,009	-0,02767
157	-0,088	-0,07	-0,04033	-0,008	-0,02667
158	-0,08833	-0,07167	-0,042	-0,00867	-0,028
159	-0,08867	-0,07133	-0,04133	-0,00833	-0,02733
160	-0,08867	-0,07167	-0,04167	-0,008	-0,02833
161	-0,08867	-0,07133	-0,041	-0,00833	-0,027
162	-0,09033	-0,07333	-0,04333	-0,00967	-0,029
163	-0,09	-0,07333	-0,042	-0,00833	-0,02867
164	-0,091	-0,07333	-0,04233	-0,00967	-0,02933
165	-0,092	-0,07433	-0,044	-0,01	-0,029

166	-0,09133	-0,07433	-0,04267	-0,00933	-0,028
167	-0,09233	-0,07367	-0,04233	-0,00967	-0,02933
168	-0,09267	-0,07633	-0,04467	-0,00967	-0,02967
169	-0,093	-0,076	-0,044	-0,00933	-0,03
170	-0,094	-0,077	-0,044	-0,01033	-0,02933
171	-0,09433	-0,07733	-0,044	-0,01067	-0,03067
172	-0,09467	-0,076	-0,04367	-0,00967	-0,03
173	-0,09567	-0,07733	-0,04467	-0,00933	-0,03067
174	-0,095	-0,07767	-0,04533	-0,009	-0,03033
175	-0,09633	-0,07833	-0,045	-0,00967	-0,031
176	-0,097	-0,07767	-0,04533	-0,01067	-0,03067
177	-0,09667	-0,079	-0,04633	-0,01033	-0,03
178	-0,09767	-0,079	-0,047	-0,00967	-0,03133
179	-0,09833	-0,08033	-0,04733	-0,01033	-0,031
180	-0,09767	-0,07967	-0,04633	-0,00967	-0,031
181	-0,09833	-0,07933	-0,046	-0,009	-0,03067
182	-0,09967	-0,081	-0,04667	-0,01067	-0,03133
183	-0,10033	-0,081	-0,04667	-0,01067	-0,03133
184	-0,09933	-0,08033	-0,04733	-0,01033	-0,03133
185	-0,101	-0,082	-0,04833	-0,01	-0,03267
186	-0,10167	-0,08267	-0,05067	-0,011	-0,03367
187	-0,10233	-0,083	-0,04933	-0,01033	-0,03333
188	-0,102	-0,08367	-0,04733	-0,01067	-0,033
189	-0,102	-0,08367	-0,04733	-0,01167	-0,03333
190	-0,10067	-0,082	-0,046	-0,00867	-0,03067
191	-0,10133	-0,08267	-0,047	-0,00933	-0,03233
192	-0,10067	-0,08267	-0,047	-0,00933	-0,032
193	-0,10167	-0,08367	-0,04667	-0,00833	-0,032
194	-0,102	-0,083	-0,047	-0,00967	-0,03133
195	-0,103	-0,08467	-0,048	-0,00933	-0,03167
196	-0,10367	-0,084	-0,047	-0,00933	-0,03233
197	-0,104	-0,084	-0,04733	-0,00933	-0,033
198	-0,105	-0,08667	-0,04967	-0,01033	-0,03333
199	-0,10567	-0,086	-0,04867	-0,00967	-0,03267
200	-0,106	-0,086	-0,04967	-0,01033	-0,03367
201	-0,10533	-0,08633	-0,049	-0,00933	-0,03333
202	-0,10633	-0,08667	-0,04933	-0,00967	-0,03333
203	-0,106	-0,08667	-0,04933	-0,00967	-0,03333
204	-0,10767	-0,08733	-0,051	-0,01033	-0,034
205	-0,10767	-0,08833	-0,05033	-0,01067	-0,03467
206	-0,10733	-0,08733	-0,05067	-0,01067	-0,03467
207	-0,10867	-0,08833	-0,05133	-0,01033	-0,035
208	-0,10967	-0,09	-0,05167	-0,011	-0,03533
209	-0,109	-0,089	-0,05133	-0,011	-0,03533
210	-0,109	-0,089	-0,05133	-0,01	-0,03433

211	-0,11033	-0,08933	-0,052	-0,01133	-0,03533
212	-0,10967	-0,08967	-0,051	-0,00967	-0,034
213	-0,111	-0,091	-0,05233	-0,00967	-0,03467
214	-0,11233	-0,09167	-0,05367	-0,011	-0,03633
215	-0,112	-0,091	-0,05267	-0,01	-0,03533
216	-0,11233	-0,09167	-0,053	-0,01	-0,03667
217	-0,11333	-0,092	-0,054	-0,01167	-0,036
218	-0,113	-0,09133	-0,053	-0,01067	-0,036
219	-0,113	-0,09133	-0,05267	-0,009	-0,03467
220	-0,11467	-0,092	-0,055	-0,011	-0,03733
221	-0,11467	-0,09267	-0,05467	-0,01133	-0,036
222	-0,11467	-0,09267	-0,055	-0,01133	-0,037
223	-0,11467	-0,09333	-0,05467	-0,01033	-0,037
224	-0,116	-0,09333	-0,05467	-0,01	-0,036
225	-0,11633	-0,095	-0,055	-0,01033	-0,03733
226	-0,11667	-0,09367	-0,055	-0,01033	-0,037
227	-0,11633	-0,09433	-0,055	-0,00967	-0,037
228	-0,11733	-0,09433	-0,056	-0,01033	-0,03733
229	-0,11767	-0,095	-0,05533	-0,01067	-0,03733
230	-0,117	-0,09533	-0,05667	-0,01033	-0,03833
231	-0,11767	-0,09567	-0,056	-0,01	-0,03633
232	-0,11867	-0,09533	-0,05633	-0,01067	-0,03733
233	-0,11867	-0,096	-0,05633	-0,00933	-0,03767
234	-0,12067	-0,09767	-0,058	-0,01133	-0,039
235	-0,12033	-0,09733	-0,05733	-0,011	-0,03867
236	-0,121	-0,09833	-0,05733	-0,01167	-0,038
237	-0,12167	-0,097	-0,057	-0,01133	-0,03833
238	-0,122	-0,099	-0,059	-0,012	-0,03933
239	-0,12167	-0,09933	-0,059	-0,01133	-0,03933
240	-0,12267	-0,09867	-0,05867	-0,01133	-0,03867
241	-0,123	-0,09933	-0,05933	-0,01133	-0,039
242	-0,12267	-0,099	-0,059	-0,01033	-0,03833
243	-0,123	-0,099	-0,059	-0,01033	-0,03867
244	-0,125	-0,101	-0,06	-0,01167	-0,03967
245	-0,125	-0,101	-0,06033	-0,01167	-0,041
246	-0,12467	-0,10067	-0,06033	-0,011	-0,03967
247	-0,12533	-0,10033	-0,06133	-0,01067	-0,03933
248	-0,12533	-0,1	-0,06	-0,01067	-0,03967
249	-0,12633	-0,101	-0,06133	-0,01167	-0,041
250	-0,12833	-0,103	-0,062	-0,013	-0,042
251	-0,12733	-0,102	-0,061	-0,012	-0,04033
252	-0,12733	-0,103	-0,06133	-0,012	-0,041
253	-0,128	-0,10267	-0,06167	-0,011	-0,04133
254	-0,12867	-0,10333	-0,062	-0,01133	-0,04133
255	-0,129	-0,10367	-0,063	-0,013	-0,04233

256	-0,12833	-0,10333	-0,06167	-0,01033	-0,04067
257	-0,12967	-0,10367	-0,06233	-0,01133	-0,04167
258	-0,13067	-0,10367	-0,063	-0,01133	-0,04167
259	-0,131	-0,10433	-0,06367	-0,012	-0,042
260	-0,13133	-0,105	-0,06367	-0,011	-0,042
261	-0,13233	-0,105	-0,06433	-0,01167	-0,043
262	-0,13167	-0,106	-0,06433	-0,013	-0,04233
263	-0,13333	-0,10533	-0,064	-0,012	-0,04267
264	-0,13233	-0,105	-0,06333	-0,011	-0,04167
265	-0,13233	-0,10633	-0,06433	-0,01133	-0,04233
266	-0,13333	-0,107	-0,065	-0,01267	-0,043
267	-0,13333	-0,10633	-0,06533	-0,01167	-0,04267
268	-0,134	-0,10667	-0,06433	-0,011	-0,042
269	-0,13433	-0,10667	-0,065	-0,01133	-0,043
270	-0,134	-0,10733	-0,06633	-0,012	-0,044
271	-0,136	-0,108	-0,06667	-0,01167	-0,04333
272	-0,13567	-0,10667	-0,06567	-0,011	-0,043
273	-0,136	-0,10733	-0,066	-0,01167	-0,043
274	-0,13633	-0,10833	-0,066	-0,01033	-0,04433
275	-0,13667	-0,10767	-0,066	-0,011	-0,04333
276	-0,13733	-0,10933	-0,067	-0,01133	-0,04367
277	-0,13767	-0,109	-0,067	-0,011	-0,04467
278	-0,13833	-0,10867	-0,06767	-0,01167	-0,044
279	-0,138	-0,109	-0,06633	-0,011	-0,04267
280	-0,13867	-0,10833	-0,06733	-0,01067	-0,04433
281	-0,14	-0,111	-0,068	-0,01233	-0,045
282	-0,13933	-0,10933	-0,06667	-0,01067	-0,04467
283	-0,14067	-0,11067	-0,06833	-0,01133	-0,046
284	-0,14067	-0,11133	-0,06833	-0,01133	-0,045
285	-0,14233	-0,11267	-0,069	-0,01233	-0,045
286	-0,14167	-0,11133	-0,069	-0,012	-0,04367
287	-0,141	-0,11033	-0,069	-0,01133	-0,04567
288	-0,14233	-0,112	-0,06967	-0,011	-0,04567
289	-0,14333	-0,11267	-0,07067	-0,01167	-0,04567
290	-0,14433	-0,11333	-0,07033	-0,01267	-0,046
291	-0,14333	-0,113	-0,069	-0,011	-0,04533
292	-0,14367	-0,11267	-0,07	-0,01133	-0,04533
293	-0,14367	-0,113	-0,06967	-0,011	-0,04533
294	-0,14433	-0,11333	-0,071	-0,012	-0,04633
295	-0,14433	-0,11333	-0,07	-0,01067	-0,045
296	-0,14533	-0,11533	-0,072	-0,012	-0,04667
297	-0,14567	-0,11367	-0,07133	-0,012	-0,04567
298	-0,14567	-0,11433	-0,07033	-0,01133	-0,045
299	-0,14533	-0,11433	-0,07067	-0,01	-0,047
300	-0,14567	-0,114	-0,06967	-0,01067	-0,046

301	-0,146	-0,11433	-0,073	-0,012	-0,04567
302	-0,14667	-0,11633	-0,07167	-0,01167	-0,047
303	-0,148	-0,11667	-0,07333	-0,012	-0,048
304	-0,14833	-0,11633	-0,07333	-0,01233	-0,04633
305	-0,14767	-0,115	-0,07167	-0,011	-0,046
306	-0,14833	-0,11533	-0,07367	-0,011	-0,047
307	-0,14933	-0,116	-0,073	-0,01133	-0,04767
308	-0,14833	-0,11633	-0,07233	-0,011	-0,04733
309	-0,14967	-0,116	-0,07333	-0,01133	-0,047
310	-0,15	-0,117	-0,07333	-0,01167	-0,04667
311	-0,151	-0,11733	-0,07433	-0,01233	-0,04833
312	-0,15167	-0,11867	-0,076	-0,01233	-0,04867
313	-0,15133	-0,11833	-0,07567	-0,012	-0,04867
314	-0,152	-0,119	-0,074	-0,012	-0,04833
315	-0,15333	-0,12033	-0,07733	-0,013	-0,049
316	-0,15233	-0,11833	-0,07433	-0,012	-0,04867
317	-0,15367	-0,12	-0,078	-0,01267	-0,05
318	-0,15233	-0,11867	-0,076	-0,011	-0,04867
319	-0,154	-0,121	-0,078	-0,01333	-0,05
320	-0,15433	-0,12033	-0,076	-0,01267	-0,05
321	-0,154	-0,12	-0,076	-0,012	-0,04867
322	-0,15467	-0,12167	-0,07833	-0,01233	-0,04933
323	-0,15533	-0,12133	-0,07867	-0,01233	-0,05033
324	-0,155	-0,121	-0,07667	-0,01167	-0,04967
325	-0,155	-0,12067	-0,07767	-0,01133	-0,049
326	-0,15667	-0,121	-0,078	-0,012	-0,05
327	-0,156	-0,12167	-0,07833	-0,01267	-0,05
328	-0,15733	-0,12267	-0,077	-0,01233	-0,05
329	-0,157	-0,12167	-0,07967	-0,01233	-0,04967
330	-0,15733	-0,12267	-0,07967	-0,01267	-0,05067
331	-0,15733	-0,12267	-0,07933	-0,01233	-0,05033
332	-0,15767	-0,12267	-0,07867	-0,01167	-0,05067
333	-0,158	-0,122	-0,08	-0,01133	-0,05133
334	-0,15833	-0,12467	-0,08	-0,01233	-0,05033
335	-0,15867	-0,12367	-0,07867	-0,01167	-0,051
336	-0,15933	-0,124	-0,08133	-0,01233	-0,05167
337	-0,16067	-0,12467	-0,08067	-0,01267	-0,052
338	-0,15933	-0,12333	-0,07867	-0,01167	-0,05033
339	-0,15933	-0,124	-0,08	-0,012	-0,05133
340	-0,16067	-0,12433	-0,081	-0,011	-0,05067
341	-0,16167	-0,12467	-0,08	-0,01267	-0,05167
342	-0,16133	-0,12433	-0,07967	-0,012	-0,051
343	-0,16167	-0,12467	-0,081	-0,012	-0,05167
344	-0,163	-0,12633	-0,08333	-0,01333	-0,052
345	-0,161	-0,125	-0,07967	-0,01133	-0,05133

346	-0,16367	-0,12733	-0,084	-0,013	-0,05333
347	-0,162	-0,12567	-0,08133	-0,01167	-0,053
348	-0,16233	-0,125	-0,08067	-0,01067	-0,05133
349	-0,164	-0,12733	-0,08433	-0,01233	-0,05333
350	-0,16367	-0,12633	-0,08267	-0,012	-0,05233
351	-0,16367	-0,12733	-0,08233	-0,013	-0,05233
352	-0,16433	-0,127	-0,083	-0,012	-0,052
353	-0,166	-0,12733	-0,08267	-0,013	-0,053
354	-0,16633	-0,12933	-0,084	-0,01333	-0,05467
355	-0,16533	-0,12767	-0,08533	-0,01333	-0,054
356	-0,167	-0,12767	-0,08433	-0,012	-0,054
357	-0,166	-0,12833	-0,08467	-0,01233	-0,05367
358	-0,16667	-0,129	-0,08433	-0,01267	-0,05367
359	-0,16667	-0,12867	-0,08433	-0,01233	-0,05367
360	-0,16767	-0,129	-0,08433	-0,01267	-0,054
361	-0,16933	-0,13	-0,085	-0,01333	-0,05433
362	-0,168	-0,12833	-0,084	-0,01167	-0,053
363	-0,169	-0,13	-0,086	-0,01233	-0,05467
364	-0,16867	-0,12933	-0,085	-0,01233	-0,05467
365	-0,16967	-0,12867	-0,08533	-0,01233	-0,05333
366	-0,16933	-0,13033	-0,08533	-0,01233	-0,05433
367	-0,17133	-0,13167	-0,08733	-0,014	-0,05633
368	-0,17067	-0,13	-0,086	-0,01267	-0,055
369	-0,17133	-0,13133	-0,08667	-0,013	-0,05567
370	-0,17033	-0,12967	-0,086	-0,01133	-0,05433
371	-0,171	-0,13033	-0,08633	-0,01233	-0,05433
372	-0,17067	-0,131	-0,08667	-0,01267	-0,05533
373	-0,173	-0,132	-0,08733	-0,01267	-0,05567
374	-0,17267	-0,132	-0,08733	-0,01267	-0,05467
375	-0,172	-0,13133	-0,088	-0,01233	-0,05467
376	-0,173	-0,13167	-0,08833	-0,01333	-0,05567
377	-0,17367	-0,132	-0,08733	-0,01233	-0,05567
378	-0,17367	-0,13267	-0,08867	-0,01233	-0,05567
379	-0,175	-0,13233	-0,089	-0,013	-0,05633
380	-0,17567	-0,13367	-0,08967	-0,01333	-0,05667
381	-0,175	-0,13367	-0,08933	-0,013	-0,05733
382	-0,176	-0,13433	-0,09	-0,01367	-0,05733
383	-0,17567	-0,13367	-0,08967	-0,013	-0,057
384	-0,17633	-0,134	-0,089	-0,01267	-0,057
385	-0,177	-0,13533	-0,09	-0,01367	-0,05667
386	-0,177	-0,13367	-0,09	-0,01233	-0,05767
387	-0,17767	-0,13467	-0,08967	-0,013	-0,057
388	-0,177	-0,13467	-0,08933	-0,01233	-0,05667
389	-0,178	-0,135	-0,09033	-0,01367	-0,05667
390	-0,17867	-0,13533	-0,09133	-0,013	-0,05733

391	-0,17867	-0,137	-0,09167	-0,014	-0,058
392	-0,17833	-0,135	-0,091	-0,01333	-0,05833
393	-0,18033	-0,136	-0,092	-0,01333	-0,058
394	-0,17967	-0,13567	-0,09067	-0,01333	-0,057
395	-0,17867	-0,13567	-0,09167	-0,013	-0,05767
396	-0,17933	-0,136	-0,092	-0,013	-0,05833
397	-0,18067	-0,13567	-0,092	-0,01367	-0,05833
398	-0,18133	-0,137	-0,09133	-0,01233	-0,05733
399	-0,17967	-0,136	-0,09167	-0,01233	-0,05733
400	-0,18233	-0,137	-0,09233	-0,013	-0,059
401	-0,182	-0,13767	-0,09333	-0,01433	-0,058
402	-0,18267	-0,13767	-0,094	-0,01367	-0,059
403	-0,18233	-0,13767	-0,094	-0,014	-0,05933
404	-0,182	-0,13833	-0,09333	-0,01233	-0,059
405	-0,18467	-0,14	-0,095	-0,01533	-0,05967
406	-0,18433	-0,13833	-0,09433	-0,01367	-0,05967
407	-0,184	-0,13933	-0,09467	-0,01467	-0,05967
408	-0,186	-0,13967	-0,096	-0,015	-0,06033
409	-0,18467	-0,13833	-0,09467	-0,01333	-0,059
410	-0,18567	-0,14033	-0,096	-0,014	-0,06
411	-0,18433	-0,138	-0,094	-0,012	-0,059
412	-0,186	-0,13933	-0,095	-0,01267	-0,05933
413	-0,18667	-0,14033	-0,09633	-0,01467	-0,06033
414	-0,18667	-0,14033	-0,09533	-0,01333	-0,06
415	-0,18833	-0,14167	-0,098	-0,01467	-0,062
416	-0,18733	-0,13967	-0,09633	-0,015	-0,06
417	-0,188	-0,141	-0,097	-0,01467	-0,06167
418	-0,189	-0,14133	-0,098	-0,01433	-0,06133
419	-0,18933	-0,14267	-0,09767	-0,015	-0,06167
420	-0,18933	-0,14167	-0,098	-0,01367	-0,06133
421	-0,189	-0,14233	-0,09767	-0,015	-0,061
422	-0,18933	-0,143	-0,09733	-0,015	-0,061
423	-0,18867	-0,14133	-0,09767	-0,01367	-0,06067
424	-0,18967	-0,14167	-0,09833	-0,01333	-0,06167
425	-0,191	-0,143	-0,09933	-0,01433	-0,062
426	-0,19167	-0,143	-0,09933	-0,01533	-0,06167
427	-0,19167	-0,143	-0,09867	-0,014	-0,06133
428	-0,19233	-0,14333	-0,09967	-0,015	-0,062
429	-0,19167	-0,142	-0,09867	-0,01333	-0,06033
430	-0,193	-0,14467	-0,10033	-0,015	-0,06333
431	-0,193	-0,144	-0,10033	-0,01467	-0,062
432	-0,19233	-0,14367	-0,09967	-0,01433	-0,06233
433	-0,194	-0,14267	-0,09933	-0,01433	-0,06167
434	-0,19333	-0,14367	-0,10033	-0,015	-0,06267
435	-0,19467	-0,14433	-0,10033	-0,01433	-0,06333

436	-0,194	-0,14433	-0,101	-0,01533	-0,06167
437	-0,19333	-0,144	-0,10067	-0,01433	-0,06233
438	-0,194	-0,144	-0,10067	-0,01433	-0,06233
439	-0,19533	-0,14467	-0,10133	-0,015	-0,062
440	-0,19667	-0,14633	-0,10333	-0,01533	-0,06367
441	-0,19533	-0,145	-0,10133	-0,014	-0,06233
442	-0,19667	-0,145	-0,10267	-0,01467	-0,06367
443	-0,19733	-0,146	-0,10267	-0,01433	-0,06333
444	-0,19633	-0,14567	-0,10167	-0,01433	-0,06267
445	-0,197	-0,14633	-0,10267	-0,01433	-0,063
446	-0,197	-0,14533	-0,10233	-0,014	-0,063
447	-0,19767	-0,14633	-0,10267	-0,01533	-0,06433
448	-0,198	-0,14633	-0,10433	-0,015	-0,064
449	-0,199	-0,14633	-0,10333	-0,014	-0,065
450	-0,19867	-0,14633	-0,10233	-0,01433	-0,064
451	-0,19833	-0,14567	-0,104	-0,014	-0,06333
452	-0,19967	-0,14733	-0,10367	-0,015	-0,06467
453	-0,19967	-0,14733	-0,10467	-0,015	-0,064
454	-0,20033	-0,148	-0,10467	-0,01467	-0,06433
455	-0,20067	-0,148	-0,10533	-0,015	-0,06433
456	-0,20067	-0,14733	-0,10367	-0,01467	-0,064
457	-0,201	-0,14767	-0,10433	-0,01533	-0,064
458	-0,20133	-0,14833	-0,10567	-0,01533	-0,06533
459	-0,20133	-0,14833	-0,10533	-0,015	-0,066
460	-0,202	-0,14833	-0,10633	-0,01533	-0,066
461	-0,20267	-0,14933	-0,10667	-0,01633	-0,066
462	-0,20367	-0,149	-0,10567	-0,01533	-0,066
463	-0,20367	-0,14967	-0,10667	-0,01667	-0,06633
464	-0,203	-0,14867	-0,10633	-0,015	-0,06633
465	-0,204	-0,14967	-0,10767	-0,01567	-0,066
466	-0,20467	-0,15033	-0,10733	-0,01667	-0,06567
467	-0,20333	-0,14833	-0,10667	-0,01467	-0,06567
468	-0,205	-0,15	-0,10733	-0,01567	-0,06667
469	-0,20567	-0,151	-0,10833	-0,01633	-0,06767
470	-0,20567	-0,15067	-0,107	-0,01533	-0,06667
471	-0,20633	-0,15033	-0,10833	-0,01567	-0,06667
472	-0,20567	-0,15033	-0,10767	-0,015	-0,06667
473	-0,206	-0,15067	-0,10833	-0,01467	-0,066
474	-0,20667	-0,151	-0,10833	-0,01567	-0,06633
475	-0,20667	-0,151	-0,10833	-0,01467	-0,06667
476	-0,20633	-0,151	-0,10867	-0,01467	-0,066
477	-0,20767	-0,15167	-0,10967	-0,01533	-0,06633
478	-0,20833	-0,15167	-0,10967	-0,01567	-0,06667
479	-0,20933	-0,15233	-0,11067	-0,017	-0,06767
480	-0,209	-0,15133	-0,11033	-0,01533	-0,068

481	-0,21	-0,153	-0,11067	-0,01633	-0,06767
482	-0,209	-0,152	-0,111	-0,01567	-0,06767
483	-0,21	-0,15267	-0,111	-0,01567	-0,06733
484	-0,21033	-0,15167	-0,11067	-0,01667	-0,06833
485	-0,21267	-0,15367	-0,11133	-0,01733	-0,06867
486	-0,20967	-0,15167	-0,11067	-0,015	-0,067
487	-0,21	-0,15233	-0,111	-0,01567	-0,06733
488	-0,21233	-0,15367	-0,11133	-0,01733	-0,06867
489	-0,212	-0,15367	-0,11233	-0,01633	-0,069
490	-0,21267	-0,15333	-0,11133	-0,01667	-0,069
491	-0,212	-0,15267	-0,112	-0,016	-0,06933
492	-0,21333	-0,15433	-0,11267	-0,01667	-0,06967
493	-0,214	-0,15433	-0,11433	-0,017	-0,071
494	-0,21333	-0,15533	-0,11333	-0,01667	-0,069
495	-0,214	-0,15467	-0,11367	-0,01633	-0,069
496	-0,21467	-0,155	-0,114	-0,01767	-0,07
497	-0,21467	-0,15533	-0,11433	-0,017	-0,06933
498	-0,21633	-0,15567	-0,11433	-0,01767	-0,07
499	-0,21433	-0,154	-0,11367	-0,016	-0,06933
500	-0,216	-0,15567	-0,11367	-0,017	-0,07067
501	-0,21567	-0,15567	-0,11367	-0,01667	-0,07
502	-0,21567	-0,15467	-0,11367	-0,01567	-0,06967
503	-0,21567	-0,15433	-0,114	-0,01467	-0,06967
504	-0,216	-0,15533	-0,114	-0,016	-0,07
505	-0,217	-0,15567	-0,115	-0,01633	-0,07067
506	-0,21767	-0,15667	-0,11533	-0,01667	-0,07033
507	-0,21767	-0,156	-0,11567	-0,01767	-0,07033
508	-0,21733	-0,155	-0,115	-0,01567	-0,06933
509	-0,21833	-0,15667	-0,116	-0,01633	-0,07133
510	-0,21867	-0,15767	-0,11633	-0,016	-0,07133
511	-0,219	-0,15733	-0,117	-0,01667	-0,071
512	-0,21967	-0,15833	-0,11767	-0,01733	-0,07133
513	-0,21967	-0,157	-0,11733	-0,01767	-0,072
514	-0,22033	-0,15767	-0,117	-0,01833	-0,071
515	-0,221	-0,15733	-0,11767	-0,01767	-0,07233
516	-0,22133	-0,15833	-0,11767	-0,01767	-0,07233
517	-0,22033	-0,15767	-0,117	-0,01667	-0,07133
518	-0,221	-0,15867	-0,11767	-0,01733	-0,07133
519	-0,22133	-0,158	-0,11767	-0,017	-0,072
520	-0,221	-0,15867	-0,11833	-0,017	-0,07267
--	--	--	--		